Aus dem

Interfakultären Institut für Biochemie der Universität Tübingen
Abteilung Biochemie III

The protein interactome of human SOD2 mRNA

Inaugural-Dissertation
zur Erlangung des Doktorgrades
der Medizin

der Medizinischen Fakultät
der Eberhard Karls Universität
zu Tübingen

vorgelegt von

Wüst, Michaela

2020

Dekan:	Professor Dr. B. Pichler
1. Berichterstatter:	Professor Dr. R.-P. Jansen
2. Berichterstatter	Professor Dr. P. Kahle
Tag der Disputation:	22.12.2020

Table of contents

Figure index

Table index

Abbreviations

AKAP	A kinase anchor protein
AMP	Adenosine monophosphate
ARCN1	Coatomer subunit delta
ATAD3	ATPase family AAA-containing protein 3
ATP6	ATP synthase subunit a
BCIP	5-Brom-4-chlor-3-indoxylphosphat
bgH	Bovine growth hormone
BSA	Bovine serum albumin
cAMP	Cyclic adenosine monophosphate
CDC37	Hsp90 co-chaperone CDC37 (also: cell division control 37)
cDNA	Complementary deoxyribonucleic acid
Clu	Protein Clueless (Clustered mitochondria protein homolog, fly)
CLUH	Clustered mitochondria protein homolog, human
CMV	Cytomegalovirus
COPB1	Coatomer subunit beta
COPI	Coat protein complex I
DMEM	Dulbecco‘s modified Eagle‘s medium
DMSO	Dimethyl sulfoxide
DNA	Deoxyribonucleic acid
DPBS	Dulbecco’s phosphate buffered saline
DTT	Dithiothreitol
EDTA	Ethylenediaminetetraacetic acid
eGFP	Enhanced green fluorescent protein
EGTA	Ethylene glycol tetraacetic acid
eIF4G	Eukaryotic translation initiation factor 4 subunit G
ER	Endoplasmic reticulum
FACS	Fluorescence activated cell sorting
FBS	Fetal bovine serum
FLP	Flip recombinase

FMR1	Synaptic functional regulator FMR1 (Fragile X mental retardation gene 1 protein)
FRT site	FLP recombination site
FUBP3	Far upstream element-binding protein 3
FXR 1	Fragile x mental retardation syndrome – related protein 1
G418	Genetecin
GAPDH	Glyceraldehyde-3-phosphate dehydrogenase
GFP	Green fluorescent protein
GPATCH8	G patch domain-containing protein 8
HEPES	N-2-hydroxyethylpiperazine-N-2-ethane sulfonic acid
HSPA4	Heat shock protein of 70 kDa 4
Hsp70	Heat shock protein of 70 kDa
Hsp 90	Heat shock protein of 90 kDa
Hsp 110	Heat shock protein of 110 kDa
IFIB	Interfaculty Institute of biochemistry
IGF2BP1	Insulin-like growth factor 2 mRNA-binding protein 1
IGF2BP2	Insulin-like growth factor 2 mRNA binding protein 2
Larp	La-related protein, fly
LARP1	La-related protein 1, human
LB	Lysogeny broth
LRIG1	Leucine-rich repeats and immunoglobulin-like domains 1
LRPPRC	Leucine-rich PPR motif-containing protein
LRRC40	Leucine-rich repeat-containing protein 40
MAP2	Microtubule-associated protein 2
MCP	MS2 coat protein
MEF	Mouse embryonic fibroblast
MnSOD	Manganese superoxide dismutase, see also: SOD2
MPCP	Mitochondrial phosphate carrier protein-protein, also known as SLC25A3
mRNA	Messenger ribonucleic acid
mTORC1	Mechanistic target of Rapamycin complex 1
MTS	Mitochondrial targeting sequence

NAC	Nascent polypeptide-associated complex
NBT	Nitro blue tetrazolium chloride
NEAT1	Nuclear enriched abundant transcript 1
NLS	Nuclear localization sequence
NP-40	Nonyl phenoxylpolyethoxylethanol
OM14	Mitochondrial outer membrane protein OM14
ORF	Open reading frame
PABP	Poly(A) binding protein
PAGE	Polyacrylamide gel electrophoresis
PBS	Phosphate buffered saline
PCR	Polymerase chain reaction
PINK1	Serine/threonine-protein kinase PINK1
PMSF	Phenylmethyl sulfonyl fluoride
Poly(A) signal	Polyadenylation signal
PPR	Pentatricopeptide repeat
Puf3p	mRNA-binding protein PUF3, yeast
PUM1	Pumilio homolog 1, human
PUM2	Pumilio homolog 2, human
PVDF	Polyvinylidene difluoride
RAB5	Ras-related protein Rab-5
RMCE	Recombinase-mediated cassette exchange
RNA	Ribonucleic acid
RNP	Ribonucleoprotein
ROS	Reactive oxygen species
SDS	Sodium dodecyl sulfate
SOD2	Superoxide dismutase 2
STAU1	Double-stranded RNA-binding protein Staufen homolog 1
TBS	Tris-buffered saline
TBS-T	Tris-buffered saline with 0,1% Tween 20
TEMED	N, N, N’,N’-tetramethylethane-1,2-diamine
TIM	Translocase of the inner mitochondrial membrane
TOM	Translocase of the outer mitochondrial membrane

UTR	Untranslated region
VPS13D	Vacuolar protein sorting-associated protein 13D
ZMBH	Zentrum für Molekulare Biologie der Universität Heidelberg

1. Introduction

"If you base medicine on science you cure people;
If you base the design of planes on science they fly;
If you base the design of rockets on science they reach the moon."
Richard Dawkins

However contested this sentence might be in this time of fake news and full of conspiracy theories it remains as true as a mathematical equation or one of Newton's axioms. If we work thoroughly and systematically in science we will send people to space and we will cure diseases that torment humans and humanity.

Mitochondria are a hub in cell homeostasis by not only providing energy through tricarboxylic acid cycle and oxidative phosphorylation but also by taking part in signaling pathways and apoptosis, fatty acid degradation, lipid and amino acid synthesis and metal ion metabolism (reviewed in: Wiedemann and Pfanner 2017). Therefore, the biogenesis and function of mitochondria must be strictly controlled. Indeed, a single disturbance in this sensible fabric can lead to severely impaired phenotypes and various diseases (reviewed in: Nunnari and Suomalainen 2012, reviewed in: Kang et al. 2018).

The coordination of mitochondrial protein expression is a special challenge for the cell. On one hand, the expression of 37 mitochondrial (Anderson et al. 1981) and about 1100 nuclear encoded (Calvo et al. 2016, Johnson et al. 2007) genes has to be spatially and temporally matched to enable the assembly of functional protein complexes in mammalian mitochondria. On the other hand, the produced proteins have to be placed and assembled correctly within the organelle's compartments and therefore must pass up to two membranes to reach their target site. Evidence found over the past decades lead us the assumption that, beyond transcription regulation, additional posttranscriptional regulation processes are key players that create the mitochondria's composition (Schatton and Rugarli 2018). Within these processes, the correct localization of a mRNA encoding a mitochondrial protein to the vicinity of mitochondria was shown to be a matter of great importance (Margeot et al. 2002, Kaltimbacher et al. 2006, reviewed in: Schatton and Rugarli 2018).

The transport of RNAs to a specific target site in the cell has been demonstrated for various organisms from prokaryotes to mammals (reviewed in: Chin and Lécuyer 2017). mRNA targeting to cellular organelles was first observed and most extensively studied at the endoplasmatic reticulum (reviewed in: Lesnik et al. 2015). However, the localization of nuclear encoded mRNAs to the mitochondrial surface has nowadays been widely demonstrated (Marc et al. 2002, Sylvestre et al. 2003, Kaltimbacher et al 2006, Garcia et al. 2007, Fazal et al. 2019).

Advantages of mRNA localization and their subsequent translation restricted to a cellular compartment could include the reduction of potentially harmful protein activity in a non-target site as well as enabling a faster response to sudden intra- or extracellular stimuli compared to transcriptional regulation. In addition, the transport of one mRNA molecule can serve multiple rounds of translation. Thus, it seems preferable to the transport of its translation products with regard to energy efficiency (reviewed in: Golani-Armon and Arava 2016). Moreover, coupling of mRNA localization to cellular organelles with cotranslational import prevents premature folding and reduces energy expenditure of the import (reviewed in: Lesnik et al. 2015). Indeed, electron cryo-tomography has demonstrated the presence of ribosomes at the mitochondrial surface in yeast. These attached ribosomes had a characteristic orientation and clustered around the TOM complex (Gold et al. 2017) that is crucial for mitochondrial protein import (reviewed in: Wiedemann and Pfanner 2017). First evidence in this matter was found by Kellems et al. in the 1970s who already demonstrated that translating ribosomes locate to the mitochondrial outer membrane in yeast depending on metabolic changes (Kellems and Butow 1974, Kellems et al. 1975). These mitochondria-attached ribosomes were shown to bind preferentially nuclear encoded mitochondrial targeted mRNAs (Marc et al. 2002, Sylvestre et al. 2003, Garcia et al. 2007, Gadir et al. 2011, Williams et al. 2014). This was lately confirmed by Fazal and his colleagues (Fazal et al. 2019). However, it has to be noted that they found a large overlap in mitochondrial and ER-targeted mRNAs.

The findings that posttranslational import of proteins into mitochondria was demonstrated *in vitro* (Behra and Christen 1986) and that a mislocalized mRNA does not necessarily lead to mislocalization of its encoded protein (Shepard et al. 2003) question the functional impact of mRNA transport and local translation *in vivo*.

In 2002, Margeot et al. examined the impact of ATP2 mRNA mislocalization from its mitochondrial target site in yeast and reported not only a decreased import of its encoded protein but also a severely impaired respiration (Margeot et al. 2002). Consistent with that, Gehrke et al. found that a decrease in mitochondria-bound mRNAs is accompanied by reduced protein levels and decreased oxidative phosphorylation activity in HeLa cells and tissue-specific in *Drosophila melanogaster* (Gehrke et al. 2015) upon depletion of PINK1, a protein that is involved in localization.

The localization of a given mRNA is dependent on cis-elements in its sequence and trans-acting proteins that are able to recognize them (reviewed in: Jansen 2001). Although most involved factors are still unknown, some proteins and their target signals that take part in mRNA localization have been identified within the past years. It has to be noted that the distribution of mitochondria-targeted mRNAs is dependent on many external factors (reviewed in: Schatton and Rugarli 2018). For example, nuclear encoded mitochondrial RNAs can be trapped by the nuclear long non-coding RNA NEAT1 upon mitochondrial stress sensing (Wang et al. 2018) and many RNA-binding proteins change their behavior in response to metabolic stimuli (Hong et al. 2017, Lapointe et al. 2018). However, this work will focus on RNA-binding proteins acting at the mitochondrial surface and their mRNA targets.

The most common cis-acting elements for sorting of mRNAs and proteins to the mitochondrial surface are the mitochondrial targeting sequence (MTS) and the 3'UTR of target mRNAs (reviewed in: Lesnik et al. 2015). Each of this two sequence elements were shown to be sufficient for distribution of mRNAs to the mitochondrial vicinity that increased when both elements were added to a construct (Kaltimbacher et al. 2006, Eliyahu et al. 2010).

The MTS is located at a protein's N-terminus and has a typical length between 8 and 80 amino acids. In yeast, the sequence is bound by the nascent polypeptide-associated complex (NAC) upon release from the ribosomal exit tunnel (reviewed in: Hansen and Herrmann 2019). The NAC targets the nascent polypeptide and associated ribosomes to the mitochondrial surface via its interaction with OM14, a mitochondrial outer membrane protein (Lesnik et al. 2014). Finally, the presequence carrying proteins are usually recognized by the TOM complex subunit TOM20 and imported through the TOM40 channel (reviewed in: Wiedemann and Pfanner 2017). Indeed, TOM20 was

shown to recruit MTS-containing mRNAs to the mitochondrial surface in a translation-dependent manner (Eliyahu et al. 2010). Besides the N-terminal MTS, internal MTS-like structures in the ORF of proteins were recently identified (Backes et al. 2018). They are found mainly in mitochondrial matrix proteins and are especially recognized by the subunit TOM70 (yeast TOM71) receptor that also recognizes cytosolic chaperones. Although TOM70 and TOM20 prefer to bind a specific subset of mitochondrial targeted proteins, respectively, they can functionally replace each other since single knockout yeast strains show at least sufficient mitochondrial protein import for viability (reviewed in: Hansen and Herrmann 2019).

The second important cis-element is the 3' untranslated region of a mRNA. It is suggested to interact with RNA-binding proteins that mediate localization of the transcript independently of translation (reviewed in: Lesnik et al. 2015).

One of the first and best studied proteins involved in 3'UTR-mediated sorting of nuclear encoded mRNAs to the mitochondrial surface is the yeast mRNA-binding protein Puf3. It is resident on the cytosolic surface of the mitochondrial outer membrane (reviewed in: Lesnik et al. 2015) and was first identified in 2008 as a binder of mitochondrial targeted cytosolic mRNAs (Saint-Georges et al. 2008). The protein was shown to act as translational regulator and also mediates mRNA decay and stability (reviewed in: Lesnik et al. 2015). It represses translation of mitochondrial targeted mRNAs including several encoding for respiratory chain subunits, tricarboxylic acid cycle enzymes, mitochondrial lipids and proteins of the import machinery and innermitochondrial translation in fermenting *Saccharomyces cerevisiae*. This repression is released in respiring yeast cells (likely by phosphorylation of Puf3) although the protein stays bound to its mRNAs (Lapointe et al. 2018). In addition to the direct binding and impact on mitochondrial targeted mRNAs, Puf3 was found to alter the protein level of cytosolic ribosomes and to regulate a network of 65 RNA binding proteins (Wang et al 2019). Taken together, Puf3 is considered a sensor for metabolic changes in yeast cells that mediates expression of proteins for mitochondrial biogenesis under non-fermentive conditions and balances mitochondrial and cytosolic translation (Lapointe et al. 2018, Wang et al. 2019). The two mammalian Pumilio family members, PUM1 and PUM2, are also RNA-binding proteins with a posttranslational regulatory function. However,

none of them exhibits a specificity for nuclear encoded mitochondrial targeted mRNAs (Bohn et al. 2018).

PINK1, a protein associated with Parkinson's disease, was shown to recruit a subset of mitochondrial targeted mRNA to the mitochondrial outer membrane in *Drosophila melanogaster* and in Hek293 cells. In this study, in fly tissue and mammalian cells, Pum was shown to interact with PINK1's mitochondrial outer membrane targets, most likely downstream of PINK1 (Gehrke et al. 2015). Therefore, Pum might not exclusively, but also regulate mitochondrial targeted mRNAs.

PINK1 interacts with Parkin to release translation repression from its bound mRNAs and recruits the translation initiation factor eIF4G (Gehrke et al. 2015). Since the PINK1-Parkin pathway is also involved in mitophagy (Narendra et al. 2010), it might provide an interesting link between in translation and mitochondrial homeostasis (Gehrke et al. 2015).

Another study performed in *D. melanogaster* oocytes reported a novel mitochondrial outer membrane protein belonging to the AKAP family, MDI, that interacts with TOM20 and recruits the La-related protein (Larp) to the mitochondrial surface. This interaction was demonstrated essential for mitochondrial biogenesis and replication of mitochondrial DNA in *Drosophila* oocytes (Zhang et al. 2016). LARP1, the human homolog of Larp, is a known RNA binding protein that was shown to regulate the translation of cytosolic ribosomal proteins dependent on phosphorylation (Hong et al. 2017). Although the localization of mRNAs encoding mitochondrial proteins that showed alterations in expression in MDI deficient cells was not studied by Zhang and colleagues (2016), it is likely that MDI and Larp have an impact on mRNA distribution to the mitochondrial surface. In addition, another AKAP protein localized at the mitochondrial outer membrane, the mouse AKAP121 was shown to tether the nuclear encoded SOD2 mRNA to the surface of mitochondria in transfected Hela S3 cells and increases SOD2 protein level especially following cAMP stimulation (Ginsberg et al. 2003). Thus, the AKAP protein family might be an interesting field to mine for new mRNA binders at the mitochondrial outer membrane.

The clustered mitochondria protein homolog (CLUH) is nowadays considered the main interactor for mitochondrial targeted mRNAs. The protein is an evolutionary conserved RNA-binding protein (reviewed in: Schatton and Rugarli 2018) that, in mammalian

cells, was shown to bind especially mRNAs belonging to nuclear encoded mitochondrial proteins (Gao et al. 2014). Concurrently, Hela S3 cells with a CLUH knockout were impaired in oxidative phosphorylation, tricarboxylic acid cycle function and fatty acid oxidation and displayed an altered mitochondrial translation pattern (Wakim et al. 2017). In addition, a homozygote deletion of CLUH in mice lead to postnatal lethality and the mitochondrial proteome in CLUH deficient liver tissue of mice is significantly altered compared to wildtype mice (Schatton et al. 2017). The *Drosophila* homolog of CLUH, Clueless (Clu) was shown to associate with ribosomal proteins at the mitochondrial outer membrane in larval neuroblasts. Moreover, the depletion of Clu does not only exhibit the conserved phenotype of mitochondrial clustering in the examined cells, but also leads to an impairment of mitochondrial function (Sen and Cox 2016).

Although Schatton et al. observed an increased decay of investigated target mRNAs in CLUH depleted mouse embryonic fibroblasts (MEFs) (Schatton et al. 2017), Vardi-Oknin and Arava reported almost no impact on steady-state levels of examined targets in Hek293 cells. Moreover, CLUH binding transcripts exhibited a stronger localization to the mitochondrial vicinity upon transfecting with CLUH silencing RNA. Thus, the exact function of CLUH on its target mRNAs and interacting proteins are still to be elucidated (Vardi-Oknin and Arava 2019). However, CLUH's function has shown to be crucial in adipose tissue differentiation linking it obesity, hepatosteatosis and cardiovascular diseases (Cho et al. 2019).

Most of the studies presented above approach the question what factors are involved in mRNA localization to the mitochondrial surface from the view of the trans-acting proteins. Usually one or few proteins are chosen and it is examined what mRNAs are altered in their localization. In contrast, this work aims to put a specific mRNA to the center of interest and to identify potential trans-acting proteins that are involved in its transport.

The bait RNA chosen for this work is the human mitochondrial superoxide dismutase 2 (SOD2, also known as MnSOD) mRNA. SOD2 is a mitochondrial superoxide radical scavenger protein (Wong 1995) that protects proteins, lipids and nucleic acids in the organelle from reactive oxygen species (ROS), the byproducts of oxidative phosphorylation. The SOD2 and especially its active site is conserved from bacteria to

human and a deletion of the enzyme was demonstrated to be lethal in mice. In human, SOD2 mutations were observed in several cancers and neurological disorders (including Parkinson's disease). Polymorphisms within its sequence were associated with type II diabetes and hypertension. Moreover, pre-clinical studies in mice and rat using recombinant SOD2 as a drug demonstrated irradiation protection of healthy tissue and a toxic effect in tumor cells. Moreover, it seems to have a positive impact on fibrosis and to reduce inflammation (reviewed in: Azadmanesh and Borgstahl 2018).

The sequence is encoded in the nucleus (compare Anderson et al. 1981) and its mRNA was found enriched in mitochondria associated polysomes in HeLa cells (Sylvestre et al. 2003) indicating the sorting of SOD2 mRNA to the mitochondrial surface. In addition, the transcript was recruited in a cAMP-dependent manner to the vicinity of HeLa mitochondria upon transfection with a vector encoding the mouse mitochondrial membrane protein AKAP121 (Ginsberg et al. 2003). Moreover, the SOD2 MTS and its 3'UTR were characterized as sufficient to retarget the mitochondrial encoded ATP6 from a genomic locus to a successful mitochondrial import although ATP6 constructs without the SOD2 cis-elements failed to enter the mitochondria (Kaltimbacher et al. 2006).

Here, 24 MS2 loops were introduced between the SOD2 ORF and the 3'UTR to tether the mutant biotin ligase BirA* via MS2 coat proteins to the bait. This RNA-BioID method has already been proven to be successful to identify trans-acting proteins involved in ß-Actin mRNA localization (Mukherjee et al. 2019).

The work presented here seeks to find potential candidates responsible for the sorting of SOD2 mRNA to the mitochondrial vicinity by applying RNA-BioID on SOD2 mRNA in human HeLa and U2OS cells.

2. Materials and methods

2.1. Materials

Table 1: machines and equipment in the cell culture.

Sterile Hood HLB 2448	*Heraeus*
Water bath Isotemp 210	*Thermo Fisher Scientific*
Incubator CB210	*Binder GmbH*
Refridgerator	*Liebherr Profi line*
Tabletop centrifuge 5702	*Eppendorf*
Mini centrifuge	*Biozym*
Inverse Microscope	*Zeiss West Germany*
Light source Mikroskopierleuchte 1000	*Zeiss West Germany*
Freezer	*Liebherr*
Vortex Genie 2	*VWR*
Pipette 10 µl	*Eppendorf*
Pipette 20µl	*Gilson*
Pipette 200µl	*Eppendorf*
Pipette 1000µl	*Gilson*
Pipetboy Acu	*Integra Biosciences*
IBS Fireboy	*Integra Biosciences*
Laboport^{R}	*KNF*
Hemocytometer	*Brand*
Microscopy cover glass	*VWR*
10 cm dishes	*Corning*
75 cm² flasks	*Corning*
150 cm² flasks	*TPP*
300 cm² flasks	*TTP*
6 well plates with lid	*Corning*
4-well microscopy chambers with lid	*Sarstedt*

Filtertips 10 µl	*nerbe plus*
Filtertips 20 µl	*nerbe plus*
Filtertips 200 µl	*nerbe plus*
Filtertips 1000 µl	*nerbe plus*
Pipette tips 10 µl	*Sarstedt*
Pipette tips 200 µl	*Sarstedt*
Pipette tips 1000 µl	*Sarstedt*
CoStar^{R} Strippettes 2ml-25ml	*Corning*
15 ml tubes with lid	*Sarstedt*
50 ml tubes with lid	*Greiner bio-one*
1.5 ml safelock microcentrifuge tubes	*Sarstedt*
2ml Cryopure freezing tubes	*Sarstedt*

Table 2: Machines and equipment in the laboratory.

CCD Camera Axiocam 506	*Canon*
Filter cube HE 38	*Zeiss*
Filter cube F45	*AHF*
Cell observer microscope	*Zeiss*
Lambda unit with Xenon lamp	*Zeiss*
Objectives 40x-63x	*Zeiss*
Nanodrop spectral photometer	*Thermo Fisher Scientific*
SDS-page and western blotting chambers	*Bio-Rad*
SDS-page glass plates	*Bio-Rad*
Agarose gel chambers	*Thermo Fisher Scientific*
Power supply PowerPac^{TM}	*Bio-Rad*
Refridgerator	*Liebherr Profi line*
Freezer -20°C	*Liebherr Comfort line*
Freezer -80°C	*Thermo Scientific*
Tabletop centrifuge 5424	*Eppendorf*
Tabletop centrifuge 5415 R	*Eppendorf*
Centrifuge 5810 R	*Eppendorf*

Vortex Genie 2	*VWR*
Thermocycler FlexCycler	*Analytik Jena*
Thermocycler MyCycler	*Bio-Rad*
Genesys 10 spectrophotometer	*Thermo Scientific*
DeVision Dbox imaging system	*Decon Science Tec*
Microwave	*Sharp*
Odyssey imaging system	*Li-Cor Biosciences*
Thermocell mixing block MB102	*Bioer*
Incubator INCU-line	*VWR*
Minitron incubation shaker	*Infors-HT*
Milli-Q water purification system	*Millipore company*
Pipetboy Acu	*Integra Biosciences*
Pipette 10 µl	*Eppendorf*
Pipette 20 µl	*Eppendorf*
Pipette 200 µl	*Eppendorf*
Pipette 1000 µl	*Eppendorf*
IKAMAG RCT (stirrer and heating plate)	*IKA*
dounce glass homogenitizer	*Braun*
Scales	*Kern ABJ and PLS 2100-2*
Beaker glasses	*Schott*
Erlenmeyer flasks	*SIMAY*
Glass bottles 200ml-1000ml with lid	*Schott*
Glass beads	*Roth*
Rotator SB2	*VWR*
Filter tips 10 µl	*Nerbe plus*
Filter tips 200 µl	*Nerbe plus*
Filter tips 1000 µl	*Nerbe plus*
Pipette tips 10 µl	*Sarstedt*
Pipette tips 200 µl	*Sarstedt*
Pipette tips 1000 µl	*Sarstedt*
Safelock 1.5 ml microcentrifuge tubes	*Sarstedt*

1.5 ml microcentrifuge tubes	*Greiner-bio/Sarstedt*
15 ml tubes with lid	*Sarstedt*
50 ml tubes with lid	*Greiner-bio/Sarstedt*
Polystyrene Cuvettes	*Sarstedt*
2 ml microcentrifuge tubes	*Sarstedt*
CoStar^{R} Stripettes 2 ml-25ml	*Corning*
PCR tubes	*Sarstedt*
PCR stripes	*Sarstedt*
Petri dishes	*Sarstedt*
Soft-ject 2ml Syringes	*VWR*
Needles 21G	*Sterican*

Table 3: Chemicals, enzymes and antibodies in the cell culture.

1x Trypsin-EDTA	*Sigma-Aldrich*
10x Trypsin-EDTA	*Sigma-Aldrich*
FBS, heat-inactivated	*Sigma-Aldrich*
Dulbecco‘s modified Eagle‘s medium	*Sigma-Aldrich*
Opti-MEM medium	*gibco*
Trypan blue solution	*Sigma-Aldrich*
DMSO	*Sigma-Aldrich*
Hygromycin B	*Roth*
G418	*Sigma-Aldrich*
Ganciclovir	*Sigma-Aldrich*
Doxycycline hyclate	*Sigma-Aldrich*
Blasticidin S hydrochloride	*Roth*
X-treme Gene transfection reagent	*Sigma-Aldrich*
FuGENE^{R} 6 transfection reagent	*Thermo Fisher Scientific*
FuGENE^{HD} transfection reagent	*Thermo Fisher Scientific*
Biotin	*Sigma-Aldrich*
Salmon Protamine sulfate	*Sigma-Aldrich*
Penicillin/Streptomycin	*Sigma-Aldrich*

Mitotracker^{R} deepRed staining	*Thermo Fisher Scientific*
Mitotracker^{R} Green staining	*Thermo Fisher Scientific*
DPBS	*Sigma-Aldrich*

Table 4: Chemicals, enzymes and antibodies in the laboratory.

Phenol/Chloroform	*Roth*
Ethanol	*Riedel de Haen*
Agarose	*Sigma-Aldrich*
GelRed^{R} dye	*BioTrend*
Cutsmart^{R} 10x buffered	*New England BioLabs*
1kb DNA ladder	*New England BioLabs*
6xloading buffer	*New England Biolabs*
BamHI-HF enzyme	*New England Biolabs*
KpnI-HF enzyme	*New England Biolabs*
NotI Fast digest	*Fermentas*
BamHI Fast digest	*Fermentas*
Buffer "Green"	*Fermentas*
Herculase^{R} II Fusion DNA polymerase	*Stratagene*
100 mM dNTP mix	*Agilens*
5x Herculase buffer	*Stratagene*
10 T4 DNA ligase buffer	*Thermo Fisher Scientific*
T4 DNA ligase	*Thermo Fisher Scientific*
Pageruler^{TM} prestained protein ladder	*Thermo Fisher Scientific*
RiboRuler high range RNA ladder	*Thermo Fisher Scientific*
PVDF membrane	*GE Healthcare Sciences*
Immobilon-FL PVDF membrane	*Merck –Millipore*
Sodium chloride	*Sigma-Aldrich*
NBT	*Sigma-Aldrich*
BCIP	*Sigma-Aldrich*
Streptadvidin-Alkaline phosphatase	*KPL*
Streptavidin magnetic beads	*GE Healthcare*

Proteinase K	*Thermo Fisher Scientific*
Agarose	*Roth*
Methanol	*Thermo Fisher Scientific*
BSA	*Sigma-Aldrich*
Tween 20	*Roth*
Bradford reagent Roti-Quant^{R}	*Roth*
Potassium chloride	*Applichem/Roth*
Sodium hydrogen phosphate	*Merck*
Potassium hydrogen phosphate	*Applichem*
Tris	*Applichem*
NP-40	*Roche*
SDS pellets	*Roth*
Magnesium chloride	*Merck*
Mannitol	*Roth*
Magnesium acetate	*Roth*
ß-Mercaptoethanol	*Roth*
PMSF	*Roth*
HEPES	*Roth*
Glucose	*Roth*
Trehalose	*Sigma-Aldrich*
Magnesium sulfate	*Sigma-Aldrich*
Calcium chloride	*Merck*
Glycerol	*Roth*
Bromphenolblue	*Roth*
Sodium deoxycholate	*Sigma-Aldrich*
Triton X-100	*Roth*
EDTA	*Applichem*
Lithium chloride	*Applichem*
DTT	*Sigma-Aldrich*
Sucrose	*Sigma-Aldrich*
EGTA	*Sigma-Aldrich*
Ammoniumperoxidisulfate	*Roth*

TEMED	*Applichem*
Isopropanol	*Merck*
Sodium acetate	*Merck*
Glycine	*Sigma-Aldrich*
Trypton/Pepton	*Roth*
Yeast extract	*Roth*
Ampicillin	*Roth*
Sodium hydroxide	*Baker*
Anti GFP rabbit antibody	*lifeTechnologies*
Anti FLAG mouse antibody	*Sigma-Aldrich*
Anti Tom20 rabbit antibody	*Santa Cruz*
Anti Lamin A/C rabbit antibody	*Cell Signaling*
Anti GAPDH rabbit antibody	*Cell Signaling*
Goat anti mouse 680nm	*Li-Cor*
Goat anti rabbit 680nm	*Li-Cor*
Goat anti mouse 800 nm	*Li-Cor*
Goat anti rabbit 800nm	*Li-Cor*
Roti^{R} Load RNA	*Roth*
DNA ladder	*Thermo Fisher Scientific*

Table 5: Commercially available kits.

Nucleospin^{R} Plasmid Easypure kit	*Machery and Nagel*
Nucleospin^{R} Gel and PCR cleanup kit	*Machery and Nagel*
Nucleosnap^{R} plasmid Midi kit	*Machery and Nagel*
Nuckeospin^{R} RNA kit	*Machery and Nagel*
Goscript^{R} reverse transcriptase system	*Promega*

2.2. Methods

2.2.1. Plasmids and Cloning

Plasmid amplification

All plasmids were amplified in *Escherichia coli DH5α*. The purified plasmids were transformed into the competent bacteria by heat shock transformation. A maximum amount of 1 ng DNA was placed in a 1.5 ml microcentrifuge tube. $5x10^5$ competent *E. coli DH5α* were added to the plasmid DNA. The tubes were incubated on ice for 40 minutes, heat shocked in a 42°C waterbath for 42 seconds and placed on ice for another 2 minutes. After addition of 700 µl of room-temperatured LB medium without antibiotics, the bacteria were incubated at 37°C for 45-60 minutes. Following, the tubes were centrifuged with 7000 rpm for 1 minute and 600 µl of the supernatant were discarded. The prokaryotes were resuspended in the remaining medium and plated on LB plates containing the selection marker Ampicillin with the help of glass beads. The plates were incubated overnight at 37°C.

The next day, several colonies from one plate were picked to inoculate separate cultures with LB medium containing 100µg/ml Ampicillin for overnight incubation. The plasmids were purified using the Nucleospin plasmid Easypure kit following the provided protocol. The obtained DNA amount was measured by spectrophotometry using the Nanodrop system. Each plasmid was checked by restriction digestion.

Plasmid purification by phenol-chloroform extraction and ethanol precipitation

For phenol-chloroform extraction, the DNA had to be diluted to a volume of at least 50 µl. Following, the same volume of phenol/chloroform solution was added onto the plasmids. The tube was vortexed for 15-20 seconds. The sample was then kept at room temperature for 3 minutes until both phases had been separated again. Following, the tube was centrifuged at 12000 x g for 15 min at 4 °C to neatly separate the phases and the interphase layer. The upper liquid phase was then transferred into a new 1.5 ml microcentrifuge tube.

$^1/_3$ of the primary volume (e.g. if started with 100 µl plasmid solution, now 30 µl) of sodium acetate 3 M pH 5.2 was added to the new tube. Then 3 times the primary volume (e.g. 300 µl) of ice-cold 100% ethanol was added and the tubes were stored at

-80 °C for at least 4 hours, but mostly overnight for 8-10 hours. After this time, the samples were centrifuged at 13000 x g and 4 °C for 30 minutes. The supernatant was discarded and the pellet resuspended in 75 % ice-cold ethanol. The centrifugation was repeated at 4 °C and 13000 x g for 20 minutes. The supernatant was discarded and the tubes were left at room temperature for 15 minutes under an extractor fan to let the alcohol evaporate. The plasmids then were resuspended in ddH_2O and concentration was measured using the Nanodrop system.

Constructs for transient transfection and stable integration

In figure 1 the constructs that were transfected into HeLa S3, U2OS and HeLa 11ht cells are portrayed. The first shown construct is the bait mRNA, $SOD2_{MS2}$, that was developed by Joyita Mukgerjee (unpublished data, laboratory of Prof. Jansen, IFIb Tübingen). Here, the DNA coding for the FLAG epitope and the MS2 loops are inserted between the human SOD2 open reading frame and the SOD2 3'UTR. The stop codon is located after the FLAG tag, so that the SOD2 expressed from the plasmid will have a FLAG tag at its C-terminal end.

In the bottom of figure 1, the RNA-binding fusion protein constructs used for the experiments are shown. The aminoterminal nuclear localization sequence (NLS) relocates the protein to the nucleus in absence of the bound target mRNA. The MS2 coat protein (MCP) binds as a dimer to the MS2-loops. The fusion proteins contain either one or two MCP units. This segment is followed by an enhanced GFP (eGFP) that allows the detection of the protein in the cell by fluorescence microscopy. The mutant biotin ligase BirA* represents the carboxyterminal component of the fusion protein(s) (Mukherjee et al. 2019). When targeted via MCP to the MS2 loops, the fusion protein will travel with the target RNA and biotinylate surrounding proteins including the RNA-interacting proteins within the approximate range of 10nm (reviewed in: Kim and Roux 2016).

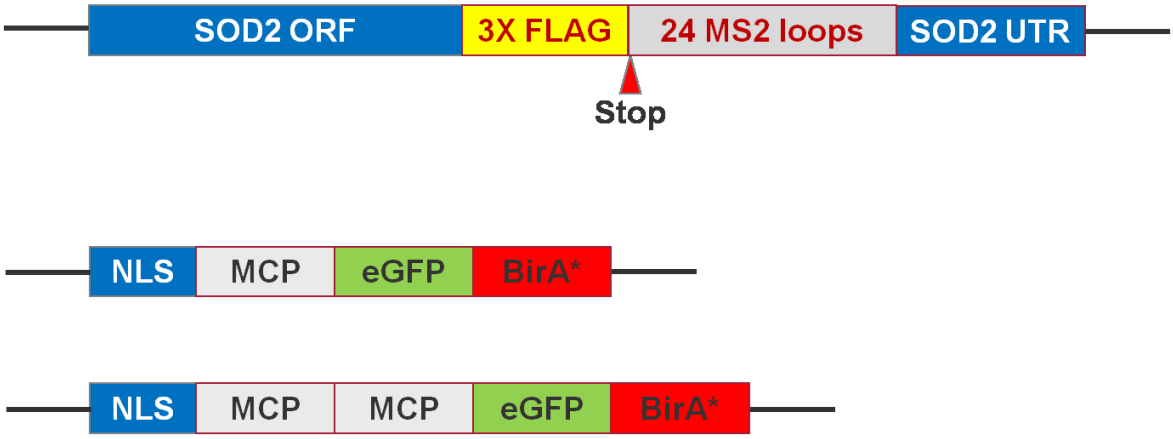

Fig. 1: SOD2 bait mRNA and BirA fusion protein constructs.*
The picture shows the constructs for the experiments developed by Joyita Mukherjee (Mukherjee et al. 2019, $SOD2_{MS2}$: unpublished data, laboratory of Prof. Jansen, IFIB Tübingen) by linking the BioID method (Roux et al. 2013) to a bait mRNA via the widely used MS2/MCP system (Mukherjee et al. 2019).
The first construct is encoded on the plasmid SOD2MS2 shown in figure 2 (see transient transfection vectors section in this chapter). The second containing one MCP is encoded on BirA$_t$ and the last one on BirA*$_{tt}$ for transient transfection. For stable integration into cells, one MS2 coat unit per protein was preferred over the construct with two.*

In addition, constructs lacking BirA* but containing MCP and eGFP were developed for first localization experiments.

Transient transfection vectors

Three plasmids were used for transient transfection experiments in the HeLa S3 cell line.

First, *SOD2MS2* was created to introduce the target RNA of human SOD2 together with 24 MS2 loops between the ORF and the 3'UTR into the cells. The plasmid has a pcDNA3 backbone and the mRNA is expressed from a CMV promotor. The plasmid was created by Joyita Mukherjee (unpublished data, laboratory of Prof. Jansen, IFIB Tübingen).

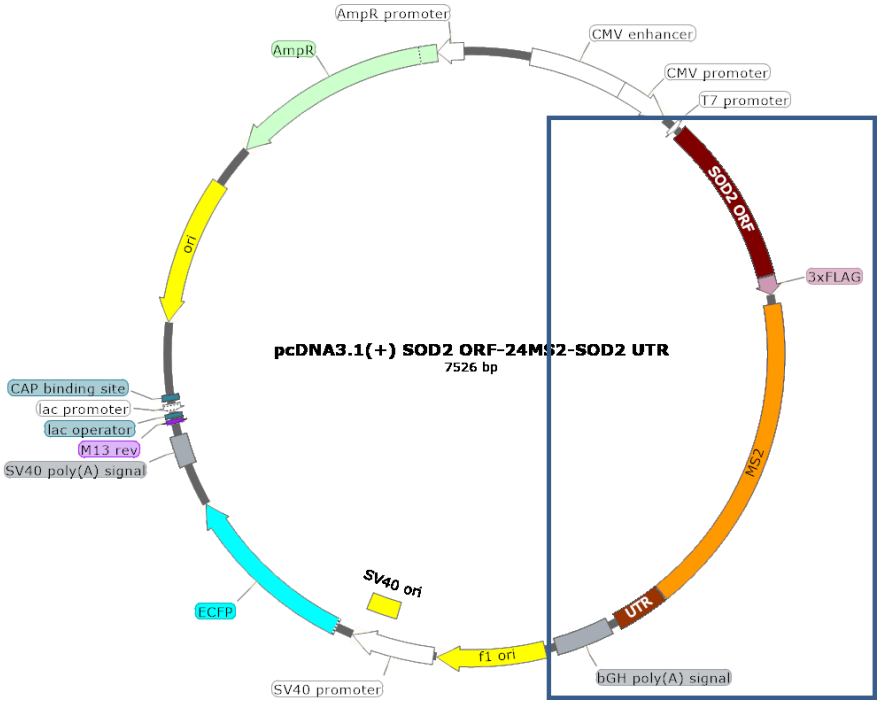

Fig. 2: SOD2MS2 (RJP 2029).

The plasmid was used to introduce the bait mRNA into the cells. The blue box highlights the region expressing the target mRNA. It consists of the ORF of human SOD2 in frame with a FLAG tag, 24 MS2 loops, the 3'UTR of human SOD2 and a bovine growth hormone polyadenylation signal.

The second plasmid *RJP 1953* was also designed by Joyita Mukherjee. The construct in a phage backbone can be seen in figure 3 and contains the sequence of the 2xMCP-eGFP-BirA* fusion protein that will bind to the $SOD2_{MS2}$ bait mRNA. In addition, another variant of this plasmid expressing the protein construct with only one MCP instead of two was designed. Here, theoretically twice the amount of biotin ligase and eGFP units can be bound per RNA molecule for a brighter signal.

Moreover, plasmids containing the sequences for fusion proteins lacking BirA*, respectively, were designed in the same backbone by Joyita Mukherjee (unpublished data, laboratory of Prof. Jansen, IFIB Tübingen).

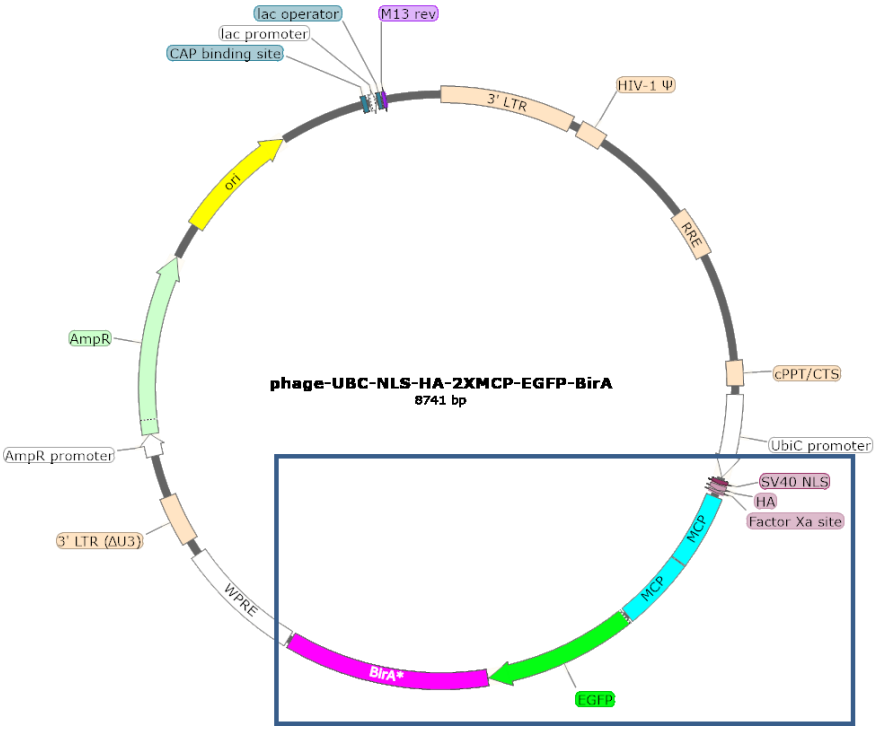

Fig. 3: The plasmid BirA$_{tt}$ (RJP 1953).*

BirA$_{tt}$ encodes the MS2 loop binding protein construct that is highlighted in the blue box. It consists of the mutant biotin ligase BirA* derived from E.coli (reviewed in: Kim and Roux 2016) that is expressed in frame with the fluorescent protein eGFP and two MS2 coat proteins. Moreover, it contains a nuclear targeting sequence that will guide the expressed protein to the nucleus unless bound to the MS2 loops (Mukherjee et al. 2019).*

Stable integration vectors

The HeLa 11ht cells and U2OS cells are optimized for different ways to achieve stable integration of added plasmids into their genome.

The used U2OS T-Rex cell line has FRT sites integrated in their genome. Therefore, the Flp/FRT system can be used to integrate a given DNA sequence at these sites. Several requirements have to be fulfilled for a successful integration in this system. First, the Flip recombinase must be produced in the cells at the time of transfection. For this, a plasmid encoding this protein has to be co-transfected with the target DNA sequence. The according plasmid map is shown below in figure 4.

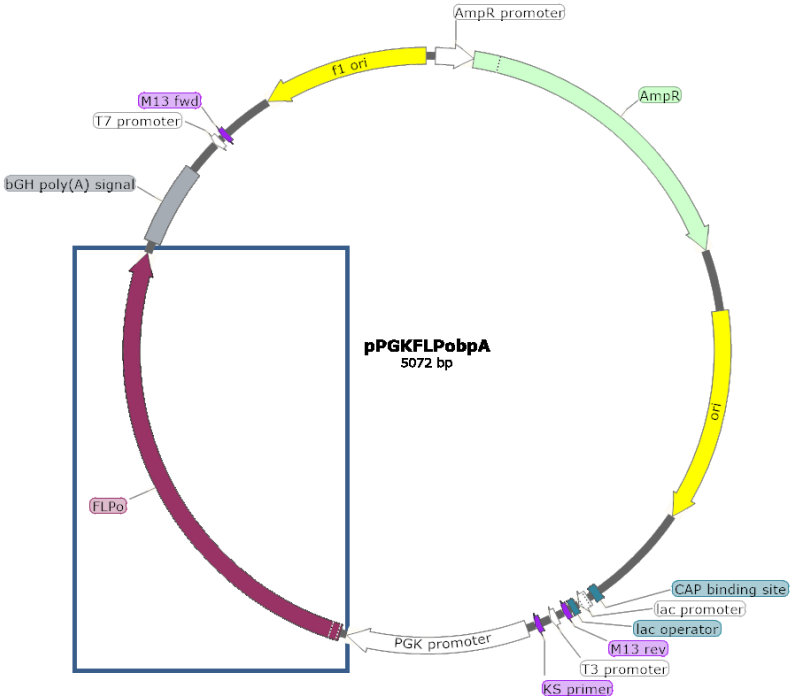

Fig. 4: Plasmid map of pPGKFLPobpA (Raymond and Soriano 2007).
The vector encodes a codon optimized Flip recombinase for mammalian cells (blue box) with a bovine growth hormone poly-A signal (Raymond and Soriano 2007). It is commercially available via Addgene.

Second, the plasmid with the DNA sequence that has to be integrated must contain the fitting FRT site to enable its insertion by the Flip recombinase.
The plasmid construct with Tet operators and two CMV promoters in a pcDNA5 backbone was created by Alfred Hanswillemenke (laboratory of Prof. Stafforst, IFIB Tübingen, unpublished data) as shown in figure 5. Box two highlights the FRT site necessary for stable integration of the plasmid into the genome of U2OS T-Rex cells.

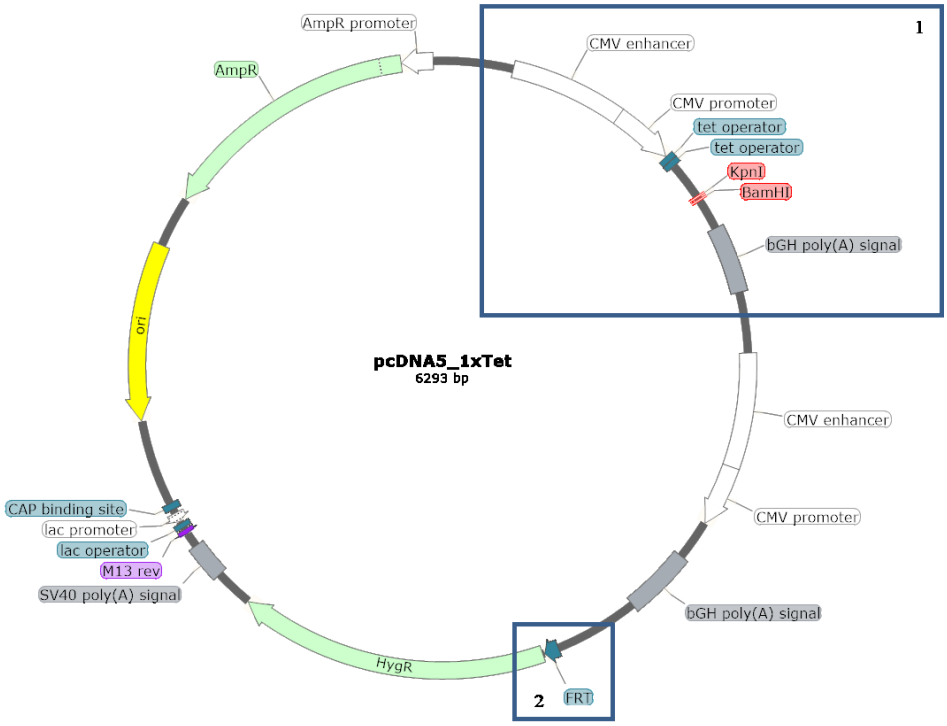

Fig. 5: Plasmid pcDNA5_1xTet (Alfred Hanswillemenke, unpublished data, laboratory of Prof. Stafforst, IFIB Tübingen).

The plasmid pcDNA5_1xTet is the backbone for transfer of genes into U2OS cells. Box number 1 shows the KpnI and BamHI restriction sites I used for inserting the fusion proteins containing the biotin ligase. Before the insertion site you find the CMV promoter and the Tet-response elements necessary for the tetracycline or doxycycline dependent expression of the inserted gene. Again, the inserted sequence is followed by a bovine growth hormone poly-A signal.

The FRT (flip recombinase target) site is highlighted in box number 2. It is needed for stable integration of the plasmid into the U2OS genome using the Flp/FRT system.

The DNA inserts containing the eGFP or eGFP+BirA* were created by PCR from the psF3 plasmids *RJP 2052* and *RJP 2053* (see figure 8) that have been cloned for stable integration of the fusion proteins' sequences in Hela 11ht cells by Joyita Mukherjee (unpublished data, laboratory of Prof. Jansen, IFIB Tübingen). The products were amplified with the primers KpnI-stop-SV40NLS_F and either BamHI-eGFPwithstop_R or BamHI-BirAwithstop_R (for sequences see appendix) for constructs without or with BirA*, respectively. The PCR program is shown in figure 6.

The primers insert a KpnI site and, to avoid frame shift, an ATG triplet in the beginning as well as a BamHI site for cloning at the end. The PCR product was purified by agarose gel electrophoresis and the correct band was extracted using the Nucleospin kit. The insert as well as the backbone vector were digested with BamHI and KpnI high fidelity enzymes in the recommended buffer. The digested DNA was again purified via agarose gel electrophoresis, extracted and following ligated with T4 DNA ligase. The ligation products were transformed into *E.coli DHα* by heat shock transformation (for protocol see plasmid amplification in this chapter). Correctly assembled plasmids were checked with colony PCR and partially by sequencing.

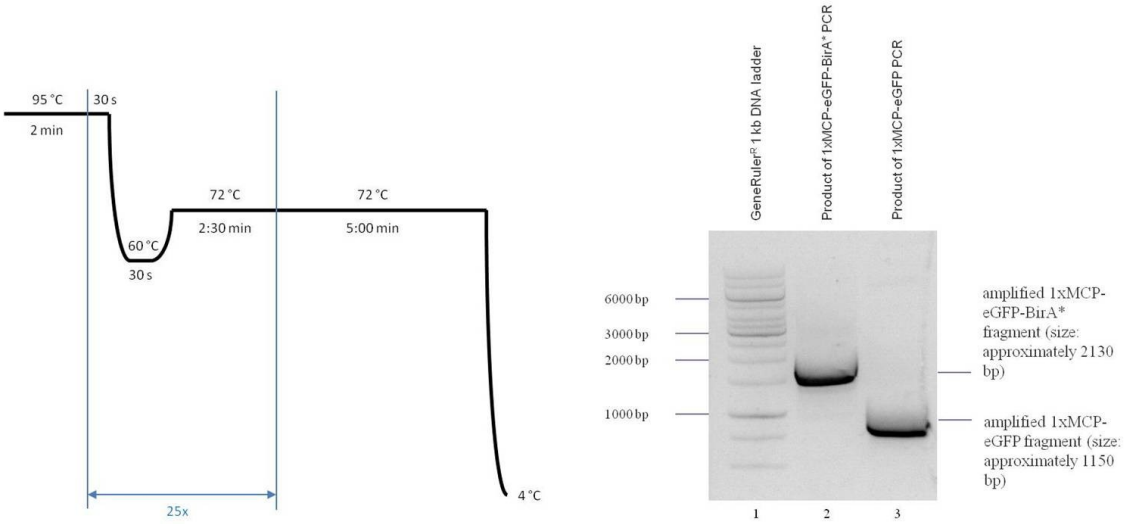

Fig. 6: Generating 1xMCP-eGFP and 1xMCP-eGFP-BirA inserts for cloning in pcDNA5_1xTet.*

Left: PCR program. Right: amplified products. Lane 2 shows the band for 1xMCP-eGFP-BirA (2127 base pairs) and lane 3 the band of 1xMCP-eGFP (1158 base pairs).*

The plasmid map below shows the final plasmid *1xTet_1xMCP eGFP BirA** used for stable integration into U2OS cells. The backbones created by Alfred Hanswillemenke (unpublished data, laboratory of Prof. Stafforst, IFIB Tübingen) contain two CMV promoters followed by multiple cloning sites. In 2xTet plasmids, both CMV promotors are controlled by Tet-response-elements, whereas in 1xTet plasmids only the first insert is expressed in a tetracycline (or doxycycline) dependent manner.

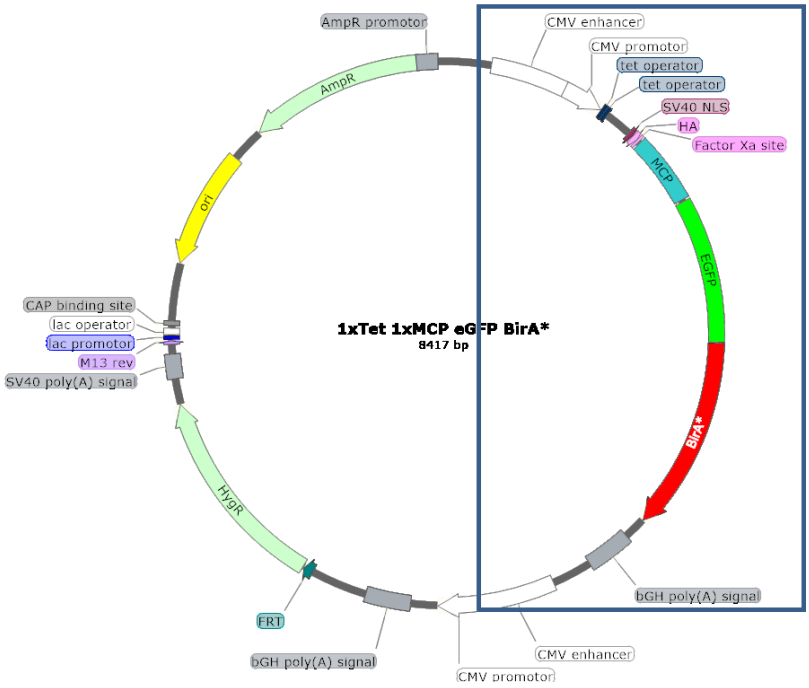

Fig. 7: 1xTet_1xMCP-eGF-BirA.*

The MCP-eGFP-biotin ligase construct integrated into pcDNA5 backbone. The blue box highlights the integrated fusion protein and its surroundings.

The other cell line used was the HeLa EM2-11ht cell line that is optimized for stable integration via recombinase mediated cassette exchange (RMCE). Instead of only one FRT site, they carry two heterologous recombination sites in their genome. Between them a target DNA sequence can be introduced. Figure 8 shows a typical vector for stable integration in HeLa 11ht cells, the two different FRT sites are highlighted in box 1 and 2. The cells as well as the psF3 vector were kindly given to the Jansen group from ZMBH Heidelberg. The cloning sites of the vector follow the bidirectional arranged promotors and tetracycline response elements. Each of the two is followed by a bovine growth hormone poly-A signal. The sequence of MCP-eGFP and MCP-eGFP-BirA* fusion proteins were integrated by Joyita Mukherjee (unpublished data, laboratory of Prof. Jansen, IFIB Tübingen,). The luciferase was already integrated and can be used as an expression reporter.

For integration into HeLa EM2-11ht, the same plasmid encoding the Flip recombinase as described above had to be cotransfected with the plasmid carrying the target DNA.

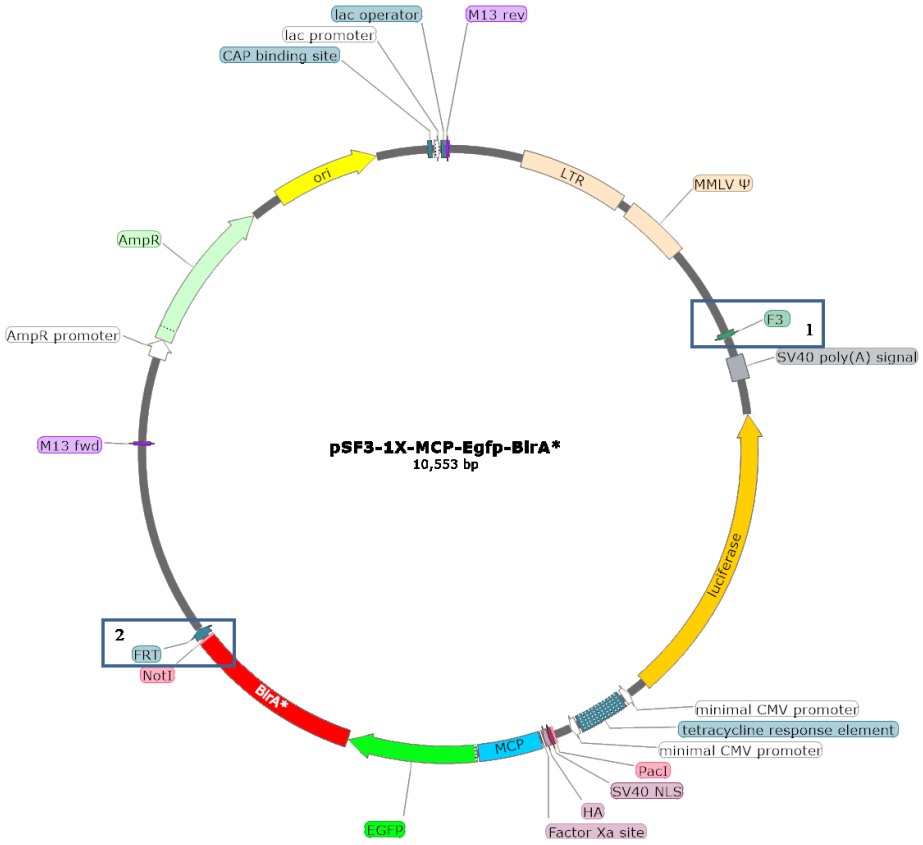

Fig. 8: Vector psF3_1xMCP-eGFP-BirA(RJP 2053).*
1xMCP-eGFP-BirA integrated in the psF3 backbone (created by Joyita Mukherjee). The boxes 1 and 2 show the two different FRT sites used for recombinase mediated cassette exchange in HeLa 11ht cells.*

The original Flp/FRT system used in U2OS cells is based on DNA insertion that works against thermodynamic and kinetic barriers. On the contrary, the RMCE works by exchanging DNA fragments instead of inserting one. It should therefore, at least theoretically, face lesser energetic hurdles which makes an insertion of the wanted DNA sequence into the genome of a target cell more likely to happen (reviewed in: Turan et al. 2011).

Cloning of mitochondrial phosphate carrier protein fusion with mCherry

For cloning of the sequence of the mitochondrial phosphate carrier protein (MPCP), RNA was extracted from HeLa S3 cells using the Nucleospin^{R} RNA extraction kit, following the large RNA purification protocol.

The MPCP cDNA was produced using the primer Q00325-2_backward (for sequence see appendix) and the Goscript^{R} reverse transcription kit in a sample volume of 20 µl per PCR tube. The thermocycler program for reverse transcription is shown in figure 9.

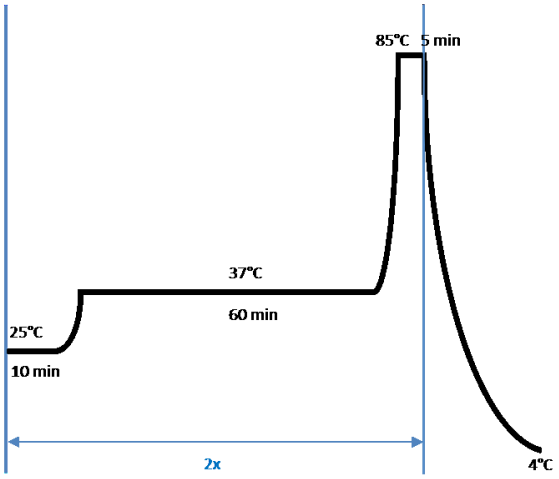

Fig. 9: Reverse transcription program for MPCP cDNA from HeLa S3 RNA with primer Q00325-2_backward.

The cDNA of the mitochondrial phosphate carrier protein was then amplified in a PCR. This time Q00325-2_backward and Q00325-2_forward (for sequences see appendix) were used as forward and backward primers, respectively. The PCR was set up with Herculase polymerase according to recommended composition. The PCR program and the gel electrophoresis of the amplification product are shown in figure 10.

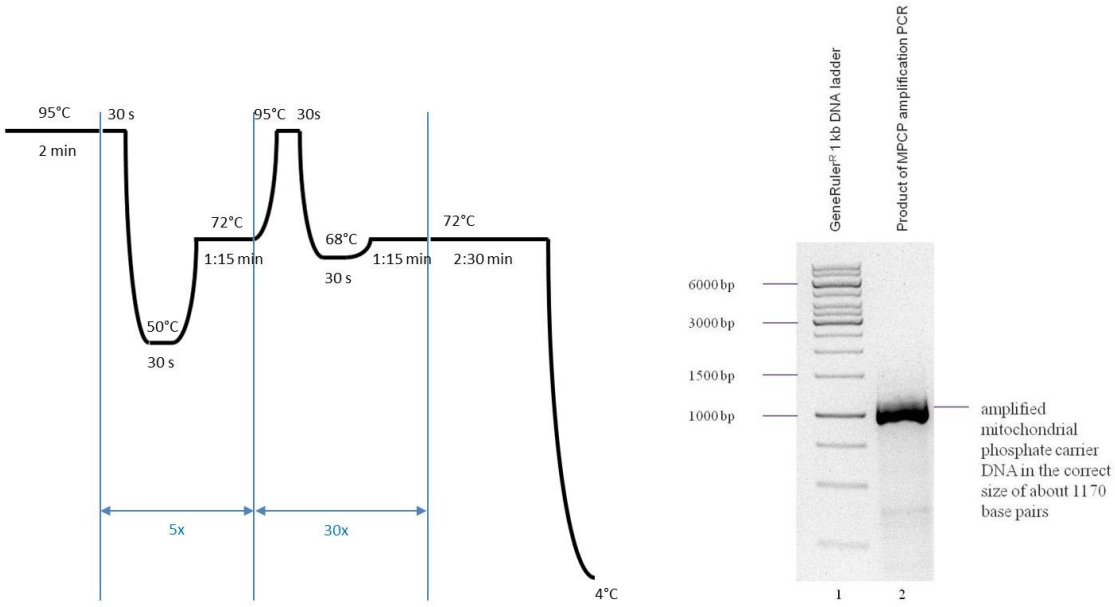

Fig 10: Amplification of mitochondrial phosphate carrier DNA.
Left: PCR program for amplification of mitochondrial phosphate carrier DNA. Right: Correctly amplified MPCP sequence (1171 base pairs).

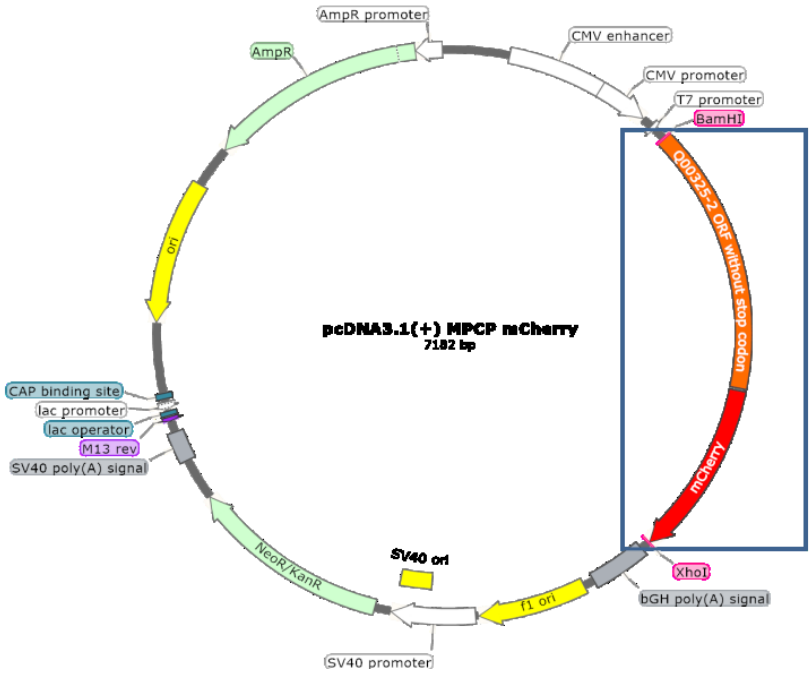

Fig. 11: The final plasmid map of Mitochondrial Phosphate Carrier Protein in frame with mCherry in a pcDNA3.1. backbone that was transfected into HeLa S3 cells.

The chosen primers help to introduce the restriction sites for BamHI and NotI at the beginning and the end of the MPCP ORF. The amplified product was ligated with restricted RJP 1987 that encodes the mCherry fluorescent protein. Therefore, the PCR product was cleaned using the Nucleospin^{R} Easypure gel and PCR cleanup kit. RJP 1987 as well as the MPCP PCR product were digested overnight with BamHI and NotI fast digest enzymes from Fermentas in the recommended buffer "Green". The digested DNA samples were purified by agarose gel electrophoresis and the correct bands were isolated using the PCR and gel cleanup kit. The ligation was performed with T4 DNA ligase in its provided buffer for 2 hours at room temperature. Vector and insert were used in at 1:5 ratio with 30 ng digested plasmid and 150ng of insert DNA. After ligation 50 µl of competent *E.coli DH5α* were directly added to the ligation mix for transformation via heat shock protocol. A set of colonies were amplified and tested via plasmid digestion for the correct insert size, one plasmid was sequenced to verify the correct integration and sequence. The final plasmid map is shown in figure 11.

2.2.2. Cell culture

HeLa S3

HeLa cells, widely used for scientific research, are human cervical cancer cells. The immortal cell strain was already cultured for about five years when Puck and Fisher (Puck and Fisher 1956) described subpopulations of cells with different growth behavior dependent on the preconditions. The S3 cell line was used for transient transfection experiments.

The cells were cultivated in DMEM with 10% heat-inactivated FBS and 1% penicillin/streptomycin. Since they grow adherently, they were kept in 75 cm² (10ml of medium) or 150 cm^2 (20 ml of medium) tissue culture flasks. These were incubated at 37°C and under 10 % CO_2 conditions in the incubator's atmosphere. The medium was changed every second to fourth day depending on the cell number in the flask.

When grown confluent, the cells were splitted in a dilution of 1:5 with fresh medium. After removing the old medium, the cells were detached by incubating them for 3 min at 37°C with 5 ml of 1x trypsin solution. The enzyme was then inactivated by adding an

equal amount of DMEM with 10%FBS. The cell suspension was transferred into a 50 ml Falcon tube and centrifuged at 2000 rpm for 5 min. The supernatant was discarded and the cells were resuspended in 5ml of growth medium. 1 ml was transferred into a new tissue culture flask with the according amount of fresh medium (if splitting the cells into a new flask of different size the cell amount must be adjusted).

For fluorescence microscopy the cells were counted to select an optimal number. For this 20 µl of the resuspended cells were mixed with the same amount of Trypan blue staining. Living cells were counted using a hemocytometer. The cell suspension was then diluted to the required concentration so the accurate cell number could be splitted.

To store the cells for a longer time, they were frozen in liquid nitrogen. Therefore, the cells were also detached, resuspended and counted. The cells then were pelleted at 2000 rpm for 5 min and diluted in DMEM with 9% FBS and 10% DMSO to a concentration of 10^6 cells per ml. They were distributed in 1ml aliquots into cryogenic tubes. The tubes were phased cooled by keeping them 30 min at 4°C, 30 min at -20°C, 2 – 8h at -80°C before finally storing the stocks in liquid nitrogen.

To avoid toxic effects of DMSO, cell stocks must be thawed quickly. They were transferred from the liquid nitrogen into a prewarmed water bath at 37°C. Immediately after thawing they were placed into a centrifuge and pelleted at 2000 rpm for 5 min. The medium was discarded, the cells were resuspended in growth medium and placed into a 75cm^2 tissue culture flask. They had to be cultured for at least two passages to recover from the stress and normalize their biochemical behavior.

HeLa EM2-11ht

The HeLa EM2-11ht cell line was designed and characterized by Weidenfeld and colleagues in 2009. Any gene can be stably inserted into the genome of this cell line. The designers have shown that the insertion site can be retargeted and that, after successful insertion of a gene, it contains a single copy of it per cell. Moreover, the transcription of the inserted genes is regulated by the addition of tetracycline or doxycycline (Weidenfeld et al. 2009).

The HeLa 11ht cells were usually grown in DMEM with 10% FBS. The cell line needs 200 µg/ml Hygromycin B and 200 µg/ml G418 in the medium for selection to keep the

FRT sites for recombinase-mediated cassette exchange. Stocks were prepared under the same conditions as described for HeLa S3 cells.

For stable integration, the cells were grown in 10 cm dishes and transfected with the plasmids encoding the Flip recombinase and the target DNA sequence in a ratio of 1:1 (2 µg per plasmid were used) using Fugene transfection reagent and following the according protocol.

For efficient recombination, the cells were grown for 1-2 days in medium containing only G418 before changing to medium that also contains 50 µM Ganciclovir. The cassette surrounded by FRT sites on the psF3 plasmid encodes a Ganciclovir-resistance gene, therefore a strict selection for the recombinant cells was possible. The cell clones producing the eGFP or eGFP-BirA* fusion protein were grown in 10 cm plates and subsequently transferred in 75 cm^2 and 150 cm^2 tissue culture flasks. To select cells with similar eGFP expression upon induction, the cell clones were seeded in 10 cm dishes, induced in medium containing 1 µg/ml doxycycline for 24h and sorted by FACS (performed by Cornelia Grimmel, FACS Core Facility of Tübingen university), the specific details of the sort are shown in the appendix.

Due to frequent contamination even of the cell stocks, this cell line was several times screened for mycoplasma infection by PCR from a whole cell lysate, but the expected bands indicating presence of mycoplasma could not be detected. However, plating medium of the cells on LB plates gave positive results in growing colonies, therefore a bacterial contamination has to be suspected. Because contamination could not be eradicated even by adding penicillin and streptomycin to the medium as for the HeLa S3 cells, the cell line was left for working with U2OS cells in later experiments.

U2OS – T-Rex

U2OS is a human cancer cell line that was derived by Ponten and Saksela in 1964 as 2T cells. The original tumor was a moderately differentiated osteosarcoma of the tibia (Ponten and Saksela 1967). Nowadays, it is a cell line widely used in scientific research. The U2OS T-Rex cells were a kind gift from Alfred Hanswillemenke (laboratory of Prof. Stafforst, IFIB Tübingen) together with the pcDNA 5 vectors containing Tet-response elements designed by himself. The genome of U2OS T-Rex cells carries a

single FRT site that allows integration of a gene using a FLP recombinase (Gordon et al. 2009).

Native U2OS cells were grown in DMEM with 10 % heat-inactivated FBS, 15 µg/ml Blasticidin S and 100 µg/ml Zeocin under the same incubation conditions as HeLa cells (see above). Also the splitting and storage of U2OS cells follow the same protocol as the one of HeLa cells.

For stable integration of a desired sequence the osteosarcoma cells were seeded into 6-well plates $1x10^5$ cells per well. For transfection the medium was changed to DMEM with 5% FBS. 4 µg of *pOG44* (encoding the Flip-recombinase) and 2µg of carrier plasmid were transfected per well. I used Fugene HD transfection reagent in a ratio of 1:3 (which means 18µl per well) according to the company's protocol. The transfection complex was prepared in Opti-MEM medium and then added to the cells. The plates were tilted carefully and then incubated for 6 h. Afterwards, the U2OS cells were washed once with DMEM containing 10% FBS and incubated overnight in medium of the same composition. After 24 h it was withdrawn from the plates and replaced by selection medium that contains 100 µg/ml Hygromycin B instead of the Zeocin. The medium was changed every second day until the forming colonies reached a diameter of approximately 3 to 5 mm. Then the cells were grown in 10 cm dishes.

To standardize the eGFP expression between the cells, they were seeded in 10 cm plates and induced with 1µg/ml doxycycline for 24h. Afterwards, cells were detached, washed twice with PBS and re-diluted in FACS buffer. The cells were sorted into a 6-well microscopy plate by FACS (performed by Cornelia Grimmel, FACS Core Facility of Tübingen university), the FACS details can be found in the appendix.

2.2.3. Laboratory methods

Fractionation protocol by Kaltimbacher et al. (2006)

The subcellular fractionation was performed with the HeLa S3 and 11ht lines. When the cells were grown confluent, they were detached with trypsin solution and washed once with PBS. After centrifugation of approximately $6x10^7$ cells at 2000rpm for 5 min, the supernatant was discarded and the cells were resuspended in 2ml of homogenization buffer (see Appendix for composition). The cells were homogenized with 15 strokes in

a dounce glass homogenizer. The lysate was centrifuged again in a 15 ml Falcon tube at 1000 x g for 8 min at 4° C. To release the mitochondria from the unbroken cells, the pellet was resuspended as suggested and homogenized with another 25 strokes. Before repeating the centrifugation a 20 µl aliquot (whole cell lysate) was removed for the western blots. To pellet the membrane fraction and unbroken cells, the lysate was centrifuged again at 1000 x g for 8 min at 4° C. As suggested in the protocol, the mitochondria were pelleted by centrifugation at 12000 x g for 30 min at 4° C and then washed four times with homogenization buffer.

Modified fractionation protocol according Frezza et al. (2007)

This protocol was performed with HeLa 11ht cells grown until they covered the surface confluently. The cells were detached with trypsin as described above. Detachment was stopped by adding FBS containing medium. The cells were re-diluted in PBS for counting and then pelleted at 600 x g for 10 minutes. The pellet was resuspended in 500 µl of ice-cold IB_C buffer (see appendix for composition) and transferred into a glass potter. The suspension was treated with 50 strokes with a teflon pestle before transferring it into a 1.5ml microcentrifuge tube and centrifuged at 600 x g for another 10 minutes for pelleting the membrane fraction.

The supernatant was transferred into another tube and spun at 7000 x g and 4° C for 10 minutes to pellet the mitochondrial fraction. This was washed 3 times with 50 µl of IB_C buffer with another centrifugation at 7000 x g at each step.

Cell dissection protocol by Shaiken et al. (2014)

U2OS cells were grown confluently and detached using trypsin solution. After centrifugation they were washed one time using PBS. Two times the packed cell volume of buffer A (see appendix for composition) was added to the cell pellet and it was left rotating at 4° C for 30 min for cell lysis. The nuclei were pelleted by centrifugation at 1000 x g 4° C for 5 minutes, the supernatant was centrifuged again at 10000 x g for 10 minutes to pellet the perinuclear fraction. The only fraction left in the supernatant should be the cytosolic one containing also the mitochondria.

Blotting experiments

All western blots were performed after SDS polyacrylamide gel electrophoresis (PAGE) using gels which composition can be found in the appendix. The PAGE was usually run at 110 V for 1 h to maximum 1.5 h.

The western blot transfers were performed by tank blotting. The PVDF membrane was activated in methanol shortly before use, washed twice in distilled water and briefly stored in cold Towbin buffer (for composition see appendix). The gels were also washed in Towbin buffer. For protein transfer the electric field was held at a constant voltage. The blots were run at 36 V for 16 h at 4° C.

After transfer the membranes were blocked with 5 % BSA in TBS for 1 h at room temperature or at 4 °C overnight. Following, the blots were washed 3 times for 5 minutes at room temperature with TBS-T 0.1 %. The biotinylated proteins were labeled with streptavidin bound alkaline phosphatase that was incubated with the membranes same as the primary antibodies (see below). For development, staining buffer (see appendix for composition) as well as 50 µl of BCIP (final concentration 150 µg/ml) and NBT stock solutions (final concentration of 300 µg/ml) were added to the membranes and the blots were developed at room temperature.

Protein tags like GFP and FLAG were detected using corresponding rabbit or mouse antibodies. The membranes were also blocked with 5% BSA and washed with TBS-T. The primary antibody were incubated with the membranes for 1 h at room temperature or at 4 °C overnight. The antibody solution was discarded and the after a second round of TBS-T washes, the secondary antibodies for Near Infrared Imaging (using Li-Cor Odyssey) were incubated the same way as the primary ones. Before imaging, the membranes again were washed in TBS-T.

Relative quantification of western blots was performed with ImageJ following the protocol of Luke Miller (https://lukemiller.org/index.php/2010/11/analyzing-gels-and-western-blots-with-image-j/, latest access 23rd of March 2020).

Microscopy

For fluorescence microscopy experiments, 20000 cells were seeded per chamber in 4-well microscopy dishes one day before beginning of the experiment.

Transient transfection of HeLa S3 cells was performed the following day. Vectors encoding MCP-eGFP constructs with or without BirA* were transfected either alone or simultaneously with *SOD2MS2*. The transfections were performed with FuGene^{R} transfection reagent according to the provided protocol at a ratio of 5:1 or 3:1. Although the transfection complex was initially incubated on the cells for a maximum time of 24 h, the transfection time was reduced in later experiments to decrease cell toxicity. In this case medium was changed to normal growth medium until the next day. At this day the cells were stained with Mitotracker^{R} Deep Red before performing microscopy.

For microscopy of the mitochondrial phosphate carrier protein with mCherry fusion protein, the cells were transfected with different concentrations of pcDNA3.1 MPCP mCherry plasmid (see chapter 2.2.1.) per well, again using FuGene transfection reagent. The cells were stained with Mitotracker^{R} Green.

For microscopy of cell lines with stably integrated biotin ligase constructs, the cells were treated similarly. The SOD2MS2 plasmid was transfected the day before microscopy. The eGFP-containing fusion protein will be transcribed only in presence of tetracycline (see plasmid maps in chapter 3.2.1.), therefore the medium was changed after 12 hours and transcription was induced by adding doxycycline containing medium.

Preparation of mass spectrometry samples for mRNA interactome

For mass spectrometry 1x10^{6} U2OS$_{1xMCP\text{-}eGFP\text{-}BirA*}$ cells were seeded in a 10cm dish and incubated overnight in selection medium. The transfection complex of 10 µg of *SOD2MS2* plasmid with 30 µl FuGene^{R} transfection reagent was prepared in 400 µl Opti-MEM medium. Subsequently it was added on the cells that were maintained for transfection in a total volume of DMEM with 5% FBS without antibiotics. The transfection was performed over 12 h, then the medium was changed to the U2OS selection medium. The cells were left to recover for another 12 h. Following, the biotin ligase production was induced by changing the medium to medium containing 10 ng/µl doxycycline and 50 µM biotin. For preparation of the last sample and control pair, the transfection was performed in medium with 8 µg/ml protamine to increase the number of transfected cells.

After 16 h the cells were washed twice with DPBS and then detached with 4 ml trypsin solution per plate for 3 minutes. Detaching was stopped by adding DMEM with 5%

FBS. After centrifugation at 2000 rpm for 5 minutes the cells were washed in 10 ml DPBS by resuspension. Following another centrifugation the U2OS cells were resuspended in 1 ml PBS and transferred into a 1.5 ml microcentrifuge tube. This again was followed by centrifugation at 2000 rpm for 5 minutes.

The cells were resuspended in 0.5 ml of lysis buffer and passaged 30 times through a 21G needle. The suspension was then centrifuged at maximum speed and 4 °C for 10 minutes to pellet the membrane fraction.

The protein concentration in the supernatant was measured using a Bradford assay. Since the experiments produced only low amounts of protein, the complete samples beside 20 µl were loaded onto the prepared beads. Before loading the proteins the magnetic beads (100 µ per sample) used for capturing the biotinylated proteins were washed in lysis buffer (for buffer composition see appendix) at room temperature twice for 5 minutes.

After addition of the samples to the beads, they were incubated rotating at 4 °C overnight. The next morning the supernatant was removed and the beads were washed once with 300 µl bead wash buffer 1, wash buffer 2 and wash buffer 3, followed by washing 3 times in buffer 4 (for detailed composition see appendix). The beads were resuspended in 500 µl of ABC buffer. 25 µl were kept at -20 °C for the western blotting, the rest of the beads were stored at -80 °C until they were used for mass spectrometry (performed by Dr. Mirita Franz-Wachtel, Proteome Center of Tübingen University).

Proteins were considered to be enriched if they were found twice as often in the samples as in the controls. For that, the arithmetical mean of the frequencies of samples and controls were compared. The properties of the captured and identified proteins, especially corresponding to their localization and RNA-binding, were extracted from the Uniprot database (https://www.uniprot.org/, latest access 05th of May 2020).

3. Results

3.1. Validation of RNA-BioID on $SOD2_{MS2}$ mRNA in transiently transfected HeLa S3 cells

First experiments where performed by transiently transfecting HeLa S3 cells. The cells were transfected either with *BirA*$_{tt}$* and *SOD2MS2* simultaneously or only with *SOD2MS2* for western blots.

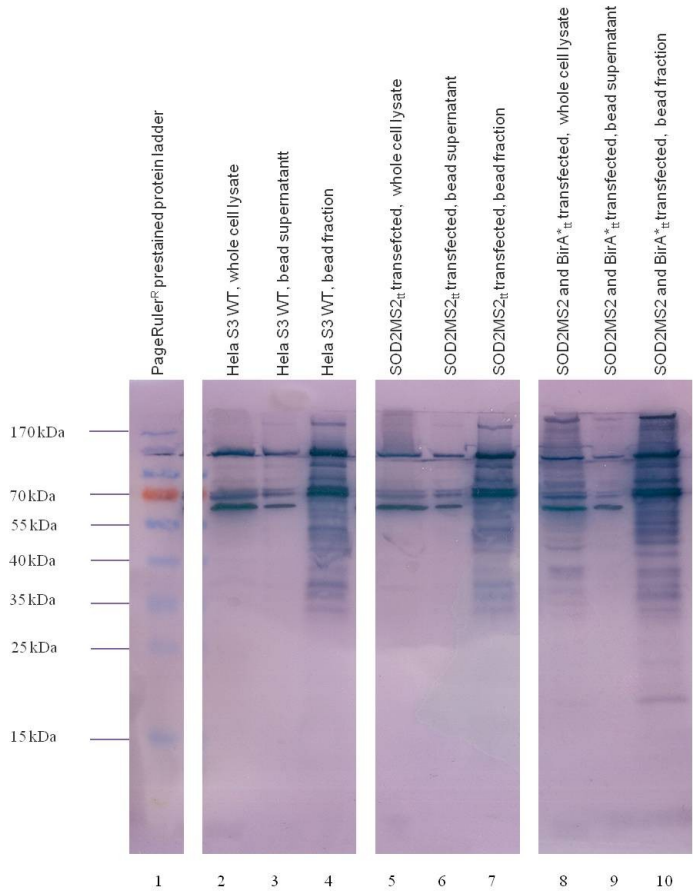

Fig. 12: Western blot against biotinylated proteins in transiently transfected HeLa S3 cells.

In the lanes 2, 5 and 8 the whole cell lysate of each population is shown. The biotinylated proteins were enriched using Streptavidin-beads. Lanes 3, 6 and 9 show the supernatants and lanes 3, 6 and 9 the bead fractions of the according lysate.

The correct expression of the construct was checked using different ways. The expression of a functional biotin ligase was detected indirectly via changes in the biotinylation pattern of cellular proteins in whole cell lysates.

The cells were grown in 50 µM biotin containing medium. Only the cells transfected with plasmid *BirA*$_{tt}$* show an expanded biotinylation pattern in whole cell lysates (compare lane 8 to 2 and 5) as well as in the streptavidin-bead captured fraction (compare lane 10 to 4 and 7). Cells only transfected with the artificial *SOD2MS2* vector show a biotinylation pattern similar to untransfected cells (compare lanes 5 to 7 with lanes 2 to 4).

Upon expression, the fusion protein containing the biotin ligase BirA* does not only produce a more intense signal in the western blot, but also leads to a change in the protein pattern. For example, in the cell population transfected with *BirA*$_{tt}$* a band between 15 and 25kDa (see streptavidin-bead enriched fraction of cotransfected cells in lane 10) as well as two additional ones (see lane 8) with a size of over 130 kDa appear.

Thus, the expression and function of the biotin ligase can be deduced from this blot.

In addition, the successful enrichment of biotinylated proteins by using streptavidin magnetic beads (see lanes 4, 7 and 10) compared to the whole cell lysates (see lanes 2, 5 and 8) could be demonstrated.

Next, the expression of the second component of the fusion protein, eGFP, was checked by western blot. eGFP expression was detected using an anti-GFP rabbit primary antibody and anti-rabbit secondary antibody coupled to a near-infrared (680 nm) fluorescent dye, using the Odyssey Near-Infrared Fluorescence detection system. The blot is shown in figure 13.

As expected there is no expression of GFP in the wildtype cells (see lines 2 to 4) or in the population that was only transfected with *SOD2MS2* (see lanes 5 to 7). On the opposite, the GFP containing product can be found in the lysate of *BirA*$_{tt}$* transfected cells (see lanes 8 to 10). Furthermore the size of the detected protein corresponds to the expected product size of about 90 kDa which demonstrates that the construct is expressed in its full size. Moreover, since the protein is enriched in the bead fraction, the biotin ligase is likely to biotinylate itself as well as its surroundings.

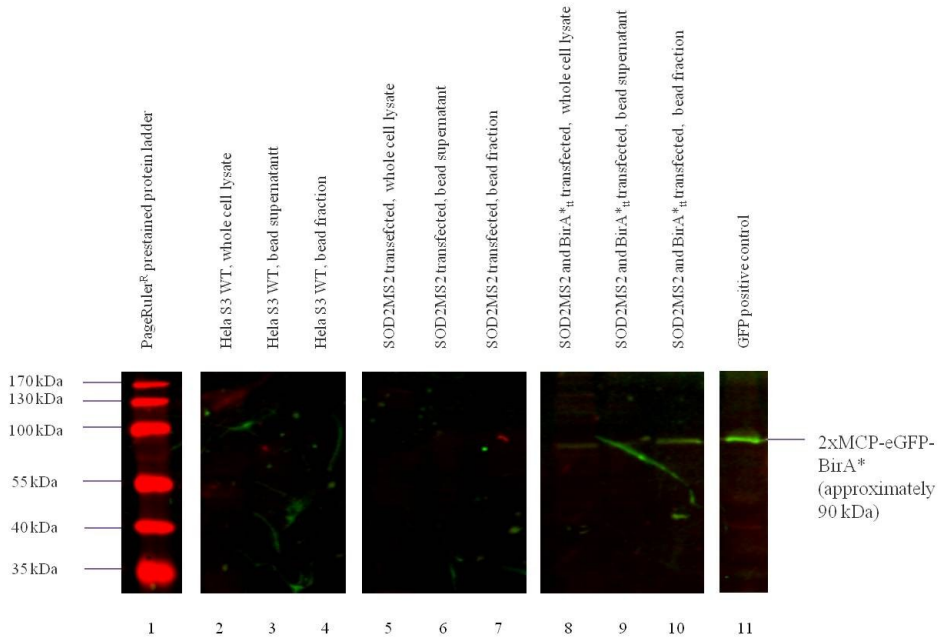

Fig. 13: Western blot against GFP in transiently transfected HeLa S3 cells.
The depicted cell lysates were arranged as described in figure 12. In the HeLa cells transfected with BirA$_{tt}$ (lanes 8 to 10) the GFP unit could be detected. The fusion protein can be detected in the the bead supernatant as well as in the bead-bound fraction (lane 10).*

The SOD2$_{MS2}$ protein encoded on *SOD2MS2* was tagged with a FLAG-tag. Therefore the expression and the correct product size could also be detected by western blotting. This was performed with a mouse anti-FLAG primary antibody and anti-mouse secondary antibodies coupled to a near-infrared (800 nm) fluorescent dye. The results are shown in figure 14.

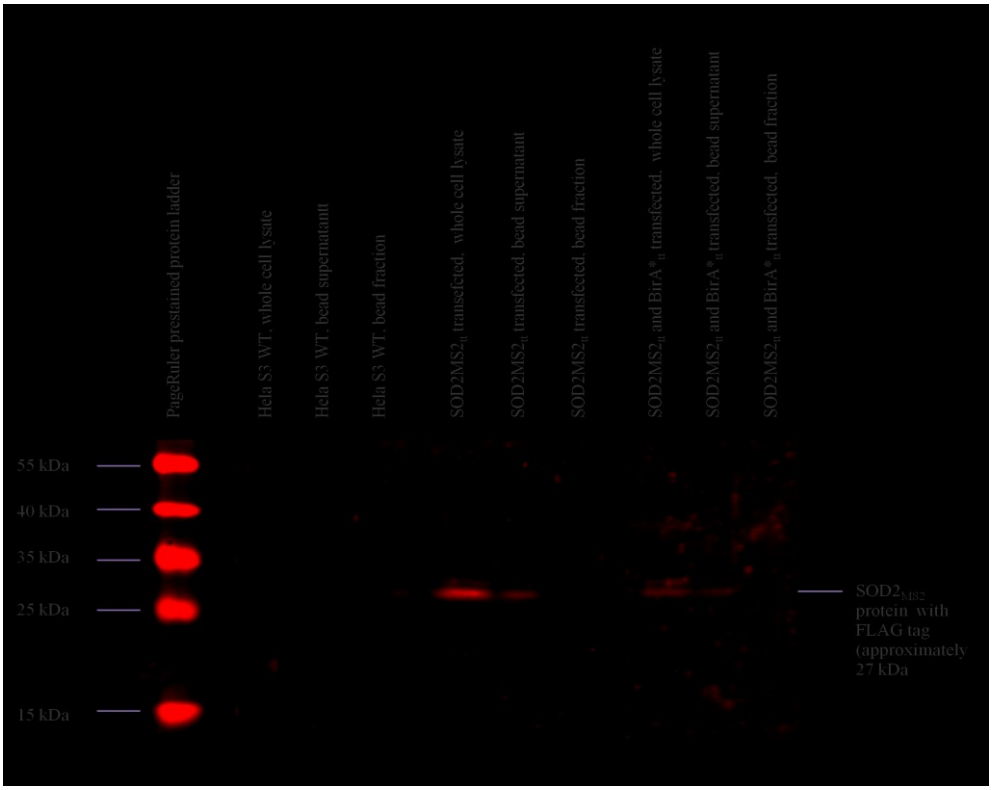

Fig. 14: Western blot against FLAG in transiently transfected HeLa S3 cells. Lysate arrangement as described in figure 12. In the lanes 5 to 7 and 8 to 10 lysates from cell samples transfected with SOD2MS2$_{tt}$ are blotted. The correct expression of the tagged SOD2 with its correct protein size of approximately 27 kDa is demonstrated.

In the cell populations transfected with SOD2MS2 the artificial SOD2$_{MS2}$ is expressed in the correct size of approximately 27 kDa. Interestingly enough the FLAG-tagged SOD2$_{MS2}$ is missing in the protein fraction that binds to the Streptavidin beads (lanes 7 and 10) even in the presence of BirA* fusion protein in the cells (lane 10). The BirA* bound mRNA and the resulting SOD2$_{MS2}$ protein are parts of the same translation process, therefore it does seem likely that the protein should be biotinylated during translation. The absence of SOD2$_{MS2}$ in the bead fraction might indicate a shielding of the protein from BirA* activity due to a cotranslational import, but could also be the effect of a sterical shielding through ribosomal proteins. However, it also has to be considered that the contact time between RNA and SOD2$_{MS2}$ protein is simply to short for an efficient biotinylation.

Next it had to be tested whether the binding of MCP to the MS2 loops is working in the HeLa S3 cells. This could be easily done using the eGFP part of the fusion protein and fluorescence microscopy.

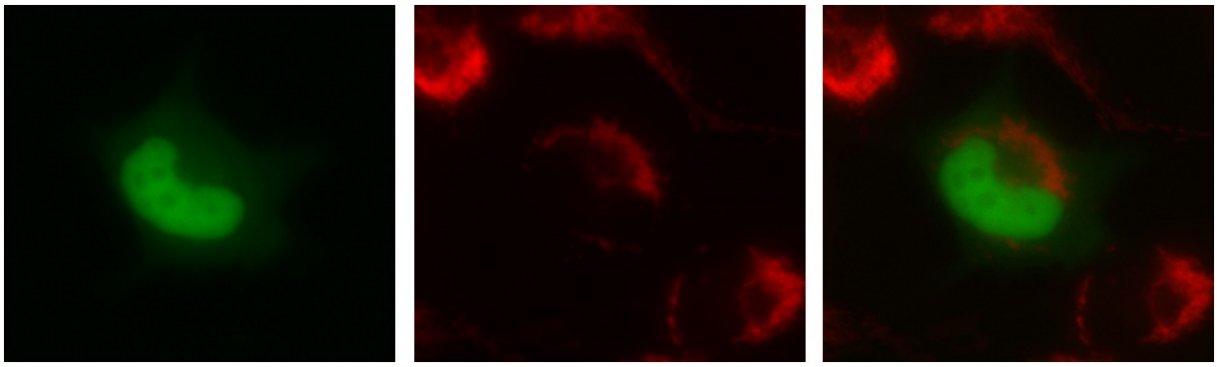

Fig. 15: Distribution of eGFP signals in a HeLa S3 cell transfected only with the vector BirA$_t$ encoding 1xMCP-eGFP-BirA* fusion protein.*
Left: Due to the NLS the eGFP-containing fusion protein is found mainly in the nucleus with a weaker background signal in the cytoplasm. The middle picture shows the distribution of mitochondria in the cell that are stained by Mitotracker^R Deep Red. Right: Merged image.

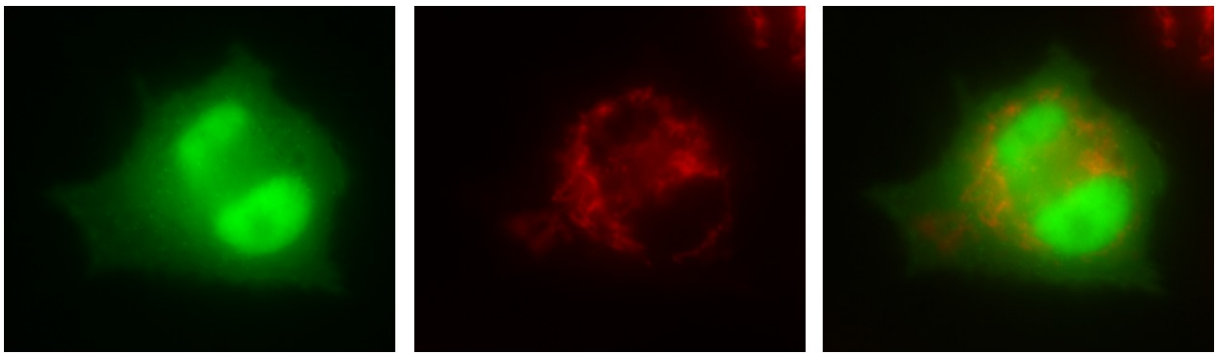

Fig. 16: Distribution of eGFP signaling in HeLa S3 cells simultaneously transfected with the plasmids BirA$_t$ and SOD2MS2.*
Middle: Mitochondria stained with Mitotracker^R Deep Red. Left: Although the cytoplasmic background signal of eGFP is high in this cell, small eGFP-spots can be detected within the cytoplasm. They likely represent the fusion protein bound to RNA particles that travel through the cell. Right: Merged.

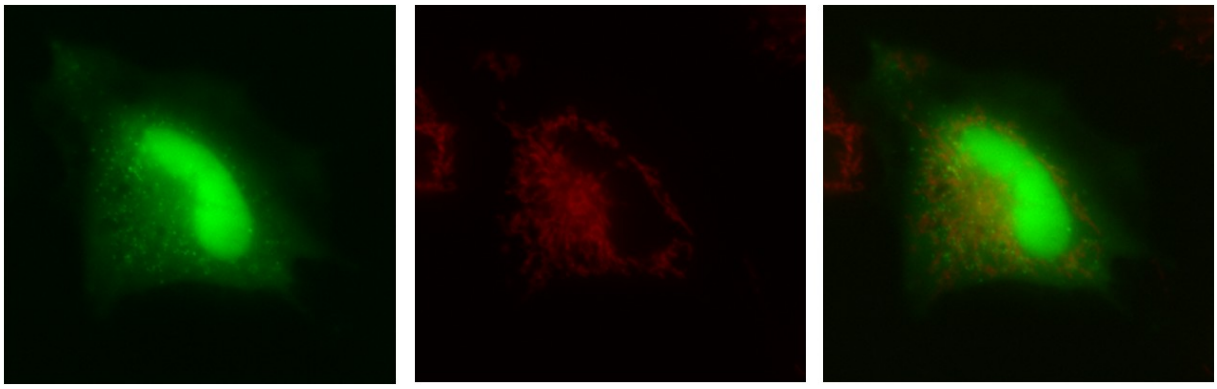

Fig. 17: HeLa cell transfected with BirA$_{tt}$ (encoding 2xMCP-eGFP-BirA* fusion protein) and SOD2MS2.*
Left: Even the bigger protein containing two MS2 coat structures leaves the nucleus with the MS2-containing mRNA and can be detected as eGFP containing granule in the cytoplasm. Middle: Mitochondria stained with Mitotracker^{R} Deep Red. Right: Merged image. The granules seem to locate mainly around the mitochondria.

Figure 15 shows that the eGFP signal of the fusion protein in cells transfected only with the biotin ligase plasmid is restricted to the nucleus with low cytoplasmic eGFP signal. This distribution was expected due to the added nuclear localization sequence in the front of the protein.
The one or two MCPs included to the fusion protein enable it to bind to MS2 loops of the bait SOD2$_{MS2}$ mRNA. Cells co-transfected with *SOD2MS2* and *BirA*$_{t}$* or *BirA*$_{tt}$* are shown in figures 16 and 17. Besides the diffuse nuclear eGFP signal, eGFP spots in the cytoplasm and around the mitochondria can be detected that likely represent the fusion protein bound in the RNA granules.

3.2. Subcellular fractionations

Since the aim of the project was to identify proteins from the mitochondrial fraction that can be labeled by an RNA-associated biotin ligase, it could be beneficial to enrich mitochondrial proteins in the samples used for mass spectrometry. There are different protocols available to perform such a subcellular fractionation.
Various protocols for subcellular fractionation were compared, using a mitochondrial marker protein (TOM20) and a cytoplasmic (GAPDH) as well as a nuclear (Lamin A/C)

protein as controls. For all performed western blots the protein amount per fraction was measured with a Bradford assays and equal amounts of protein were loaded per lane. Quantification was performed relatively to the summarized signal of all quantified bands according to the protocol of Luke Miller (https://lukemiller.org/index.php/2010/11/analyzing-gels-and-western-blots-with-image-j/, latest access 23rd of March 2020).

The protocol developed by Kaltimbacher et al. (2006) shows hardly any increase in TOM20 concentration in the final mitochondrial fraction as compared to the lysate, as shown in figure 18.

Protocol according to Kaltimbacher et al. (2006)

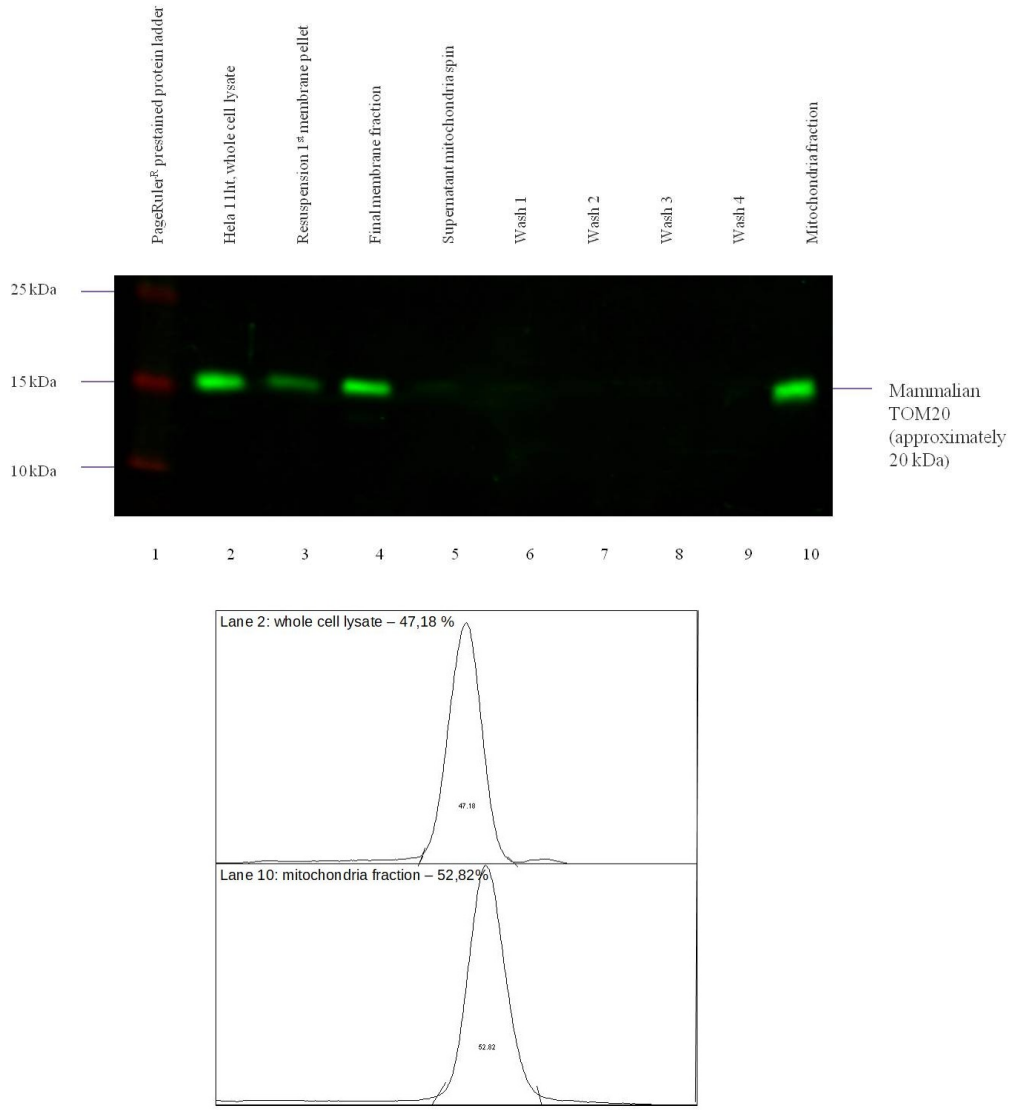

Fig. 18: Subcellular fractionation according to Kaltimbacher et al. (2006). Western blot against mammalian TOM20.

Top: Blot membrane. Bottom: Quantification of lane 2 (whole cell lysate) and lane 10 (final mitochondrial fraction). In the mitochondrial fraction (lane 10) only a slightly higher concentration (52.82% of the summarized signal) of this TOM20 can be detected than in the whole cell lysate (lane 2). Therefore, the enrichment of mitochondrial proteins in this fraction is not as high as expected.

In addition, the cytosolic control protein GAPDH is also enriched in the mitochondrial fraction, as shown in figure 19. Thus, the fractionation might not fulfill the aim to cleanly separate a mitochondrial fraction from cytosolic components.

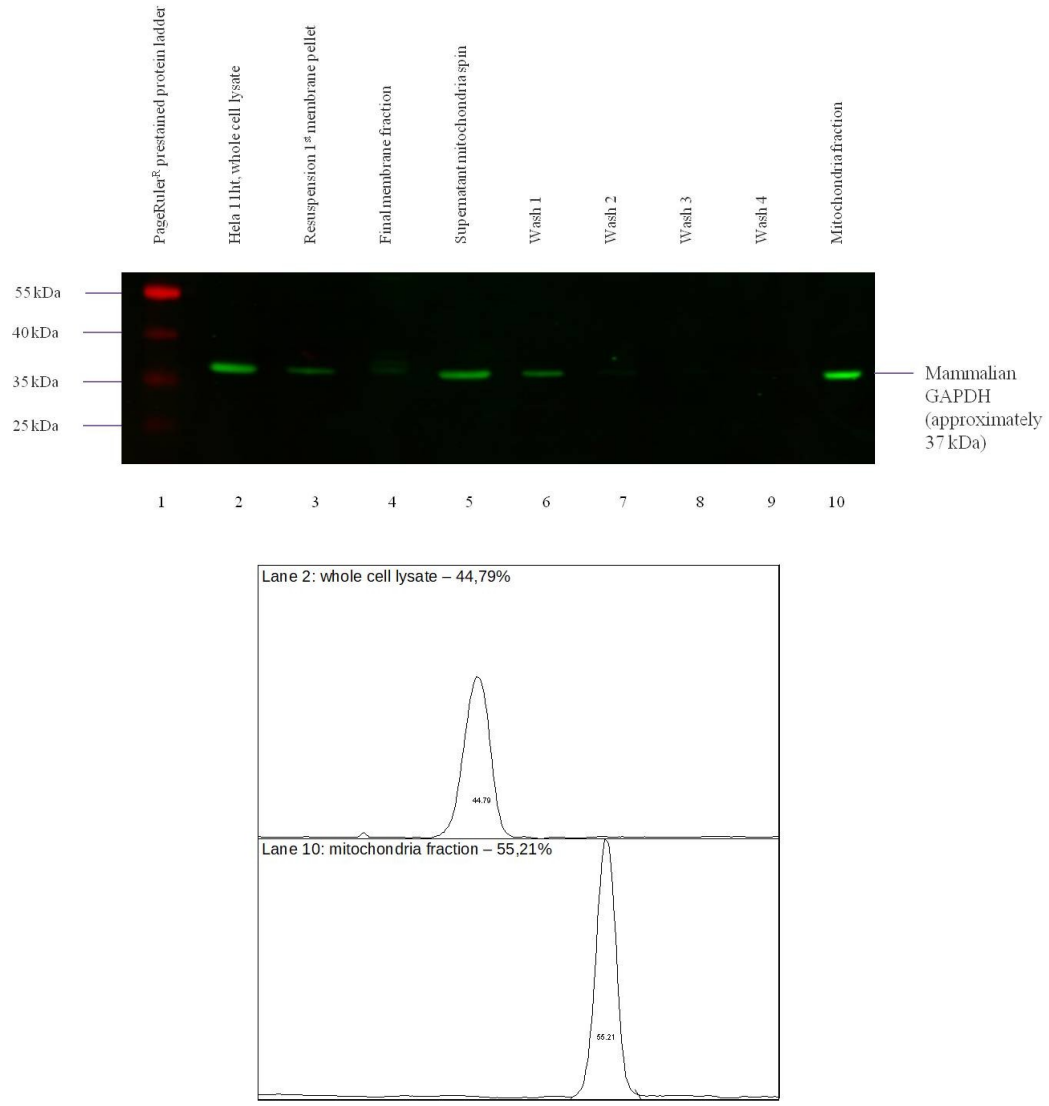

Fig. 19: Subcellular fractionation according to Kaltimbacher et al. (2006). Western blot against mammalian GAPDH, a cytosolic protein.
Top: Blot membrane. Bottom: Quantification of lane 2 (whole cell lysate) and lane 10 (mitochondrial fraction). The mitochondrial fraction (lane 10) shows even a higher concentration of GAPDH than the whole cell lysate (lane 2).

Protocol according to Frezza et al. (2007)

In figure 20 the enrichment of TOM20 using the subcellular fractionation protocol of Frezza and his colleagues (Frezza et al. 2007) is demonstrated by western blotting. A portion of mitochondria gets lost with the initial membrane fraction (see lane 3), but the final mitochondrial fraction shows a stronger TOM20 signal than the whole cell lysate – clearly indicating an enrichment. However, there is a detectable loss of TOM20 during the washing steps. Therefore, the protocol results in an increased enrichment of mitochondrial proteins, but a decreased protein amount.

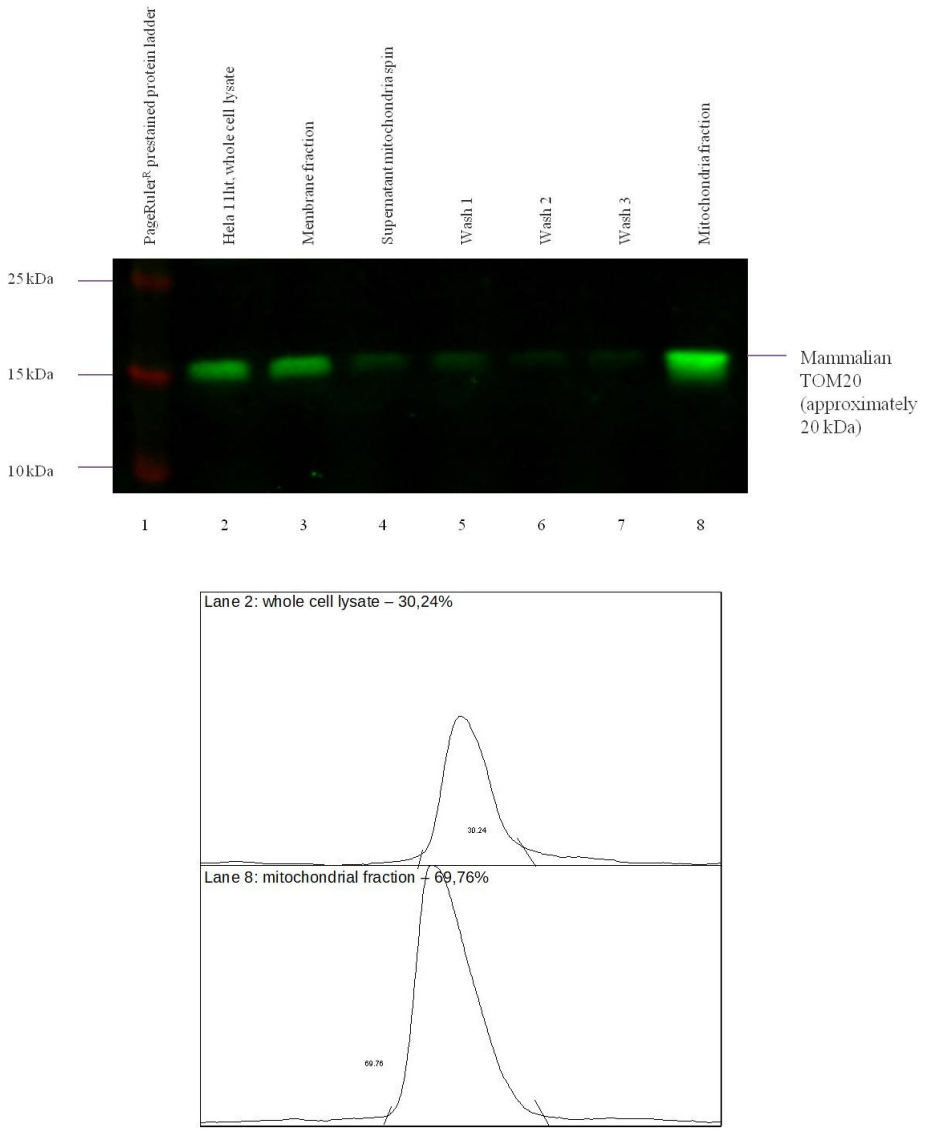

Fig. 20: Subcellular fractionation according to Frezza et al (2007). Western blot against mammalian TOM20.

Top: Blot membrane. Bottom: Quantification of lane 2 (whole cell lysate) and lane 8 (final mitochondrial fraction). Throughout every fractionation and washing step (lane 3 to 7) a loss of mitochondrial protein could be detected. However, the protocol results in an enrichment of TOM20 in the final mitochondrial fraction (almost 70% of the summarized signal of lane 2 and 8).

Shown in figure 21 is the GAPDH distribution in the fractions when using this protocol. In the mitochondrial fraction GAPDH is clearly reduced compared to the whole cell lysate (compare lanes 2 to 8 and quantification), but still well detectable. However, the reduction of GAPDH in the mitochondrial fraction is definitely an advantage compared to the protocol described above.

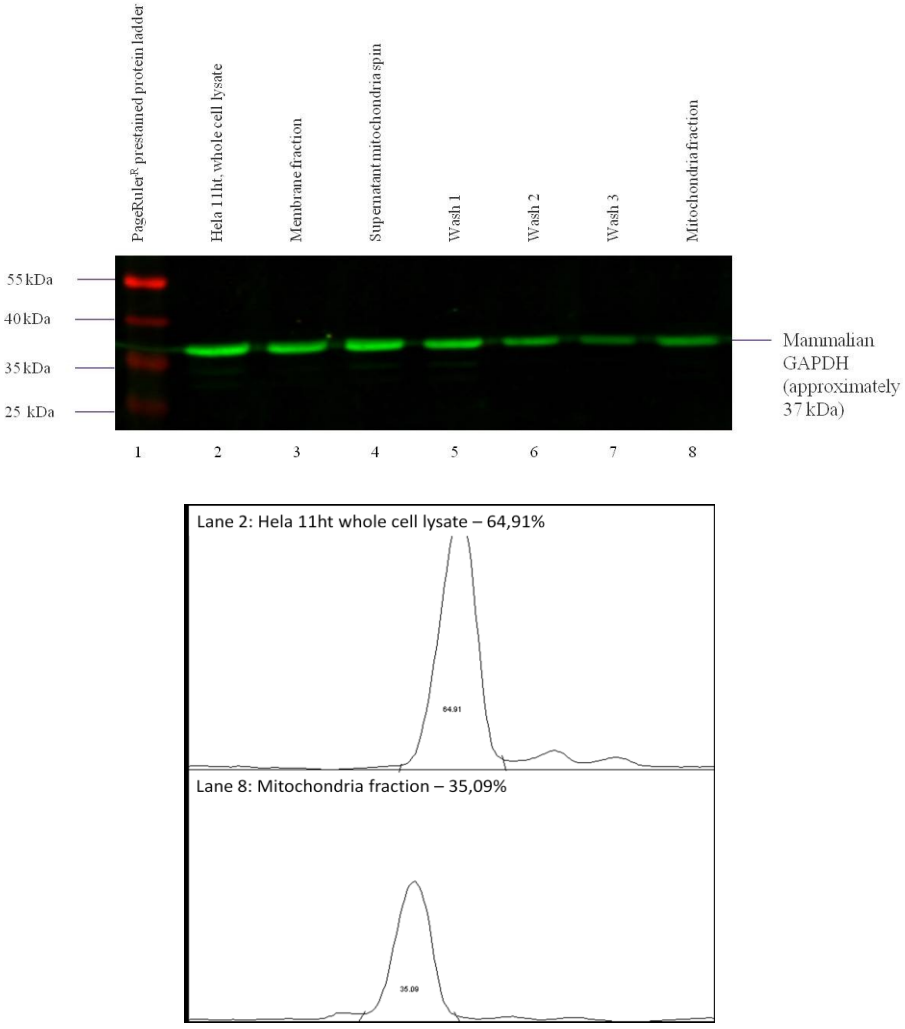

Fig. 21.: Subcellular fractionation according to Frezza et al. (2007). Western blot against mammalian GAPDH.

Top: Blot membrane. Bottom: Quantification of lane 2 (whole cell lysate) and lane 8 (mitochondrial fraction). The mitochondrial fraction (lane 8) still shows a significant contamination with cytoplasmic GAPDH (35% of the summarized signal of lanes 2 and 8).

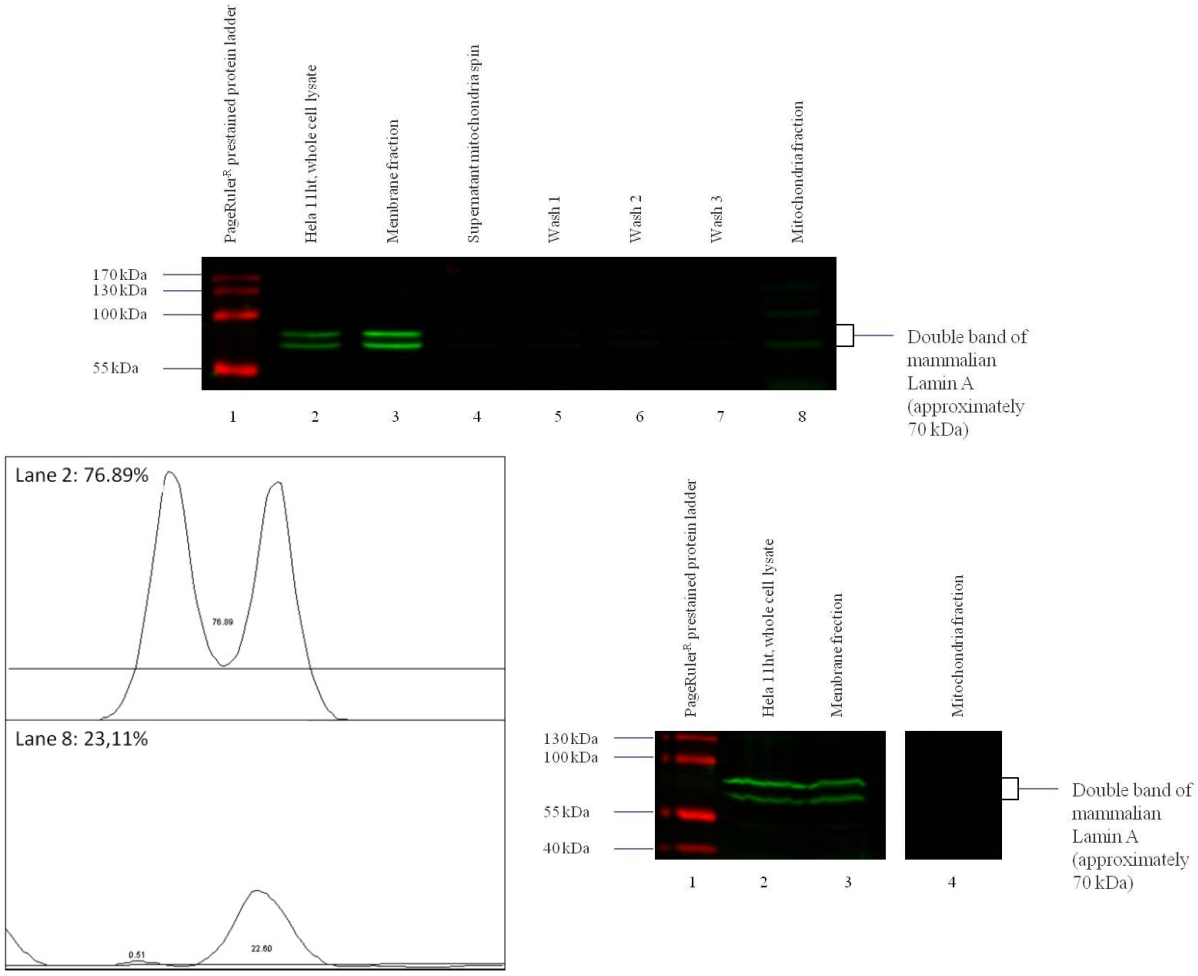

Fig. 22.: Fractionation protocol according to Frezza et al. (2007). Western blot against mammalian Lamin A.

Top: First western blot membrane against Lamin A. High amounts of nuclear Lamin A pellet in the membrane fraction (lane 2). Bottom left: The Lamin A contamination of the mitochondrial fraction (lane 8) was quantified up to 23% of cumulated GFP-signal compared to the whole cell lysate (lane 2).The baseline was adjusted to a clear double band. Bottom right: Western blot of the technical replicate. The mitochondrial fraction (lane 4) seems free of nuclear contamination.

The Lamin A as a marker for nuclear contamination is shown in figure 22. In the first experiment the mitochondrial fraction (lane 8 on membrane at the top) is contaminated with Lamin A (quantification left bottom). However, several shady bands are visible in lane 8 (for example at 100 kDa and 130 kDa), suggesting crossreacting bands or a

contamination. In a technical replicate of the blot (see bottom right), the mitochondrial fraction seemed devoid of a Lamin A signal.

In summary, the protocol developed by Frezza and colleagues seems to result in a better separation of a mitochondrial fraction from contaminating cytoplasm than the Kaltimbacher protocol. However, this protocol also needs a high number of cells to obtain a detectable mitochondria mass, e.g. an amount of 6 million cells resulted in only 20 µg of mitochondrial protein. This required mass of cells cannot easily be handled under the given circumstances, e.g. they would require high amounts of plasmid for transfection. In addition, both shown protocols are time-consuming and are hence difficult to integrate into the already time-consuming experimental approach.

Modified cell dissection protocol according to Shaiken et al. (2014)

Shaiken and colleagues (Shaiken et al. 2014) have suggested another fractionation protocol. The protocol does not aim to separate the mitochondria from the cytosolic fraction, but at least to extract it from nuclear contamination. Figure 23 shows the distribution of TOM20 at various steps of the experiment. Some mitochondrial marker protein is lost over the washing steps resulting in a similar concentration of mitochondrial marker protein (50.21% in the whole cell lysate compared to 49.79% in the mitochondrial fraction) in the final mitochondrial fraction compared to the whole cell lysate, but an overall decreased protein amount.

Figure 24 shows the western blot against nuclear Lamin A. It is clearly reduced, but still detectable in the mitochondrial fraction. Therefore the protocol does not give as good results as the protocol from Frezza et al. in terms of reduction of nuclear contamination. The protocol needs definitely less time than the both presented above, but also has the problem that only little amounts of mitochondrial protein can be obtained from many cells. Moreover, using this protocol a separation of mitochondria from the cytosolic proteins is not possible.

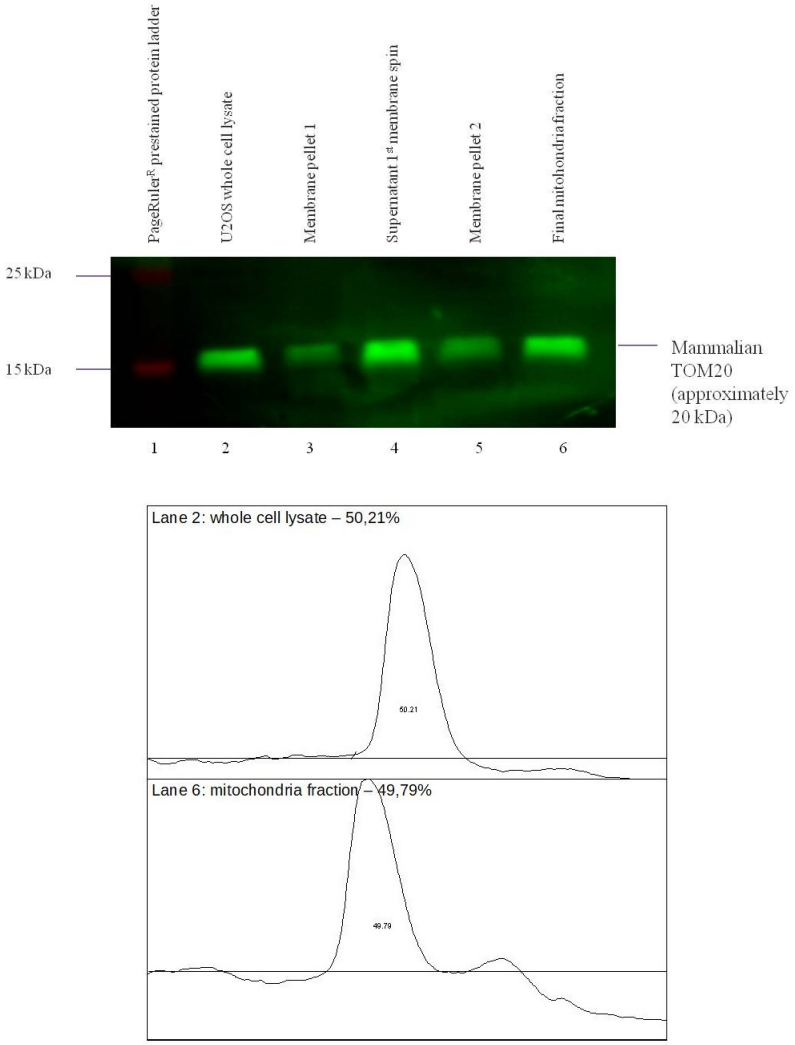

Fig. 23: Modified cell dissection protocol according to Shaiken et al. (2014). Western blot against mammalian TOM20.

Top: Blot membrane with TOM20 signal. Bottom: Quantification of lane 2 (whole cell lysate) and lane 6 (mitochondrial fraction). After subtracting the different background signals by manually adjusting the baseline for quantification, the bands show almost an equal concentration for TOM20 in the mitochondria fraction as well as in the whole cell lysate.

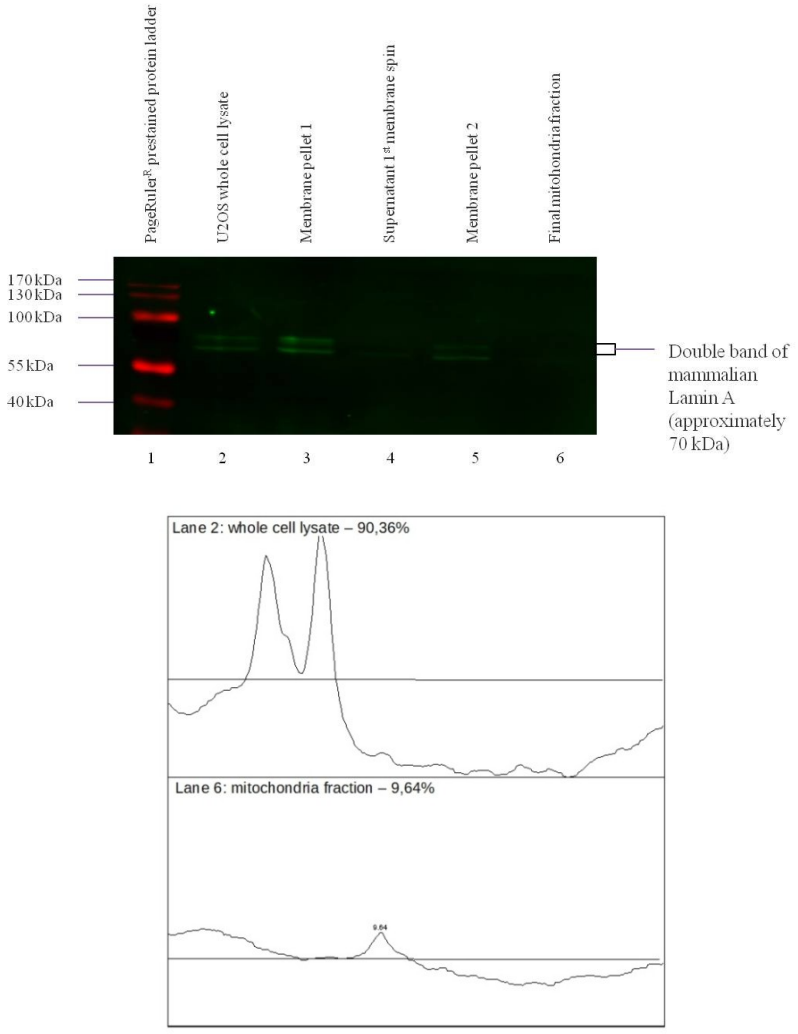

Fig. 24: Modified cell dissection protocol according to Shaiken et al. (2014).Western blot against mammalian Lamin A.

Top: Blot membrane with typical double band signal for Lamin A. Bottom: Quantification of lane 2 (whole cell lysate) and lane 6 (mitochondrial fraction). The background line was manually adjusted to measure only the characteristic double band in lane 2. The mitochondrial fraction shows a slight (about 10% of the concentration in the whole cell lysate) contamination with the nuclear protein Lamin A.

3.3. Validation experiments with stably integrated BirA* fusion proteins in HeLa EM2-11ht cells and U2OS T-Rex cells

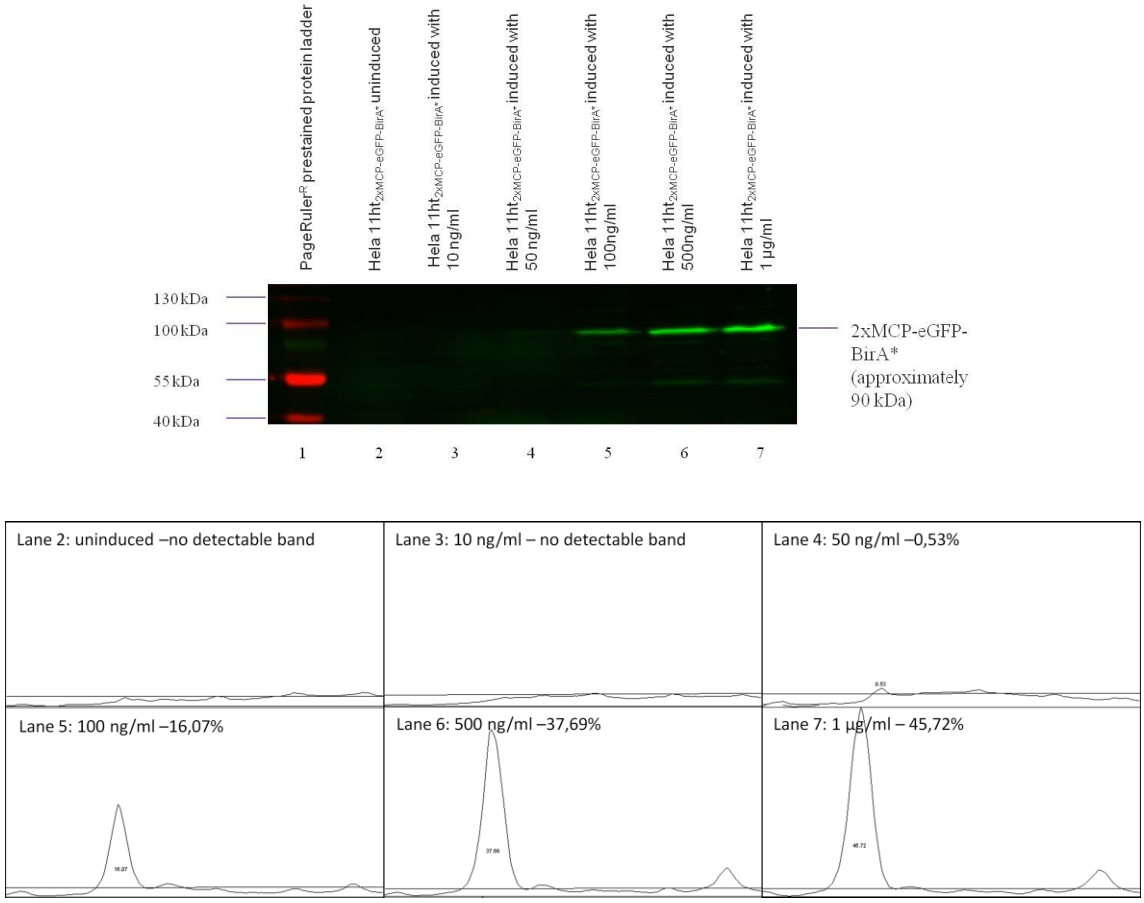

Fig. 25: Expression of 2xMCP-eGFP-BirA fusion protein dependent on doxycyline concentration.*

Top: Western blot membrane with GFP signal. Bottom: Quantification of lanes 2 to 7. HeLa 11ht$_{2xMCP\text{-}eGFP\text{-}BirA*}$ cells were induced with different concentrations of doxycycline for 24 h. In the plots a sufficient expression starting from 500 ng/ml doxycycline can be detected.

The biotin ligase fusion protein was first integrated into the genome of HeLa EM2-11ht cells and first validation experiments were performed in this cell line. The fusion constructs were expressed under a tetracycline dependent promoter. Hence, the concentration of doxycycline for an optimal expression needed to be determined by western blot against eGFP. The result is shown in figure 25. With an induction time of

24 h a concentration of at least 100 ng/µl doxycycline (lane 5, 16.07% of the summarized signal of lanes 2 to 7) was needed for a well detectable signal. An induction with 500 ng/µl (lane 6, 37.69%) gives a clearly better result, an increase up to a concentration of 1 µg/ml does not result in a similar enhancement of GFP signal (lane 7, increase only up to 45.72%).

In parallel, HeLa 11ht cells were induced and grown in medium with different biotin concentrations to find the best concentration for the biotinylation experiments. Whole cell lysates were prepared for the western blot that was developed using streptavidin coupled alkaline phosphatase. The blot is shown in figure 26.

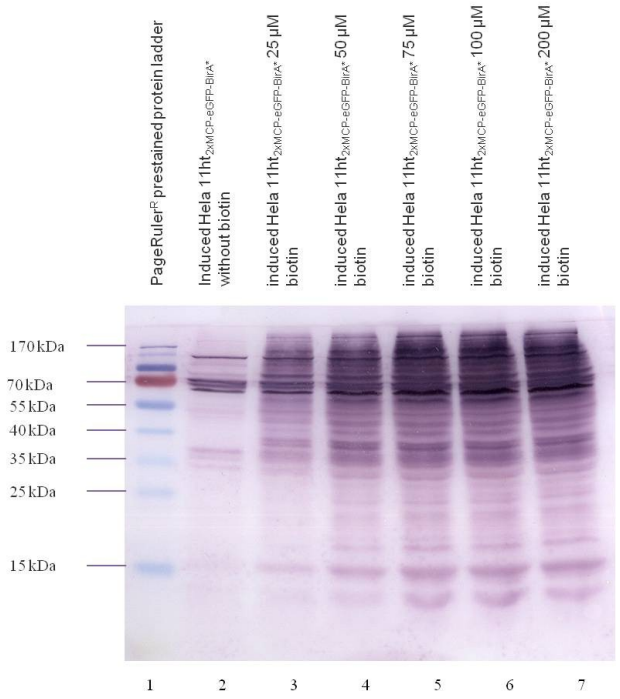

Fig. 26: Assessing the optimal concentration of biotin for in vivo biotinylation. HeLa$_{2xMCP\text{-}eGFP\text{-}BirA*}$ 11ht cells were induced with 1µg/ml doxycycline in media of different biotin concentrations. Beginning with a concentration of 50 µM biotin (see lane 4) a saturation of labeling is reached as shown by the identical pattern of biotinylated proteins.

Due to better handling and, more than that, a highly resilient contamination in the HeLa EM2-11ht cell cultures, later experiments were performed in U2OS T-Rex cells.

The fusion protein consisting of biotin ligase, eGFP and one MCP together with its nuclear localization sequence was successfully integrated into the genome of U2OS cells as shown by its expression (figure 27). In U2OS cells the gene is expressed under a tetracycline dependent promotor that is activated in the presence of tetracycline or its derivate doxycycline (Das et al. 2016). Thus, the cells were induced with 10 ng/ml of doxycycline as suggested by Alfred Hanswillemenke (unpublished data, laboratory of Prof. Stafforst, IFIB Tübingen), who constructed the backbone of the plasmid.

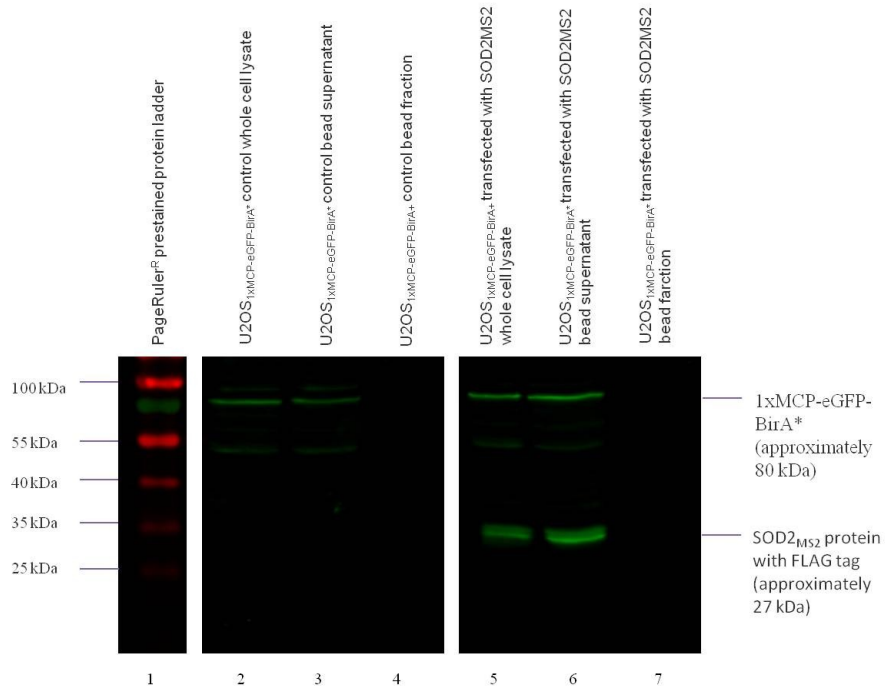

Fig. 27: Confirmation of integration of 1xMCP-eGFP-BirA fusion protein into the genome of U2OS cells.*
Western blot against GFP and FLAG. The $U2OS_{1xMCP\text{-}eGFP\text{-}BirA*}$ cells have been induced with 10 ng/ml doxycycline for 16 h. If compared to the similar HeLa cell system (shown in figure 25), the GFP signal is weaker although well detectable. The cell population that has been transfected with SOD2MS2 (lanes 5 to 7) shows $SOD2_{MS2}$ protein expression.

The expression is detectable, but could be improved in future experiments. It also shows the expression of tagged SOD2 by detecting the FLAG protein. In transfected cells, as expected, a FLAG signal can be found. Strikingly, the biotin ligase fusion protein itself cannot be detected in the bead fraction (see lanes 4 and 7) – unlike in the transient

transfection experiment shown in figure 13. However, the $SOD2_{MS2}$ protein is consistently absent in the bead fractions (lane 7).

Next, the required time of biotinylation was checked by western blotting. $U2OS_{1xMCP\text{-}eGFP\text{-}BirA*}$ cells were induced with 10 ng/µl doxycycline for 16 h. The biotin was added to the cells at different time points from 16 h to 3 h before lysation. As shown below, saturation in the biotinylation pattern starts after 6 h of biotin presence.

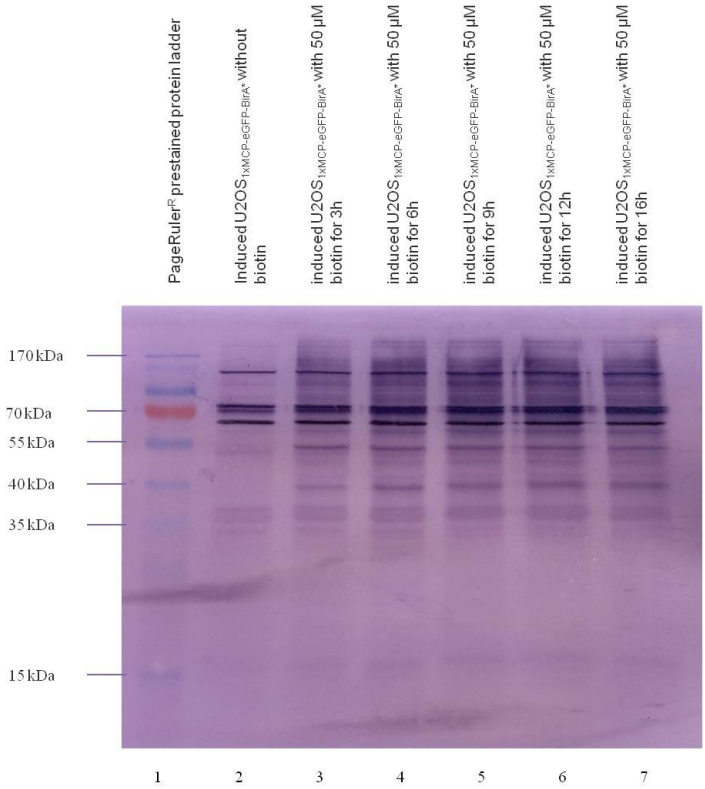

Fig. 28: Saturation of biotinylation in U2OS cells expressing 1xMCP-eGFP-BirA fusion protein induced for 16h (10 ng/ml doxycycline).*
Shown is a western blot against biotinylated proteins. The biotin was added to medium at the according timepoints. From lane 4 to lane 7 the same protein pattern occurs. Therefore I expect a sufficient time of biotin supply for in vivo biotinylation from 6 h in 50 µM biotin containing medium.

In addition, the distribution of the eGFP signal in cells with stably integrated biotin ligase fusion protein was controlled by fluorescence microscopy. The cells were induced and transfected with *SOD2MS2*. The result can be seen in figure 29. In transfected cells, the GFP signal is not only present in the nucleus, but the protein is

also included in particles (most likely RNA particles) that are distributed through the cytoplasm and also seem to localize around the mitochondria. However, as also shown in this figure, there are two problems with this approach. The first is the low transfection rate by transiently transfecting *SOD2MS2*, as (RNA) particles can only be detected in few cells. Secondly, different expression levels were detected in the cells although they were pre-sorted by FACS. As seen in figure 29, two cells are stained by Mitotracker^{R} Deep Red staining, but do not express GFP-BirA* fusion protein.

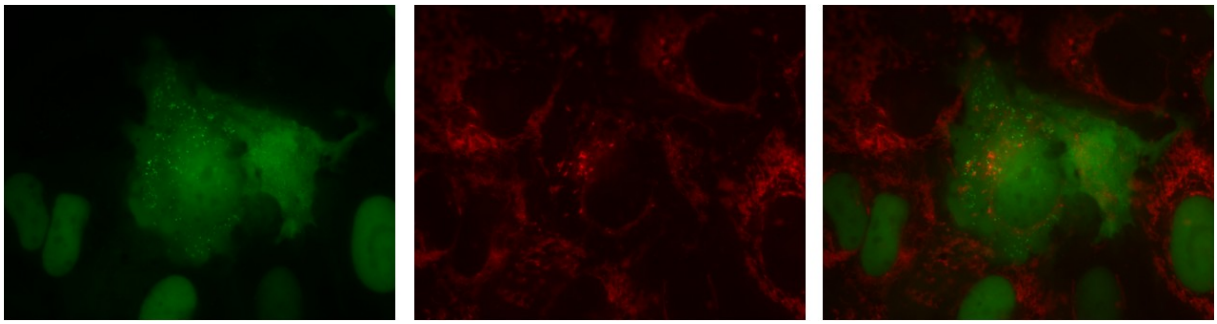

Fig. 29: U2OS$_{1MCP\text{-}eGFP\text{-}BirA*}$ transfected with SOD2MS2.
Left: eGFP signal. Middle: Staining with Mitotracker^{R} Deep Red. Right: Merged image. The RNA-particles with bound GFP can easily be detected in the cell body. The cell is surrounded by untransfected cells where the GFP signal is restricted to the nuclei and two without detectable GFP production.

3.4. Identification of SOD2$_{MS2}$ bait RNA interactome by mass spectrometry of transfected U2OS$_{1xMCP\text{-}eGFP\text{-}BirA*}$ cells

Although the experiments were initially planned for Hela 11ht cells and the validation of the U2OS cell lines can still be improved, the U2OS$_{1MCP\text{-}eGFP\text{-}BirA*}$ were chosen for upscaling the proximity labeling experiments. For this, cells were transiently transfected with *SOD2MS2*, biotinylated, and the biotinylated protein fraction was extracted with magnetic streptavidin beads from the whole cell lysate. The beads with the captured proteins were sent for mass spectrometry to identify the interactome of SOD2$_{MS2}$ mRNA. Four samples and two non-transfected controls (lacking *SOD2MS2*) were analyzed by Dr. Mirita Franz-Wachtel (Proteome Center of Tübingen University).

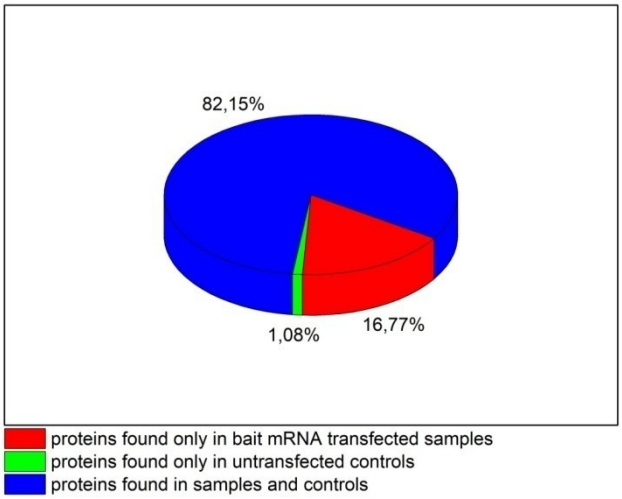

Fig. 30: Summary of the mass spectrometric analysis of the $SOD2_{MS2}$-dependent proximity labeling.
The majority of identified proteins were found in the samples expressing $SOD2_{MS2}$ mRNA as well as in the untransfected controls. However, 16.77% of all identified proteins were found only in the samples transfected with SOD2MS2. Only 1% of identified proteins were restricted to the controls.

Altogether, 1765 proteins were identified by mass spectrometry. Figure 30 shows the distribution of proteins found only in samples, only in controls or on both. Proteins that are found in samples as well as in the controls have a similar distribution within the cell as proteins that were only found in the transfected samples. Within the few proteins only found in the controls are two mitochondrially localized proteins.
Promising candidates (see table 6 in chapter 4.4) to interact with $SOD2_{MS2}$ bait RNA that were only found in the *SOD2MS2* transfected samples but not in untransfected controls are the insulin-like growth factor 2 mRNA binding protein 2 (IGF2BP2), the leucine-rich repeat-containing protein 40 (LRRC40) and the G patch domain-containing protein 8 (GPATCH8).

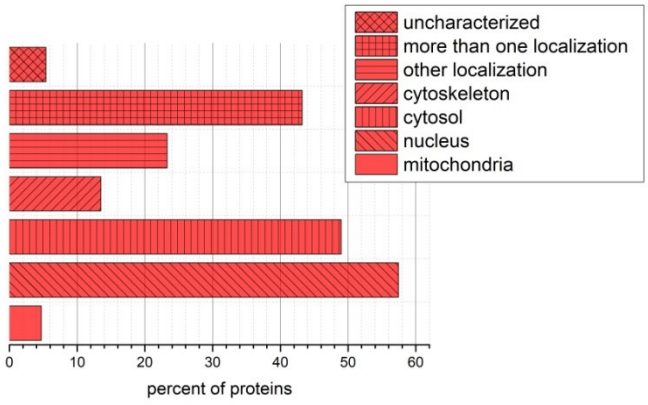

1

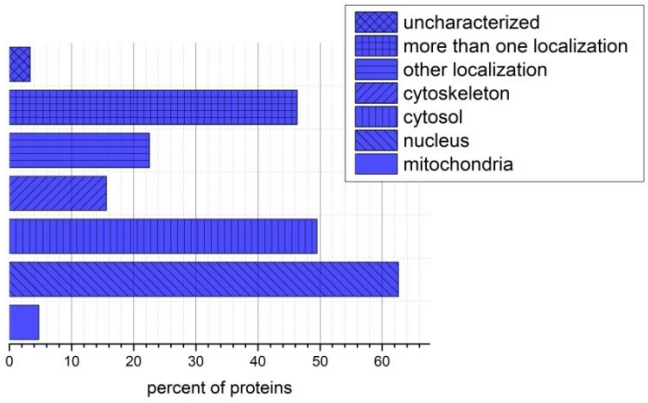

2

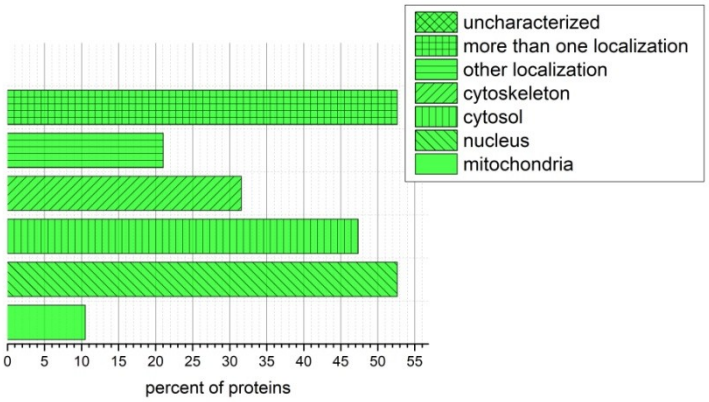

3

Fig. 31: Localization of proteins identified by mass spectrometry.

(1) shows the localization of proteins found only in the samples of cells that were transfected with SOD2MS2 (red). (2) shows the distribution of proteins found in the controls as well as in the samples (blue), (3) shows the localization pattern of proteins that have been identified only in the controls (green).

The first one is an RNA-binding protein located in the cytoplasm in ribonucleoproteins and less abundant in the nucleus. Its paralog IGF2BP1 is involved in mRNA transport, stability and translation processes. In *igf2bp2*$^{-}$/*igf2bp2*$^{-}$ deletion mice, the translation level of 15 proteins including 13 mitochondrial ones were altered and in glioblastoma cells the protein was shown to take part in the localization and localized translation of proteins in the vicinity of mitochondria (reviewed in: Cao et al. 2018). Moreover, IGF2BP2 was shown to bind SOD2 mRNA as well as many others by RNA immunoprecipitation experiments in mouse cardiomyocytes (Hosen et al. 2018).

Even more interesting in this context is LRRC40, a so far uncharacterized protein that is found in none of the controls but in every transfected sample. Neither its function nor its localization was investigated so far. However, it is known to interact with the tumor suppressor leucine-rich repeats and immunoglobulin-like domains 1 (LRIG1) (Faraz et al. 2018).

GPATCH8 seemed primarily another candidate of interest due to its possible RNA-binding domain, but was identified as a nuclear protein located in paraspeckles, most possibly involved in splicing (Chapman et al. 2019).

None of these proteins was determined to sit at the mitochondrial outer membrane using proximity biotinylation (Hung et al. 2017).

In contrast, the Ras-related protein RAB5C was identified as so far unknown mitochondrial outer membrane protein in their publication (Hung et al. 2017). No interaction with mRNA was described so far, instead, the RAB5 proteins are involved in membrane and vesicle trafficking as well as in mitophagy (reviewed in: Hervé and Bourmeyster 2018, Nepal et al. 2020, Yamano et al. 2018). The RAB5C could not be detected for sure in our mass spectrometry samples due to its sequence similarity to RAB5A as well as RAB5B and its low overall abundance, but the cluster of RAB5 was found in all *SOD2MS2* transfected samples and none of the controls. Therefore, it should be considered as protein interacting directly or indirectly with the $SOD2_{MS2}$ bait mRNA.

Some proteins that are found enriched in cells that express $SOD2_{MS2}$ mRNA are already known or suspected to take part in the transport of mRNAs through the cytoplasm. One of the most interesting of them is the Clustered mitochondria protein homolog (CLUH)

that is known to play a role in the local translation of mRNAs for nuclear encoded mitochondrial proteins (Gao et al. 2014). It is enriched in the samples transfected with *SOD2MS2* although it also occurs, less frequently, in the controls.

Another protein of interest might be the fragile x mental retardation syndrome – related protein 1 (FXR1) which is also found enriched in the cells producing $SOD2_{MS2}$ mRNA. It is a RNA-binding protein (reviewed in: Bardoni et al. 2001) that was shown to take part in translation regulation of proinflammatory transcripts (Herman et al. 2018) and its family member FMR1 was early associated to mRNA transport and translation regulation (reviewed in: Bardoni et al. 2001). CLUH as well as FXR1 are mainly localized in the cytoplasm (reviewed in: Schatton and Rugarli 2019, Herman et al. 2018).

Also, the leucine-rich PPR motif-containing protein LRPPRC can be noted enriched in the samples compared to the controls. LRPPRC has various subcellular localizations and can therefore be found in the nucleus as well as in mitochondria (reviewed in: Cui et al. 2019). It was shown to take part in the cellular energy metabolism by regulating the mitochondrial encoded mRNAs, but so far is not expected to regulate the expression of nuclear encoded mitochondrial genes (reviewed in: Cui et al. 2019).

Other proteins known to be involved in mRNA localization were found enriched in the samples with $SOD2_{MS2}$ mRNA, among them the La-related protein 1 (LARP1). Its homolog Larp, a translation regulator, was previously reported to be recruited to the mitochondria by the mitochondrial outer membrane protein MDI in *Drosophila melanogaster* (Zhang et al. 2016). However, AKAP1, the human homolog to MDI, has not at all been found in our mass spectrometry data. Other AKAP proteins, including the AKAP2 (also known as AKAP-KL), show a trend to be more abundant in the transfected cells than in the controls, but none of them passes the cut-off criteria. Six isoforms of AKAP2 derive from its genes via alternative splicing that are expressed in a tissue-specific matter and have been suggested to differ in subcellular localization (Dong et al. 1998).

Larp is known to interact with the eukaryotic translation initiation factor 4 gamma 1 (eIF4G), a cytosolic protein (Nousch et al. 2007) that is involved in recruiting mRNAs to ribosomes (reviewed in: Pévot et al. 2003), and the polyadenylate binding proteins (PABPs) that bind the poly(A) tail of mRNAs and are involved in many tasks of mRNA

metabolism and regulation (Smith et al. 2014, Tcherkezian et al. 2014). Although eIF4G is similarly enriched in *SOD2MS2* transfected cells and controls, the poly A binding proteins are enriched in the transfected samples. Additionally, ATAD3 proteins passed the threshold of a twofold enrichment in the samples. The homolog of ATAD3A was copurified with MDI in *Drosophila melanogaster* and mammalian ATAD3 was thought to tether the mtDNA at contact sites of mitochondria and ER (Zhang et al. 2016), but ATAD3 also pops up in the list of mitochondrial outer membrane orphans from 2017 (Hung et al. 2017).

In addition, the far upstream element-binding protein 3 (FUBP3) that was lately discovered to be involved in ß-actin mRNA localization (Mukherjee et al. 2019) is also found enriched in samples transfected with $SOD2_{MS2}$ mRNA.

Another protein passing the threshold for possible interacting proteins is the Double-stranded RNA-binding protein Staufen homolog 1 (STAU1). It is a common RNA-binding protein involved in mRNA transport in neurons and mRNA decay after binding preferentially to complex secondary structures of its targets (Vessey et al. 2008, Mitsumori et al. 2017, Gowravaram et al. 2019).

In yeast, vesicular trafficking has been reported to participate in mRNA transport to the mitochondrial surface (reviewed in: Schatton and Rugarli 2018). In fact, four coatomer proteins were detected as biotinylated in the lysates. Two of them, the coatomer subunits beta and delta are enriched in the transfected samples. Also the subunits gamma-2 and alpha showed a trend to be more enriched in the presence of SOD2MS2 mRNA, but both did not cross the threshold. It has to be mentioned, that in one sample there was no hit at all for the coatomer subunits beta and delta which over all makes it unlikely that this proteins interact with the target mRNA directly (for detailed table see appendix).

Beside them, Vacuolar protein sorting-associated protein 13D (VPS13D) was lately identified as an outer mitochondrial membrane orphan (Hung et al. 2017) and is, despite it lacks a suggested or known function as RNA-binder, highly enriched in the samples expressing $SOD2_{MS2}$ bait mRNA. It further was suggested involved in mitochondrial homeostasis and clearance (Anding et al. 2018). Except VPS13D and the RAB5B protein (that is also involved in vesicle trafficking) mentioned above none of the other

orphan mitochondrial outer membrane proteins detected by Hung et al. were found in our dataset (Hung et al. 2017).

Despite the crucial role the TOM complex has in mitochondrial protein import (reviewed in: Wiedemann and Pfanner 2017), only the cytosolic chaperone TOM34 that is suggested to interact with TOM70 targeted mitochondrial precursor proteins (Faou et al. 2012) shows up in our dataset. It is not found in the controls, but also not frequent in the samples expressing the artificial SOD2 (for detailed table see appendix). Indeed, in one of the samples no TOM34 was detected.

Furthermore, heat shock proteins, especially Hsp70 and Hsp90, are known to be involved in the so-termed "carrier pathway" of mitochondrial protein import (reviewed in: Wiedemann and Pfanner 2017). Two of their co-chaperones are enriched in the samples transfected with my target RNA. The heat shock 70 kDa protein 4 (HSPA4) is a protein of the Hsp110 family interacting with the Hsp70 proteins (Cabrera et al. 2019) that play a role in mitochondrial protein import (Young et al. 2003). The second protein passing the threshold is the CDC37 co-chaperone of Hsp90. Units of the heat shock proteins 90 were found mostly equally enriched in mass spectrometry samples of *SOD2MS2* transfected and untransfected cells. CDC37 helps to sort the client proteins to Hsp90 itself. However, its target proteins were widely studied and it was shown to interact exclusively with protein kinases (Li et al. 2018). Indeed, a list of CDC37 target proteins lacks the SOD2. Taken together, to my knowledge, none of the two proteins were shown to interact with mitochondrial targeted proteins directly so far. In addition, no other heat shock protein showed a difference in abundance that passed our threshold.

Finally, peptides of the artificially integrated biotin ligase BirA* were identified by mass spectrometry, giving us the certainty of its expression in the cells. It was found at almost the same rates in controls and transfected samples.

3.5. Mitochondrial phosphate carrier protein

The mitochondrial phosphate carrier protein (MPCP) is a protein that has been identified in the vicinity of $SOD2_{MS2}$ RNA in earlier mass spectrometry experiments performed by Joyita Mukherjee (unpublished data, laboratory of Prof. Jansen, IFIB Tübingen) with transiently transfected HeLa S3 cells.

As an initial experiment to verify this potential interaction of MPCP with SOD2 mRNA, I designed a construct of MPCP ORF in frame with a mCherry fluorescent protein, keeping the 3'UTR of MPCP. The localization of this fusion was tested by fluorescence microscopy. Figure 32 shows the distribution of the mCherry signal in a transiently transfected HeLa S3 cell. The distribution of MPCP mCherry fusion protein overlaps with the Mitotracker^{R} Green, confirming its mitochondrial localization.
However, the mitochondrial phosphate carrier protein was not found in mass spectromety experiments with U2OS T-Rex cells.

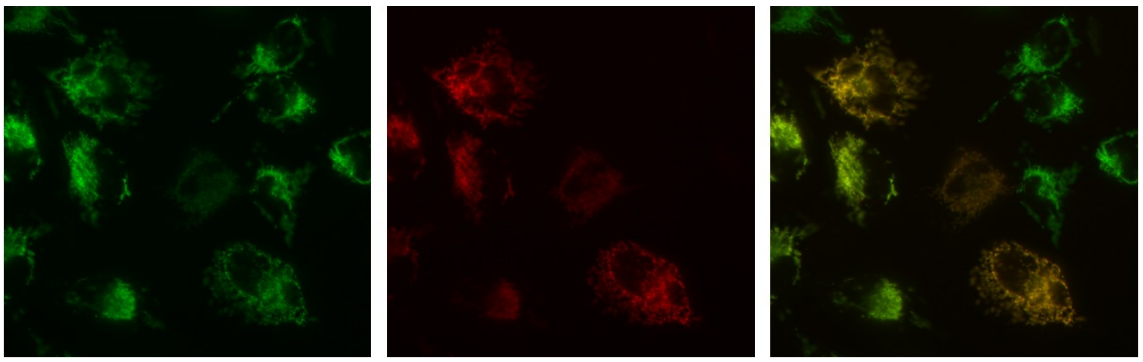

Fig. 32: Localization of MPCP-mCherry fusion protein in transiently transfected HeLa S3 cells.
Left: Mitochondria stained with Mitotracker^{R} Green. Middle: Distribution of MPCP mCherry fusion protein. Right: Merged image. The MPCP-mCherry is localized only in the mitochondria, the merged picture shows a perfect overlap signal in transfected cells.

4. Discussion

The importance of RNA localization was brought into focus by many studies over the past few years (reviewed in: Chin and Lécuyer 2017, reviewed in: Schatton ans Rugarli 2018). This work aims to extend our current knowledge about the factors involved in the targeting of SOD2 mRNA to the mitochondrial surface. Therefore, the RNA-BioID method (Mukherjee et al. 2019) was applied on a $SOD2_{MS2}$ bait mRNA in Hela S3 and $U2OS_{1xMCP\text{-}eGFP\text{-}BirA*}$ cells.

4.1.Validation of SOD2 RNA-BioID in transiently transfected HeLa S3 cells

The correct expression of the biotin ligase fusion protein and the FLAG-tagged bait $SOD2_{MS2}$ protein could be verified by western blotting of transfected HeLa S3 whole cell lysates (figure 13 and 14). In addition, a western blot using Streptavidin coupled alkaline phosphatase demonstrated the biotinylating activity of BirA* in cells transfected with the encoding vector (see figure 12). The successful enrichment of biotinylated proteins by streptavidin magnetic beads used for extraction of biotin marked proteins before mass spectrometry could also be demonstrated (figure 12).
In addition, the correct localization of the fusion protein could be determined by fluorescence microscopy. Transfecting cells with vectors encoding eGFP-BirA* or eGFP containing fusion proteins, the correct nuclear localization due to the C-terminal nuclear localization sequence (NLS) was observed (figure 15). Upon cotransfection with *SOD2MS2,* the fusion protein was also detected outside the nucleus in small particles suggesting its correct binding to $SOD2_{MS2}$ bait mRNA (see figures 16 and 17).

4.2.Fractionation protocols

Several protocols were tested for an enrichment of mitochondrial proteins. As mentioned before (see chapter 3.2.), the rationale for this was to find a protocol to enrich for mitochondrial or mitochondrial outer membrane proteins after biotinylation. By applying any of the tested protocols, a loss of mitochondrial TOM20 could be detected during the fractionation steps, and most mitochondrial proteins are lost in the

membrane pellets (figures 18, 20 and 23). In addition, the protocols of Kaltimbacher and Frezza failed in clearing cytosolic GAPDH from the mitochondrial fraction (figures 19 and 21). The protocol of Shaiken and colleagues did not aim to isolate a clean mitochondrial fraction. However, their protocol was clearly able to separate the nuclear Lamin A containing fraction from mitochondrial proteins such as TOM20 (figure 24). The protocol performed according to Frezza et al. showed a large variation in technical replicates of Lamin A blotting. Therefore a successful separation of mitochondrial TOM20 and nuclear Lamin A could not be determined.

All applied protocols suffer from a high requirement of cells whereas resulting in few micrograms of final mitochondrial protein. The idea of fractionating cells prior to pulldown of biotinylated proteins via streptavidin beads was therefore abandoned.

4.3. Validation of SOD2 RNA-BioID in HeLa EM2-11ht and U2OS T-Rex cells with stably integrated BirA* fusion protein

The first experiments with stably integrated BirA* fusion proteins were performed in HeLa EM2-11ht cells. The doxycyline concentration needed for sufficient expression of the fusion protein under the Tet-dependent promotor was confirmed by western blot (figure 25) with at least 100 ng/ml doxycycline for 24 h.

The optimal biotin concentration in HeLa 11ht cells and the corresponding time were examined in HeLa 11ht cells and U2OS cells, respectively. The results are similar to those published for RNA-BioID of beta-actin (Mukherjee et al. 2019), suggesting that a 50 µM concentration and 6 h of biotin in the cells' medium are sufficient for an effective BirA*-dependent biotinylation (figures 26 and 28).

In addition, the correct expression of 1xMCP-eGFP-BirA* fusion protein in U2OS cells and of the $SOD2_{MS2}$ protein were demonstrated. Consistent with the results of transiently transfected HeLa S3 cells (figure 14, lane 6 and 9) the $SOD2_{MS2}$ protein is absent in the fraction binding to streptavidin beads (figure 27, lane 7). This might support the thesis of a cotranslational import of $SOD2_{MS2}$, but could also be considered as a result of short contact time between mRNA and protein at the ribosome or a sterical shielding.

In contrast, the BirA* fusion protein was found to be enriched in the fraction of biotinylated proteins in transiently transfected HeLa S3 cells (figure 13, lane 10). However, it is missing when the vector is stably integrated in the genome of U2OS T-Rex cells (figure 27, lanes 4 and 7). This pattern is consistent in control and in transfected cells (figure 27). The result might reflect the lower expression of inducible 1xMCP-eGFP-BirA* compared to the overexpressed 2xMCP-eGFP-BirA* expressed from a plasmid backbone. Taken together, the expression of the fusion proteins as well as the successful transfection of *SOD2MS2* with expression of its encoded protein could be demonstrated. Moreover, a cytoplasmic granular distribution of the 1xMCP-eGFP-BirA* in *SOD2MS2* transfected $U2OS_{1xMCP\text{-}eGFP\text{-}BirA*}$ cells was shown (figure 29), which is similar to the one in transiently transfected HeLa S3 cells (figure 16 and 17). As some validation experiments (e.g. the assessment of biotin concentration, figure 26) were performed only with Hela EM2-11ht cells, they should be repeated in U2OS cell lines to exactly adjust the conditions for further RNA-BioID experiments.

In addition, it has to be noted that one property of carcinoma cells is the shift in energy metabolism from oxidative phosphorylation to glycolysis, called the Warburg effect (Warburg 1956). The impaired mitochondrial function might be associated with reduced protein levels and protein import that might be a drawback in studying localization of mRNA and localized translation at the mitochondrial surface. Similar to that, the Crabtree effect describes the inhibition of mitochondrial respiration upon glucose excess (reviewed in: Barros et al. 2020) as it is usually found in standard cell culture medium as DMEM. Thus, changing to a system of cells resistant to low glucose medium and starvation could be beneficial for further investigation of localized translation near the mitochondrial outer membrane.

4.4. Identification of $SOD2_{MS2}$ bait RNA interactome by mass spectrometry of transfected $U2OS_{1xMCP\text{-}eGFP\text{-}BirA*}$ cells

Table 6 shows a list of 13 identified proteins that might interact with SOD2 mRNA (for mass spectrometry details see appendix, tables 9 and 10).

Table 6: Potential interactors of the $SOD2_{MS2}$ bait mRNA.

Gene name	Protein name	Known function
Known RNA-binding proteins		
IGF2BP2	Insulin-like growth factor 2 mRNA binding protein 2	IGF2BP2 binds and regulates several mRNAs including mitochondrial ones. The according proteins play role for example in energy homeostasis and lipid metabolism as well as cell differentiation, development and carcinogenesis (reviewed in: Cao et al. 2018).
CLUH	Clustered mitochondria protein homolog	CLUH regulates translation, decay and localization of mitochondrial targeted transcripts (Gao et al. 2014, Schatton et al. 2017)
FXR1	Fragile X mental retardation syndrome-related protein 1	FXR1 is a translation repressor of proinflammatory transcripts (Herman et al. 2018). The whole family of fragile x mental retardation associated proteins (FMR, FXR1 and FXR2) are linked to mRNA transport and translation regulation (reviewed in: Bardoni et al. 2001).
LRPPRC	Leucine-rich PPR motif-containing protein	LRPPRC is a protein of a RNA-binding family that regulates among others the mRNAs of mitochondrial encoded proteins. It is abundant in many cell compartments where it takes part in mRNA processing and regulation through direct or indirect interactions (reviewed in: Cui et al. 2019).
PABP	Poly(A) binding protein	Different isoforms are involved in the whole life cycle of many mRNAs. Suggested to play a role in localized translation (reviewed in: Gray et al. 2015).
FUBP3	Far upstream element-binding protein 3	Involved in ß-actin mRNA localization in MEFs (Mukherjee et al. 2019) and MAP2 mRNA localization in rat neurons (Rehbein et al. 2000).
STAU1	Double-stranded RNA-binding protein Staufen homolog 1	Common RNA-binder responsible for mRNA transport in neurons (reviewed in: Ohashi and Shiina 2020) and decay of target mRNAs (reviewed in: Park and Maquat 2013).
Other proteins linked to mitochondrial RNA localization		
ATAD3 (isoforms ATAD3A and ATAD3B)	ATPase family AAA domain-containing protein 3A/3B	ATAD3 is a inner mitochondrial membrane protein with contact to the outer mitochondrial membrane. It is so far known to be involved in cristae formation and mtDNA replication (Peralta et al. 2018). Its fly homolog copurified with MDI (Zhang et al. 2016).
LARP1	La-related protein 1	LARP1 is an mRNA-binding protein altering the expression of its targets dependent on mTORC1-mediated phosphorylation (Hong et al. 2017). Its fly homolog is recruited to the outer mitochondrial membrane through interaction with MDI (Zhang et al. 2016).
Proteins involved in vesicle trafficking		
ARCN1	Coatomer subunit delta	Subunit of the coatomer complex involved in COPI vesicle budding from golgi apparatus and ER (Lee and Goldberg 2010).
COPB1	Coatomer subunit beta	Subunit of the coatomer complex involved in COPI vesicle budding from golgi apparatus and ER (Lee and Goldberg 2010).
RAB5 group (Rab5A; Rab 5B; Rab5C)	Ras-related protein 5A/5B/5C	Rab proteins guide vesicle transport through the a cell from budding to fusion (reviewed in Hervé and Bourmeyster 2018). Rab5c was shown to move from endosomes to the mitochondria upon mitochondrial damage as part of PINK/Parkin dependent mitophagy (Yamano et al. 2018).
Other proteins linked to mitochondrial homeostasis		
VPS13D	Vacuolar protein sorting-associated protein 13D	A ubiquitin-binding protein that takes part in mitochondrial clearance and autophagy (Anding et al. 2018).

Proteins involved in mitochondrial protein import		
TOM34	Mitochondrial import receptor subunit TOM34	Co-chaperone of Hsp70 and Hsp90 essential for mitochondrial targeting of the complex (Faou and Hoogenraad 2012).
Uncharacterized proteins		
LRRC40	Leucine-rich repeat containing protein 40	Unknown

Some of them are already known to take part in mRNA transport and regulation including CLUH (Gao et al. 2014), FXR1 (Herman et al. 2018), FUBP3 (Mukherjee et al. 2019), STAU1 (reviewed in: Park and Maquat 2013) and PABP (Tcherkezian et al. 2014).

FUBP3 was so far shown to contribute to the localization of ß-actin mRNA in MEFs (Mukherjee et al. 2019) and the transport of MAP2 mRNA in rat neurons (Rehbein et al. 2000). Finding it in our dataset, FUBP3 may be a more general interactor involved in RNP assembly and transfer. Poly(A) binding proteins basically bind to all mRNAs, which is likely the reason why it is found in our dataset. A bundle of evidence links PABPs to localized translation (reviewed in Gray et al. 2015). Interesting for us, one shortened isoform of PABP5 is enriched in mitochondria (reviewed in: Gray et al. 2015), although no peptides of this isoform were found enriched in our dataset.

STAU1 is a cytosolic protein binding to complex secondary structures that are preferentially located in the 3'UTR of its targets (Sugimoto et al. 2015). Staufen proteins have been shown to be involved in mRNA transport in fly embryos (Micklem et al. 2000) and in neurons (reviewed in: Ohashi and Shiina 2020). STAU1, in addition, has also a prominent role in mRNA decay (reviewed in: Park and Maquat 2013).

By binding targets of a more specific pathway, FXR1 was shown to inhibit the translation of proinflammatory mRNAs (Herman et al. 2018). Possibly, this protein might also co-regulate a network of anti-inflammatory transcripts, one of which could be SOD2 that was shown to act beneficial in inflammation reduction (reviewed in: Azadmanesh and Borgstahl 2018). In addition, its relative FMR interacts in a network of posttranscriptional regulators together with mammalian Pumilio proteins (Zhang et al. 2017). Here it might be important to mention that the yeast pumilio protein Puf3p specifically binds to transcripts encoding mitochondrial proteins (Saint-Georges et al. 2008).

Similar to alterations in the SOD2 sequence (reviewed in: Azadmanesh and Borgstahl 2018), a single nucleotide polymorphism in IGF2BP2 was shown associated with type

II diabetes. In addition, the protein was linked to colorectal and breast cancer as well as esophageal adenocarcinoma wherein high expression was a predictor for short survival due to enhanced proliferation and migration rates (reviewed in: Cao et al. 2018). In addition, IGF2BP2 deletion mice showed a prolonged lifespan and were resistant to diet-induced obesity and development of a fatty liver. Moreover, they did not become resistant to insulin and were more glucose tolerant (Dai et al. 2016). Regarding the phenotype contrary to SOD2 deletion and IGF2BP2's known binding to mRNA including mitochondrial targeted ones (reviewed in: Cao et al. 2018), the protein seems likely to interact with SOD2 mRNA in a posttranscriptional manner.

CLUH was already shown to select mitochondrial targeted transcripts for binding and to direct their localization to the mitochondrial surface (Gao et al. 2014). However, it was also shown that CLUH depletion might increase the abundance of its transcripts in the mitochondrial vicinity (Vardi-Oknin and Arava 2019) suggesting a more complex mechanism of targeting the concerning mRNAs. The recent work of Pla-Martín et al. shed a first light on the network and conditions of CLUH-dependent mRNA regulation (Pla-Martín et al. 2020). Interestingly, they connected CLUH to the mTORC1 signaling (Pla-Martín et al. 2020) that was already described to be regulated by LARP1 (Hong et al. 2017). LARP1's fly homolog, Larp, was demonstrated to be involved in mRNA localization in *D. melanogaster* (Zhang et al. 2016). The mammalian protein is enriched in the $SOD2_{MS2}$ mRNA interactome, making it an interesting candidate for further investigation.

The *Drosophila* Larp also interacts with the AKAP family protein MDI on the mitochondrial surface (Zhang et al. 2016). Our dataset did not reveal any AKAP protein significantly more enriched in the transfected cells than in the control. Instead, we found the ATAD3 protein. It has been located to the outer mitochondrial membrane by proximity biotinylation (Hung et al. 2017), but it was also associated with mtDNA organization (Peralta et al. 2018), making its exact localization unclear. The homolog of ATAD3A copurified with MDI in *Drosophila melanogaster* (Zhang et al. 2016). Therefore, ATAD3 could be a first mitochondrial outer membrane candidate involved in the localization of mRNAs to the organelle's surface. Another quite interesting candidate could be the LRRC40, a protein occurring only and in all in transfected

samples. However, no function or cellular localization has been attributed to this protein so far.

Beside these proteins whose RNA-binding has been shown, lately other proteins have been demonstrated to be involved in mRNA transport, including the COP I coatomer. COP I dependent mRNA transport was reported in *Saccharomyces cerevisiae* (Zabezhinsky et al. 2016). Interenstingly, we found that the coatomer complex subunit beta became biotinylated in cells transcribing $SOD2_{MS2}$ bait mRNA. Another protein group linked to vesicle transport (reviewed in: Hervé and Bourmeyster 2018) and enriched upon transfection of $U2OS_{1xMCP\text{-}eGFP\text{-}BirA*}$ with *SOD2MS2* are Rab5 proteins. Yamano et al. demonstrated that RAB5 is recruited to damaged mitochondria and linked the protein to mitophagy and the PINK/Parkin pathway (Yamano et al. 2018). The LRPPRC protein, also passing our threshold, contains domains associated with vesicular trafficking. Its protein family is also characterized by the PPR motif enabling them to bind RNA (reviewed in: Cui et al. 2019). As many members of its family, LRPPRC is involved in mRNA processing and regulation via interactions with mRNAs and effector proteins. Overexpression of LRPPRC that is abundant in many cell compartments as the nucleus, the endoplasmic reticulum and mitochondria, leads to increased mitochondrial respiration, but was also associated with carcinogenesis (reviewed in: Cui et al. 2019). In addition, the protein seems to interact with PINK1 and was linked to Parkinsons's disease and mitophagy. However, LRPPRC was so far shown to regulate mRNAs of proteins encoded in the mitochondrial genome but not of nuclear encoded mitochondrial proteins (reviewed in: Cui et al. 2019). So its role in the regulation of SOD2 mRNA has to be questioned.

Besides that, VPS13D is a protein that has previously been linked to protein degradation and mitophagy. Neither VPS13D in *Drosophila melanogaster* nor RAB5C in mammalian cells were initially reported to localize to the mitochondria (Anding et al. 2019, Yamano et al. 2018), but were identified at least as localized near the mitochondrial membrane by proximity biotinylation (Hung et al. 2017). Taking in account their involvement in mitochondrial homeostasis and their possible recruitment to mitochondria, they seem interesting for further investigation.

In addition, a mRNA could be delivered to the mitochondria in a translation-dependent manner. Proteins involved in mitochondrial protein import enriched in our data set are

TOM34, HSPA4 and CDC37. While HSPA4 was only shown to interact with Hsp70, CDC37 delivers proteins to Hsp90 (Cabrera et al. 2019; Li et al. 2018). The latter could therefore theoretically interact with a mitochondrial targeted protein during translation, but was shown to preferentially bind protein kinases (Li et al. 2018). TOM34 was also demonstrated to be a cytosolic co-chaperone of Hsp70 and Hsp90 and necessary for mitochondrial targeting of the complexes (Faou and Hoogenraad 2012).

Despite their essential roles in mitochondrial protein import (reviewed in: Wiedemann and Pfanner 2017), neither Hsp70 and Hsp90 nor any component of the membrane-bound TOM complex, especially not the Hsp70/90 interacting TOM70, were found enriched cells transfected with $SOD2_{MS2}$ bait mRNA. Taken together, this raises the question whether our bait mRNA interacts with the main import machinery consistent of TOM and TIM complex. However, that $SOD2_{MS2}$ protein is not captured by streptavidin beads suggests its shielding from biotinylation which could happen due to cotranslational import of the protein. Due to the integration of the MS2 loops 3' of the open reading frame the proteins interacting with the 5' end of our bait mRNA might be sterically shielded from biotin-AMP by other proteins, e.g. translating ribosomes or other RNA-binding proteins. If that is the case or if the SOD2 mRNA or its evolving protein indeed does not interact with the translocase of the outer mitochondrial membrane has to be elucidated. It has to be mentioned that despite its presence in mitochondria-associated polysomes (Sylvestre et al. 2003) the SOD2 mRNA was not identified in a set of mRNAs located to the outer mitochondrial membrane by APEX-Seq (Fazal et al. 2019). Here again, we cannot distinguish for sure between a possible spatial division of the SOD2 mRNA from the outer mitochondrial membrane by maybe a cluster of RNA-binding proteins and chaperones or the simple absence of SOD2 mRNA near the mitochondrial outer membrane. Although Kaltimbacher et al. showed that cis-elements of the SOD2 mRNA target the ORF of a nuclear encoded ATP6 to the mitochondrial outer membrane (Kaltimbacher et al. 2006), we cannot exclude that this targeting may rely on more factors e.g. metabolic conditions and cell type. Indeed, several mRNA binding proteins were shown to act (including their binding to their respective targets) dependent on specific stimuli (Hong et al. 2017; Schatton et al. 2017). This could not only result in a difference in translation regulation but also in a different transcript localization. Therefore, the localization of eGFP-containing particles

in transfected cells must be quantified in their relation to the cells' mitochondria in further experiments to determine the localization in of SOD2 mRNA in used cell lines and conditions.

5. Summary

Through the past decades, the model of a cotranslational import of nuclear encoded proteins into cellular organelles moved from the edge to the spotlight of attention. Indispensable for such a process is the correct targeting of an according mRNA or the ribosome-mRNA complex. mRNA localization has been studied for many cell compartments and organelles in different cell types throughout all kingdoms of life. However, involved proteins and cis-elements are yet widely unknown.

This work concentrates on the mitochondrial localized SOD2 mRNA. It aims to identify its interactome and especially the interacting factors at the mitochondrial surface by applying the RNA-BioID method on a bait mRNA that contains 24 MS2 loops between the ORF and the 3'UTR of the human superoxide dismutase 2.

The expression of all components – the $SOD2_{MS2}$ mRNA and a 2xMCP-eGFP-BirA* fusion protein – could be successfully validated in transiently transfected HeLa S3 cells. In addition, the nuclear localization of the fusion protein mediated by a C-terminal NLS and its distribution into cytoplasmic granules upon transfection with a $SOD2_{MS2}$ encoding vector (*SOD2MS2*) were visualized via fluorescence microscopy.

The fusion protein 2xMCP-eGFP-BirA* and a variant, 1xMCP-eGFP-BirA*, were integrated into the genomes of HeLa EM2-11ht and U2OS T-Rex cells and expressed under a promoter regulated by tetracycline response elements. Validation of the system was not fully performed for both cell lines, but the expression of 2xMCP-eGFP-BirA* in HeLa EM2-11ht cells and 1xMCP-eGFP-BirA* in U2OS T-Rex cells could be demonstrated by western blotting after doxycycline induction. Moreover, the expression of $SOD2_{MS2}$ in *SOD2MS2* transfected U2OS T-Rex cells was shown and the best conditions for biotin and doxycycline pulses were adjusted. The correct localization of the construct was verified via fluorescence microscopy.

Finally, RNA-BioID was performed in $U2OS_{1xMCP\text{-}eGFP\text{-}BirA*}$ cells. *SOD2MS2* transfected cells as well as untransfected controls were induced with doxycycline and maintained in biotin containing medium. Biotinylated proteins were determined by mass spectrometry. Although not a quantitative method, the mass spectrometry data allowed the identification of several candidates for proteins interacting with $SOD2_{MS2}$ mRNA. Among them were cytosolic proteins involved in mRNA regulation and transport as

CLUH, FXR1, PABP, STAU1, FUBP3 and LARP1. In addition, proteins involved in membrane and vesicle trafficking passed our threshold, as well as the TOM-complex associated cytosolic protein TOM34. Potential interactors at the mitochondrial surface were ATAD3, Rab5c and IGF2BP2. Other proteins of interest might be LRPPRC and the so far uncharacterized LRRC40. All these candidates must be carefully evaluated in further experiments to elucidate the interacting factors of SOD2 mRNA and the mode of SOD2 protein import into mitochondria, in particular since SOD2 mRNA was lately not found associated to the mitochondrial surface and no component of TOM complex, the main mitochondrial protein importer, is found in our dataset.

Further experiments will have to address an improvement of the RNA-BioID system in stably expressing cells and profound validation as well as the characterization of the possible candidates. If performed carefully, they may build the foundations to develop drugs for diseases related misregulation of SOD2 as the knowledge about gravity has built the basis for reaching the moon.

5. Zusammenfassung

In den letzten Jahrzehnten rückte die Theorie eines an die Translation gekoppelten Proteinimports in verschiedene Zellorganellen von einer hypothetischen Randbetrachtung in das Zentrum der Aufmerksamkeit. Unabdingbar für diesen Prozess ist der Transport vom mRNAs an den Zielort des zugehörigen Proteins.

Diese Arbeit befasst sich mit der mRNA von SOD2, welche in der Nähe von Mitochondrien nachgewiesen wurde. Mittels der Anwendung der RNA-BioID Methode sollten Proteine identifiziert werden, die potentiell am Transport der SOD2 mRNA und insbesondere an deren Verankerung an der mitochondrialen Oberfläche beteiligt sind.

Zunächst wurde das System in transient transfizierten HeLa S3 Zellen validiert. Hier konnte die korrekte Expression des 2xMCP-eGFP-BirA* Fusionsproteins sowie von $SOD2_{MS2}$ Protein gezeigt werden. $SOD2_{MS2}$ Protein ist auf dem Vektor *SOD2MS2* kodiert, zwischen seinem ORF und der 3'UTR finden sich 24 MS2 loops, die eine Bindung des Fusionsproteins an diese mRNA ermöglichen.

Darüber hinaus konnte fluoreszenzmikroskopisch die Umverteilung des eGFP enthaltenden Fusionsproteins von einem – durch eine c-terminale NLS bedingt – rein nukleären Signal zum Auftreten von zytoplasmatischen Punktmustern nach Transfektion mit *SOD2MS2* beobachtet werden.

2xMCP-eGFP-BirA* beziehungsweise seine Variation 1xMCP-eGFP-BirA* konnten erfolgreich in HeLa EM2-11ht und U2OS T-Rex Zellen integriert werden. Die Expression ist in beiden Zelllinien abhängig von Tet-response-Elementen. Beide Systeme konnten bisher nur unvollständig validiert werden, jedoch konnte nach Induktion mit Doxycylin das jeweilige Fusionsprotein sowie nach Transfektion in U2OS Zellen $SOD2_{MS2}$ mittels Westernblot nachgewiesen werden. Auch die notwendigen Konzentrationen und Pulszeiten für Doxycyclin und Biotin wurden teilweise ermittelt, die Untersuchungen sind jedoch für die einzelnen Zelllinien unvollständig und sollten ergänzt werden.

Mit *SOD2MS2* transfizierte $U2OS_{1xMCP\text{-}eGFP\text{-}BirA*}$ Zellen sowie untransfizierte Kontrollen wurden schließlich für die Identifikation interagierender Protein durch Massenspektrometrie verwendet. Hierfür wurden die Zellen mit Doxycyclin induziert

und dem Medium Biotin zugefügt, bevor die Zellen lysiert und biotinylierte Proteine mittels magnetischen Streptavidinperlen extrahiert wurden.

Unter den potentiellen Kandidaten finden sich viele Proteine, deren Rolle in Transport und Regulation von mRNAs bereits untersucht wird. Dazu gehören CLUH, FXR1, PABP, STAU1, FUBP3 und LARP1. Daneben fanden sich Proteine, die mit Membran- und Vesikeltransport in Verbindung gebracht werden sowie zwei Co-Chaperone und das zytosolische Protein TOM34, das üblicherweise mit den Chaperonen Hsp70/90 und dem TOM-Komplex interagiert. Weitere Komponenten dieser Hauptimportmaschinerie oder Hitzeschockproteine fanden sich nicht.

Als Kandidaten, die insbesondere im Bereich der Mitochondrien mit der $SOD2_{MS2}$ mRNA interagieren könnten, finden sich ATAD3, RAB5C und IGF2BP2. Daneben könnten auch LRPPRC sowie das bisher uncharakterisierte Protein LRRC40 von Interesse sein. Alle identifizierten Kandidaten müssen in kommenden Experimenten sorgfältig überprüft und validiert werden, insbesondere, da vor kurzem durchgeführte Experimente die SOD2 mRNA nicht in ihrer Assoziation zur mitochondrialen Außenmembran bestätigt haben. Auch hier sind dementsprechend weitere Untersuchungen notwendig.

Weitere Experimente müssen nun die RNA-BioID Methode für mRNAs mitochondrialer Proteine verfeinern, vollständig validieren und die beschriebenen sowie neuen Kandidaten untersuchen. Sorgfältig durchgeführt vermögen diese Experimente gegebenenfalls die Grundlage zur Behandlung von Erkrankungen legen, die mit veränderter Expression von SOD2 einhergehen, wie die Beschreibung der Gravitation die Grundlage bildete, um Raketen zum Mond zu schicken.

6. References

1. Anderson S, Bankier A, Barrell B, de Bruijn MH, Coulson AR, Drouin J, Eperon IC, Nierlich DP, Roe BA, Sanger F, Schreier PH, Smith AJ, Staden R, Young IG. Sequence and organization of the human mitochondrial genome. *Nature* 1981 Apr 9;290(5806):457-65. Doi: 10.1038/290457a0
2. Anding AL, Wang C, Chang TK, Sliter DA, Powers CM, Hofmann K, Youle RJ, Baehrecke EH. Vps13D Encodes a Ubiquitin-Binding Protein that Is Required for the Regulation of Mitochondrial Size and Clearance. *Curr Biol*. 2018;28(2):287–295.e6. doi:10.1016/j.cub.2017.11.064
3. Azadmanesh J, Borgstahl GEO. A Review of the Catalytic Mechanism of Human Manganese Superoxide Dismutase. *Antioxidants (Basel)*. 2018;7(2):25. Published 2018 Jan 30. Doi:10.3390/antiox7020025
4. Backes S, Hess S, Boos F, Woellhaf MW, Gödel S, Jung M, Mühlhaus T, Herrmann JM. Tom70 enhances mitochondrial preprotein import efficiency by binding to internal targeting sequences. *J Cell Biol*. 2018;217(4):1369–1382. Doi:10.1083/jcb.201708044
5. Bardoni B, Schenck A, Mandel JL. The fragile X mental retardation protein. *Brain Res Bull.* 2001 Oct-Nov 1;56(3-4):375-82. Doi: 10.1016/s0361-9230(01)00647-5
6. Barros LF, Ruminot I, San Martín A, Lerchundi R, Fernández-Moncada I, Baeza-Lehnert F. Aerobic Glycolysis in the Brain: Warburg and Crabtree Contra Pasteur. *Neurochem Res* 2020 Jan 24 doi: 10.1007/s11064-020-02964-w
7. Behra R, Christen P. In vitro import into mitochondria of the precursor of mitochondrial aspartate aminotransferase. *J Biol Chem* 1986 Jan 5;261(1):257-63.
8. Bohn JA, Van Etten JL, Schagat TL, Bowman BM, McEachin RC, Freddolino PL, Goldstrohm AC. Identification of diverse target RNAs that are functionally regulated by human Pumilio proteins. *Nucleic Acids Res*. 2018;46(1):362–386. Doi:10.1093/nar/gkx1120
9. Cabrera Y, Dublang L, Fernández-Higuero JA, Albesa-Jové D, Lucas M, Viguera AR, Guerin ME, Vilar JMG, Muga A, Moro F. Regulation of Human Hsc70 ATPase and Chaperone Activities by Apg2: Role of the Acidic Subdomain. *J Mol Biol.* 2019 Jan 18;431(2):444-461. Doi: 10.1016/j.jmb.2018.11.026
10. Calvo SE, Clauser KR, Mootha VK. MitoCarta2.0: an updated inventory of mammalian mitochondrial proteins. *Nucleic Acids Res*. 2016;44(D1):D1251–D1257. Doi:10.1093/nar/gkv1003
11. Chin A, Lécuyer E. RNA localization: Making its way to the center stage. *Biochim Biophys Acta Gen Subj.* 2017 Nov;1861(11 Pt B):2956-2970. Doi: 10.1016/j.bbagen.2017.06.011
12. Cao J, Mu Q, Huang H. The Roles of Insulin-Like Growth Factor 2 mRNA-Binding Protein 2 in Cancer and Cancer Stem Cells. *Stem Cells Int*. 2018;2018:4217259. Published 2018 Mar 15. Doi:10.1155/2018/4217259
13. Cdc37 interacting proteins. (https://www.picard.ch/downloads/Cdc37interactors.pdf). Accessed 23rd of March 2020

14. Chapman RM, Tinsley CL, Hill MJ, Forrest MP, Tansey KE, Pardiñas AF, Rees E, Doyle AM, Wilkinson LS, Owen MJ, O'Donovan MC, Blake DJ. Convergent Evidence That ZNF804A Is a Regulator of Pre-messenger RNA Processing and Gene Expression. *Schizophr Bull*. 2019;45(6):1267–1278. Doi:10.1093/schbul/sby183
15. Cho E, Jung W, Joo HY, Park ER, Kim MY, Kim SB, Kim KS, Lim YB, Lee KH, Shin HJ. Cluh plays a pivotal role during adipogenesis by regulating the activity of mitochondria. *Sci Rep*. 2019;9(1):6820. Published 2019 May 2. Doi:10.1038/s41598-019-43410-4
16. Cui J, Wang L, Ren X, Zhang Y, Zhang H. LRPPRC: A Multifunctional Protein Involved in Energy Metabolism and Human Disease. *Front Physiol*. 2019;10:595. Published 2019 May 24. Doi:10.3389/fphys.2019.00595
17. Dai N, Zhao L, Wrighting D, Krämer D, Majithia A, Wang Y, Cracan V, Borges-Rivera D, Mootha VK, Nahrendorf M, Thorburn DR, Minichiello L, Altshuler D, Avruch J. IGF2BP2/IMP2-Deficient mice resist obesity through enhanced translation of Ucp1 mRNA and Other mRNAs encoding mitochondrial proteins. *Cell Metab*. 2015;21(4):609–621. Doi:10.1016/j.cmet.2015.03.006
18. Das AT, Tenenbaum L, Berkhout B. Tet-On Systems For Doxycycline-inducible Gene Expression. *Curr Gene Ther*. 2016;16(3):156-167. Doi:10.2174/1566523216666160524144041
19. Dong F, Feldmesser M, Casadevall A, Rubin CS. Molecular characterization of a cDNA that encodes six isoforms of a novel murine a kinase anchor protein. *J Biol Chem*. 1998 Mar 13;273(11):6533-41. Doi: 10.1074/jbc.273.11.6533
20. Eliyahu E, Pnueli L, Melamed D, Scherrer T, Gerber AP, Pines O, Rapaport D, Arava Y. Tom20 mediates localization of mRNAs to mitochondria in a translation-dependent manner. *Mol Cell Biol*. 2010;30(1):284–294. Doi:10.1128/MCB.00651-09
21. Faou P, Hoogenraad NJ. Tom34: A cytosolic cochaperone of the Hsp90/Hsp70 protein complex involved in mitochondrial protein import. *Biochim Biophys Acta.* 2012 Feb;1823(2):348-57. Doi: 10.1016/j.bbamcr.2011.12.001
22. Faraz M, Herdenberg C, Holmlund C, Henriksson R, Hedman H. A protein interaction network centered on leucine-rich repeats and immunoglobulin-like domains 1 (LRIG1) regulates growth factor receptors. *J Biol Chem*. 2018;293(9):3421–3435. Doi:10.1074/jbc.M117.807487
23. Fazal FM, Han S, Parker KR, Kaewsapsak P, Xu J, Boettiger AN, Chang HY, Ting AY. Atlas of Subcellular RNA Localization Revealed by APEX-Seq. *Cell.* 2019 Jul 11;178(2):473-490.e26. doi: 10.1016/j.cell.2019.05.027
24. Frezza C, Cipolat S, Scorrano L. Organelle isolation: functional mitochondria from mouse liver, muscle and cultured fibroblasts. *Nat Protoc.* 2007;2(2):287-95. Doi: 10.1038/nprot.2006.478
25. Gadir N, Haim-Vilmovsky L, Kraut-Cohen J, Gerst JE. Localization of mRNAs coding for mitochondrial proteins in the yeast Saccharomyces cerevisiae. *RNA*. 2011;17(8):1551–1565. Doi:10.1261/rna.2621111
26. Gao J, Schatton D, Martinelli P, Hansen H, Pla-Martin D, Barth E, Becker C, Altmueller J, Frommolt P, Sardiello M, Rugarli EI. CLUH regulates mitochondrial biogenesis by binding mRNAs of nuclear-encoded mitochondrial proteins. *J Cell Biol*. 2014;207(2):213–223. Doi:10.1083/jcb.201403129

27. Garcia M, Darzacq X, Delaveau T, Jourdren L, Singer RH, Jacq C. Mitochondria-associated yeast mRNAs and the biogenesis of molecular complexes. *Mol Biol Cell*. 2007;18(2):362–368. Doi:10.1091/mbc.e06-09-0827
28. Gehrke S, Wu Z, Klinkenberg M, Sun Y, Auburger G, Guo S, Lu B. PINK1 and Parkin control localized translation of respiratory chain component mRNAs on mitochondria outer membrane. *Cell Metab*. 2015;21(1):95–108. Doi:10.1016/j.cmet.2014.12.007
29. Ginsberg MD, Feliciello A, Jones JK, Avvedimento EV, Gottesman ME. PKA-dependent binding of mRNA to the mitochondrial AKAP121 protein. *J Mol Biol.* 2003 Apr 4;327(4):885-97. Doi: 10.1016/s0022-2836(03)00173-6
30. Golani-Armon A, Arava Y. Localization of Nuclear-Encoded mRNAs to Mitochondria Outer Surface. *Biochemistry (Mosc).* 2016 Oct;81(10):1038-1043. Doi: 10.1134/S0006297916100023
31. Gold VA, Chroscicki P, Bragoszewski P, Chacinska A. Visualization of cytosolic ribosomes on the surface of mitochondria by electron cryo-tomography. *EMBO Rep*. 2017;18(10):1786–1800. Doi:10.15252/embr.201744261
32. Gordon WR, Vardar-Ulu D, L'Heureux S, Ashworth T, Malecki MJ, Sanchez-Irizarry C, McArthur DG, Histen G, Mitchell JL, Aster JC, Blacklow SC. Effects of S1 cleavage on the structure, surface export, and signaling activity of human Notch1 and Notch2. *PloS One*. 2009;4(8):e6613. Doi:10.1371/journal.pone.0006613
33. Gowravaram M, Schwarz J, Khilji SK, Urlaub H, Chakrabarti S. Insights into the assembly and architecture of a Staufen-mediated mRNA decay (SMD)-competent mRNP. *Nat Commun*. 2019;10(1):5054. Doi:10.1038/s41467-019-13080-x
34. Gray NK, Hrabálková L, Scanlon JP, Smith RW. Poly(A)-binding proteins and mRNA localization: who rules the roost? *Biochem Soc Trans.* 2015 Dec;43(6):1277-84. Doi: 10.1042/BST20150171
35. Hansen KG, Herrmann JM. Transport of Proteins into Mitochondria. *Protein J.* 2019 Jun;38(3):330-342. Doi: 10.1007/s10930-019-09819-6
36. Herman AB, Vrakas CN, Ray M, Kelemen SE, Sweredoski MJ, Moradian A, Haines DS, Autieri MV. FXR1 is an IL-19-Responsive RNA-Binding Protein that Destabilizes Pro-inflammatory Transcripts in Vascular Smooth Muscle Cells. *Cell Rep.* 2018 Jul 31;24(5):1176-1189. Doi: 10.1016/j.celrep.2018.07.002
37. Hervé JC, Bourmeyster N. Rab GTPases, master controllers of eukaryotic trafficking. *Small GTPases*. 2018;9(1-2):1–4. Doi:10.1080/21541248.2018.1428853
38. Hong S, Freeberg MA, Han T, Kamath A, Yao Y, Fukuda T, Suzuki T, Kim JK, Inoki K. LARP1 functions as a molecular switch for mTORC1-mediated translation of an essential class of mRNAs. *Elife*. 2017;6:e25237. Published 2017 Jun 26. Doi:10.7554/eLife.25237
39. Hosen MR, Militello G, Weirick T, Ponomareva Y, Dassanayaka S, Moore JB 4th, Döring C, Wysoczynski M, Jones SP, Dimmeler S, Uchida S. *Airn* Regulates Igf2bp2 Translation in Cardiomyocytes. *Circ Res*. 2018;122(10):1347–1353. Doi:10.1161/CIRCRESAHA.117.312215

40. Hung V, Lam SS, Udeshi ND, Svinkina T, Guzman G, Mootha VK, Carr SA, Ting AY. Proteomic mapping of cytosol-facing outer mitochondrial and ER membranes in living human cells by proximity biotinylation [published correction appears in Elife. 2019 Aug 05;8:]. *Elife*. 2017;6:e24463. Published 2017 Apr 25. Doi:10.7554/eLife.24463
41. Jansen RP. mRNA localization: message on the move. *Nat Rev Mol Cell Biol.* 2001 Apr;2(4):247-56. Doi: 10.1038/35067016
42. Johnson DT, Harris RA, French S, Blair PV, You J, Bemis KG, Wang M, Balaban RS. Tissue heterogeneity of mammalian mitochondrial proteome. *Am J Physiol Cell Physiol.* 2007 Feb;292(2):C689-97. Doi: 10.1152/ajpcell.00108.2006
43. Kaltimbacher V, Bonnet C, Lecoeuvre G, Forster V, Sahel JA, Corral-Debrinski M. mRNA localization to the mitochondrial surface allows the efficient translocation inside the organelle of a nuclear recoded ATP6 protein. *RNA*. 2006;12(7):1408–1417. Doi:10.1261/rna.18206
44. Kang Y, Fielden LF, Stojanovski D. Mitochondrial protein import in health and disease. *Semin Cell Dev Biol.* 2018 Apr;76:142-153. Doi: 10.1016/j.semcdb.2017.07.028
45. Kellems RE, Butow RA: Cytoplasmic 80 S ribosomes associated with yeast mitochondria. 3. Changes in the amount of bound ribosomes in response to changes in metabolic state. *J Biol Chem.* 1974 May 25;249(10):3304-10.
46. Kellems RE, Allison VF, Butow RA. Cytoplasmic type 80S ribosomes associated with yeast mitochondria. IV. Attachment of ribosomes to the outer membrane of isolated mitochondria. *J Cell Biol*. 1975;65(1):1–14. Doi:10.1083/jcb.65.1.1
47. Lapointe CP, Stefely JA, Jochem A, Hutchins PD, Wilson GM, Kwiecien NW, Coon JJ, Wickens M, Pagliarini DJ. Multi-omics Reveal Specific Targets of the RNA-Binding Protein Puf3p and Its Orchestration of Mitochondrial Biogenesis. *Cell Syst*. 2018;6(1):125–135.e6. doi:10.1016/j.cels.2017.11.012
48. Micklem DR, Adams J, Grünert S, St Johnston D. Distinct roles 89luore conserved Staufen domains in oskar mRNA localization and translation. *EMBO J*. 2000;19(6):1366-1377. Doi:10.1093/emboj/19.6.1366
49. Lee C, Goldberg J. Structure of coatomer cage proteins and the relationship among COPI, COPII, and clathrin vesicle coats. *Cell*. 2010;142(1):123–132. Doi:10.1016/j.cell.2010.05.030
50. Lesnik C, Golani-Armon A, Arava Y. Localized translation near the mitochondrial outer membrane: An update. *RNA Biol*. 2015;12(8):801–809. Doi:10.1080/15476286.2015.1058686
51. Lesnik C, Cohen Y, Atir-Lande A, Schuldiner M, Arava Y. OM14 is a mitochondrial receptor for cytosolic ribosomes that supports co-translational import into mitochondria [published correction appears in Nat Commun. 2015;6:6813]. *Nat Commun*. 2014;5:5711. Doi:10.1038/ncomms6711
52. Li T, Jiang HL, Tong YG, Lu JJ. Targeting the Hsp90-Cdc37-client protein interaction to disrupt Hsp90 chaperone machinery. *J Hematol Oncol*. 2018;11(1):59. Published 2018 Apr 27. Doi:10.1186/s13045-018-0602-8
53. Marc P, Margeot A, Devaux F, Blugeon C, Corral-Debrinski M, Jacq C. Genome-wide analysis of mRNAs targeted to yeast mitochondria. *EMBO Rep*. 2002;3(2):159–164. Doi:10.1093/embo-reports/kvf025

54. Margeot A, Blugeon C, Sylvestre J, Vialette S, Jacq C, Corral-Debrinski M. In Saccharomyces cerevisiae, ATP2 mRNA sorting to the vicinity of mitochondria is essential for respiratory function. *EMBO J.* 2002;21(24):6893–6904. Doi:10.1093/emboj/cdf690
55. Miller L. Analyzing gels and western blots with ImageJ (https://lukemiller.org/index.php/2010/11/analyzing-gels-and-western-blots-with-image-j/). Accessed 23rd of March, 2020
56. Mitsumori K, Takei Y, Hirokawa N. Components of RNA granules affect their localization and dynamics in neuronal dendrites. *Mol Biol Cell*. 2017;28(11):1412–1417. Doi:10.1091/mbc.E16-07-0497
57. Mukherjee J, Hermesh O, Eliscovich C, Nalpas N, Franz-Wachtel M, Maček B, Jansen, RP. B-Actin mRNA interactome mapping by proximity biotinylation. *Proc Natl Acad Sci U S A*. 2019;116(26):12863–12872. Doi:10.1073/pnas.1820737116
58. Narendra DP, Jin SM, Tanaka A, Suen DF, Gautier CA, Shen J, Cookson MR, Youle RJ. PINK1 is selectively stabilized on impaired mitochondria to activate Parkin. *PloS Biol*. 2010;8(1):e1000298. Doi:10.1371/journal.pbio.1000298
59. Nepal A, Wolfson DL, Ahluwalia BS, Jensen I, Jørgensen J, Iliev DB. Intracellular distribution and transcriptional regulation of Atlantic salmon (Salmo salar) Rab5c, 7a and 27a homologs by immune stimuli. *Fish Shellfish Immunol.* 2020 Apr;99:119-129. Doi: 10.1016/j.fsi.2020.01.058
60. Nousch M, Reed V, Bryson-Richardson RJ, Currie PD, Preiss T. The eIF4G-homolog p97 can activate translation independent of caspase cleavage. *RNA*. 2007;13(3):374–384. Doi:10.1261/rna.372307
61. Nunnari J, Suomalainen A. Mitochondria: in sickness and in health. *Cell*. 2012;148(6):1145–1159. Doi:10.1016/j.cell.2012.02.035
62. Ohashi R, Shiina N. Cataloguing and Selection of mRNAs Localized to Dendrites in Neurons and Regulated by RNA-Binding Proteins in RNA Granules. *Biomolecules*. 2020;10(2):167. Doi:10.3390/biom10020167
63. Park E, Maquat LE. Staufen-mediated mRNA decay. *Wiley Interdiscip Rev RNA*. 2013;4(4):423–435. Doi:10.1002/wrna.1168
64. Peralta S, Goffart S, Williams SL, Diaz F, Garcia S, Nissanka N, Area-Gomez E, Pohjoismäki J, Moraes CT. ATAD3 controls mitochondrial cristae structure in mouse muscle, influencing mtDNA replication and cholesterol levels. *J Cell Sci*. 2018;131(13):jcs217075. Doi:10.1242/jcs.217075
65. Pla-Martín D, Schatton D, Wiederstein JL, Marx MC, Khiati S, Krüger M, Rugarli EI. CLUH granules coordinate translation of mitochondrial proteins with mTORC1 signaling and mitophagy. *EMBO J.* 2020 Mar 9:e102731. Doi: 10.15252/embj.2019102731
66. Pontén J, Saksela E. Two established in vitro cell lines from human mesenchymal tumours. *Int J Cancer.* 1967 Sep 15;2(5):434-47. Doi: 10.1002/ijc.2910020505
67. Prévôt D, Darlix JL, Ohlmann T. Conducting the initiation of protein synthesis: the role of eIF4G. *Biol Cell.* 2003 May-Jun;95(3-4):141-56. Doi: 10.1016/s0248-4900(03)00031-5
68. Puck TT, Fisher HW. GENETICS OF SOMATIC MAMMALIAN CELLS : I. DEMONSTRATION OF THE EXISTENCE OF MUTANTS WITH DIFFERENT GROWTH REQUIREMENTS IN A HUMAN CANCER CELL

STRAIN (HELA). *J Exp Med*. 1956;104(3):427–434. Doi:10.1084/jem.104.3.427
69. Raymond CS, Soriano P. High-efficiency FLP and PhiC31 site-specific recombination in mammalian cells. *PloS One*. 2007;2(1):e162. Published 2007 Jan 17. Doi:10.1371/journal.pone.0000162
70. Rehbein M, Kindler S, Horke S, Richter D. Two trans-acting rat-brain proteins, MARTA1 and MARTA2, interact specifically with the dendritic targeting element in MAP2 mRNAs. *Brain Res Mol Brain Res.* 2000 Jun 23;79(1-2):192-201. Doi: 10.1016/s0169-328x(00)00114-5
71. Roux KJ, Kim DI, Burke B. BioID: A screen for protein-protein interactions. *Curr Protoc Protein Sci.* 2013 Nov 5;74:19.23.1-19.23.14. doi: 10.1002/0471140864.ps1923s74
72. Saint-Georges Y, Garcia M, Delaveau T, Jourdren L, Le Crom S, Lemoine S, Tanty V, Devaux F, Jacq C. Yeast mitochondrial biogenesis: a role for the PUF RNA-binding protein Puf3p in mRNA localization. *PloS One*. 2008;3(6):e2293. Doi:10.1371/journal.pone.0002293
73. Sen A, Cox RT. Clueless is a conserved ribonucleoprotein that binds the ribosome at the mitochondrial outer membrane. *Biol Open*. 2016;5(2):195–203. Published 2016 Feb 1. Doi:10.1242/bio.015313
74. Schatton D, Pla-Martin D, Marx MC, Hansen H, Mourier A, Nemazanyy I, Pessia A, Zentis P, Corona T, Kondylis V, Barth E, Schauss AC, Velagapudi V, Rugarli EI. CLUH regulates mitochondrial metabolism by controlling translation and decay of target mRNAs. *J Cell Biol*. 2017;216(3):675–693. Doi:10.1083/jcb.201607019
75. Schatton D, Rugarli EI. A concert of RNA-binding proteins coordinates mitochondrial function. *Crit Rev Biochem Mol Biol.* 2018 Dec;53(6):652-666. Doi: 10.1080/10409238.2018.1553927.
76. Shaiken TE, Opekun AR. Dissecting the cell to nucleus, perinucleus and cytosol. *Sci Rep*. 2014;4:4923. Doi:10.1038/srep04923
77. Shepard KA, Gerber AP, Jambhekar A, Takizawa PA, Brown PO, Herschlag D, DeRisi JL, Vale RD. Widespread cytoplasmic mRNA transport in yeast: identification of 22 bud-localized transcripts using DNA microarray analysis. *Proc Natl Acad Sci U S A*. 2003;100(20):11429–11434. Doi:10.1073/pnas.2033246100
78. Smith RW, Blee TK, Gray NK. Poly(A)-binding proteins are required for diverse biological processes in metazoans. *Biochem Soc Trans*. 2014;42(4):1229–1237. Doi:10.1042/BST20140111
79. Sugimoto Y, Vigilante A, Darbo E, Zirra A, Militti C, D'Ambrogio A, Luscombe NM, Ule J. hiCLIP reveals the in vivo atlas of mRNA secondary structures recognized by Staufen 1. *Nature*. 2015;519(7544):491–494. Doi:10.1038/nature14280
80. Sylvestre J, Margeot A, Jacq C, Dujardin G, Corral-Debrinski M. The role of the 3' untranslated region in mRNA sorting to the vicinity of mitochondria is conserved from yeast to human cells. *Mol Biol Cell*. 2003;14(9):3848–3856. Doi:10.1091/mbc.e03-02-0074
81. Tcherkezian J, Cargnello M, Romeo Y, Huttlin EL, Lavoie G, Gygi SP, Roux PP. Proteomic analysis of cap-dependent translation identifies LARP1 as a key

regulator of 5'TOP mRNA translation. *Genes Dev*. 2014;28(4):357–371. Doi:10.1101/gad.231407.113
82. Turan S, Galla M, Ernst E, Qiao J, Voelkel C, Schiedlmeier B, Zehe C, Bode J. Recombinase-mediated cassette exchange (RMCE): traditional concepts and current challenges. *J Mol Biol.* 2011 Mar 25;407(2):193-221. Doi: 10.1016/j.jmb.2011.01.004
83. Uniprot database (https://www.uniprot.org/). Accessed 5th of May, 2020
84. Vardi-Oknin D, Arava Y. Characterization of Factors Involved in Localized Translation Near Mitochondria by Ribosome-Proximity Labeling. *Front Cell Dev Biol*. 2019;7:305. Doi:10.3389/fcell.2019.00305
85. Vessey JP, Macchi P, Stein JM, Mikl M, Hawker KN, Vogelsang P, Wieczorek K, Vendra G, Riefler J, Tübing F, Aparicio SA, Abel T, Kiebler MA. A loss of function allele for murine Staufen1 leads to impairment of dendritic Staufen1-RNP delivery and dendritic spine morphogenesis. *Proc Natl Acad Sci U S A*. 2008;105(42):16374–16379. Doi:10.1073/pnas.0804583105
86. Wakim J, Goudenege D, Perrot R, Gueguen N, Desquiret-Dumas V, Chao de la Barca JM, Dalla Rosa I, Manero F, Le Mao M, Chupin S, Chevrollier A, Procaccio V, Bonneau D, Logan DC, Reynier P, Lenaers G, Khiati S. CLUH couples mitochondrial distribution to the energetic and metabolic status. *J Cell Sci.* 2017 Jun 1;130(11):1940-1951. Doi: 10.1242/jcs.201616
87. Wang H, Tan MS, Lu RC, Yu JT, Tan L. Heat shock proteins at the crossroads between cancer and Alzheimer's disease. *Biomed Res Int*. 2014;2014:239164. Doi:10.1155/2014/239164
88. Wang Y, Hu SB, Wang MR, Yao RW, Wu D, Yang L, Chen LL. Genome-wide screening of NEAT1 regulators reveals cross-regulation between paraspeckles and mitochondria. *Nat Cell Biol.* 2018 Oct;20(10):1145-1158. Doi: 10.1038/s41556-018-0204-2
89. Wang Z, Sun X, Wee J, Guo X, Gu Z. Novel insights into global translational regulation through Pumilio family RNA-binding protein Puf3p revealed by ribosomal profiling. *Curr Genet*. 2019;65(1):201–212. Doi:10.1007/s00294-018-0862-4
90. Warburg O. On the origin of cancer cells. *Science.* 1956 Feb 24;123(3191):309-14. Doi: 10.1126/science.123.3191.309
91. Weidenfeld I, Gossen M, Löw R, Kentner D, Berger S, Görlich D, Bartsch D, Bujard H, Schönig K. Inducible expression of coding and inhibitory RNAs from retargetable genomic loci. *Nucleic Acids Res*. 2009;37(7):e50. Doi:10.1093/nar/gkp108
92. Wiedemann N, Pfanner N. Mitochondrial Machineries for Protein Import and Assembly. *Annu Rev Biochem.* 2017 Jun 20;86:685-714. Doi: 10.1146/annurev-biochem-060815-014352
93. Williams CC, Jan CH, Weissman JS. Targeting and plasticity of mitochondrial proteins revealed by proximity-specific ribosome profiling. *Science*. 2014;346(6210):748–751. Doi:10.1126/science.1257522
94. Winge DR. Filling the mitochondrial copper pool. *J Biol Chem*. 2018;293(6):1897–1898. Doi:10.1074/jbc.H118.001457
95. Wong GH. Protective roles of cytokines against radiation: induction of mitochondrial MnSOD. *Biochim Biophys Acta.* 1995 May 24;1271(1):205-9. Doi: 10.1016/0925-4439(95)00029-4

96. Yamano K, Wang C, Sarraf SA, Münch C, Kikuchi R, Noda NN, Hizukuri Y, Kanemaki MT, Harper W, Tanaka K, Matsuda N, Youle RJ. Endosomal Rab cycles regulate Parkin-mediated mitophagy. *Elife*. 2018 Jan 23;7:e31326. Doi:10.7554/eLife.31326
97. Young JC, Hoogenraad NJ, Hartl FU. Molecular chaperones Hsp90 and Hsp70 deliver preproteins to the mitochondrial import receptor Tom70. *Cell.* 2003 Jan 10;112(1):41-50. Doi: 10.1016/s0092-8674(02)01250-3
98. Zabezhinsky D, Slobodin B, Rapaport D, Gerst JE. An Essential Role for COPI in mRNA Localization to Mitochondria and Mitochondrial Function. *Cell Rep.* 2016 Apr 19;15(3):540-549. Doi: 10.1016/j.celrep.2016.03.053
99. Zhang Y, Chen Y, Gucek M, Xu H. The mitochondrial outer membrane protein MDI promotes local protein synthesis and mtDNA replication. *EMBO J.* 2016;35(10):1045–1057. Doi:10.15252/embj.201592994

Appendix

Table of contents

I. Buffer compositions

Growth medium HeLa 11ht

DMEM

10%FBS

200 µg/ml G418

200 µg/ml Hygromycin B

Selection medium HeLa 11ht

DMEM

10%FBS

200µg/ml G418

50 µM Ganciclovir

Selection medium U2OS

DMEM

10%FBS

15 µg/ml Blasticidin S

100 µg/ml Hygromycin B

Imaging medium for HeLa S3 and HeLa 11ht

DMEM w/o Phenolred

5% FBS

Phosphate buffered saline (PBS)

137 mM NaCl

2,7 mM KCl

10 mM Na_2HPO_4

1,8 mM K2HPO_4

pH 7.4

TBS-T

20 mM Tris

150 mM NaCl

0,1% Tween 20

Antibody solution

1xTBS

1% FBS

0,1% Tween 20

RIPA buffer

150 mM NaCl

1.0% NP-40 or Triton X-100

0.5% sodium deoxycholate

0.1% SDS

50 mM Tris

pH 8.0

10x TBS

200 mM Tris

1,5 M NaCl

pH 7.4

Blocking buffer for western blots

1x TBS (20 mM Tris and 150mM NaCl, pH 7.4)

5%BSA

Developing buffer (for western blots with Streptavidin bound alkaline phosphatase)

100 mM Tris

50 mM $MgCl_2$

100 mM NaCl

pH 9.5, total volume 5 ml per blot

Homogenization buffer (HB) (Kaltimbacher et al., 2006)

0.6 M Mannitol

30 mM Tris-Cl pH 7.6

5 mM MgAc

100 mM KCl

0.1 % BSA

5 mM β-mercaptoethanol

1 mM PMSF

Imaging buffer for fluorescence microscopy (laboratory of Prof. Garcia, IFIB Tübingen)

2mM HEPES pH 7.4

150 mM NaCl

15 mM Glucose

20 mM Trehalose

54 mM KCl

0.58 mM $MgSO_4$

0.7 mM $CaCl_2$

filter sterilized

SDS sample buffer

10 % Glycerol

50 mM Tris-Cl pH 6.8

2 % SDS

0.005 % Bromphenolblue

1 % ß-Mercaptoethanol

Bead wash buffers #1

2 % SDS

Bead wash buffer #2

0.1 % Deoxychlate

1 % Triton X-100

1mM EDTA

500 mM NaCl

50 mM HEPES pH 7.4

Bead wash buffer #3

0.5 % Deoxycholate

0.5 % NP40

1 mM EDTA

250 mM LiCl

10 mM Tris-Cl pH 7.4

Bead wash buffer #4 (ABC buffer)

50 mM NaCl

50 mM Tris pH 7.4

Lysis buffer

50 mM Tris pH 7.5

150 mM NaCl

2.5 mM $MgCl_2$

1 mM DTT

1 % Tween 20

1 x Proteinase inhibitor (freshly added before use)

IB_C buffer (Frezza et al., 2007)

10 mM Tris-MOPS

200 mM Sucrose

1 mM EGTA/Tris

pH 7.4

Buffer A (Shaiken et a., 2014)

40 mM HEPES pH 7.4

120 mM KCl

2 mM EGTA

0.4 % Glycerol

0.4 % NP-40

1x Protease inhibitor (freshly added before use)

12% SDS page 10ml

3.2 ml ddH_2O

2.6 ml 1.5M Tris pH 8.8

0.1 ml SDS 10 %

0.1 ml Ammoniumpersulfate 10 %

10 µl TEMED

4 ml Acrylamide/Bisacrylamide 30 %/0.8 %

The surface of separating gels was straightened with 200 µl isopropanol.

Stacking gel SDS page 5ml

3.6 ml ddH_2O

0.625 ml Tris-HCl 1M pH 6.8

50 µl SDS 10%

50 µl Ammoniumpersulfate 10 %

5µl TEMED

0.67 ml Acrylamide/Bisacrylamide 30 %/0.8 %

Staining buffer for Biotin blots

100 mM NaCl

100 mM Tris

50 mM $MgCl_2$

pH 9.5

6x DNA loading dye

10 mM Tris-HCl pH 7.6

60 mM EDTA

60 % Glycerol

0.03 % bromphenol blue

0.03 % xylene cyanol

FACS buffer

1 x PBS without magnesium and calcium

2 % FBS

0.5 mM EDTA

10x Towbin buffer

250 mM Tris

190 mM Glycine

1 % SDS

LB medium

25 g yeast extract

50 g trypton

25 g sodium chloride

diluted in ddH_2O in a total volume of 5 liters

LB plates

600 ml LB medium

10g agarose

100 µg/ml Ampicillin

II. Cell lines and primer sequences

Table 1: Cell lines

Cell line	**Integrated fusion protein**
HeLa S3	-
HeLa EM2-11ht	-
$HeLa_{2xMCP\text{-}eGFP\text{-}BirA*}$	NLS-2xMCP-eGFP-BirA*
$HeLa_{1xMCP\text{-}eGFP\text{-}BirA*}$	NLS-1xMCP-eGFP-BirA*
$HeLa_{2xMCP\text{-}eGFP}$	NLS-2xMCP-eGFP
$HeLa_{1xMCP\text{-}eGFP}$	NLS-1xMCP-eGFP
U2OS T-Rex	-
$U2OS_{1xMCP\text{-}eGFP\text{-}BirA*}$	NLS-1xMCP-eGFP-BirA*
$U2OS_{1xMCP\text{-}eGFP}$	NLS-1xMCP-eGFP

Table 2: Primer sequences

Primer name	**Sequence**
Q00325-2_backward	5‘-AAGGAAAAAAGCGGCGCTGAGTTAACCCAAGCTTCTTCTT-3‘
Q00325-2_forward	5‘-CGCGGATCCATGTTCTCGTCCGTGGCGCACCTG-3‘
BamHI-eGFPwithstop_R	5‘-CGCGGATCCTTACTTGTACAGCTCGTCCATGCC-3‘
KpnI-stop-SV40NLS_F	5‘-CGGGGTACCTAAATGGGCCCAAAAAAGAAAAGAAAAGTTGG-3‘
BamHI-BirAwithstop_R	5‘-CGCGGATCCTTACTTCTCTGCGCTTCTCAGGGAG-3‘

III. Quantification of western lanes

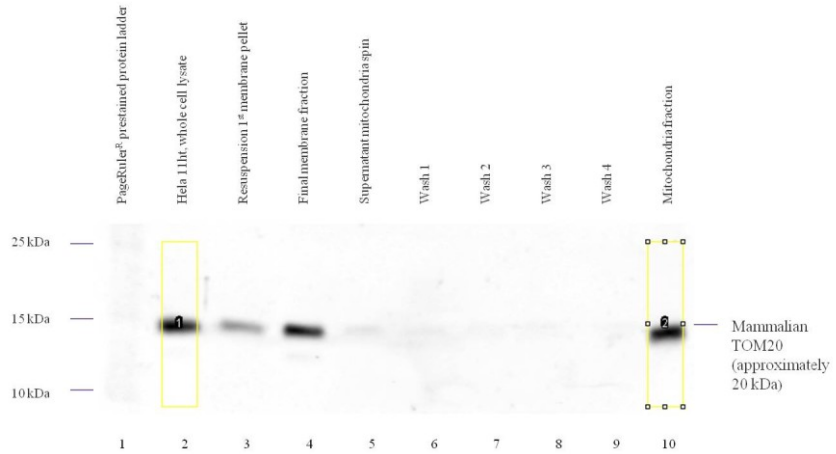

Fig. 1: Blotting windows chosen from blot in figure 18. Lane 2 (marked as nr. 1) and lane 10 (marked as nr. 2) were analyzed in the shown windows.

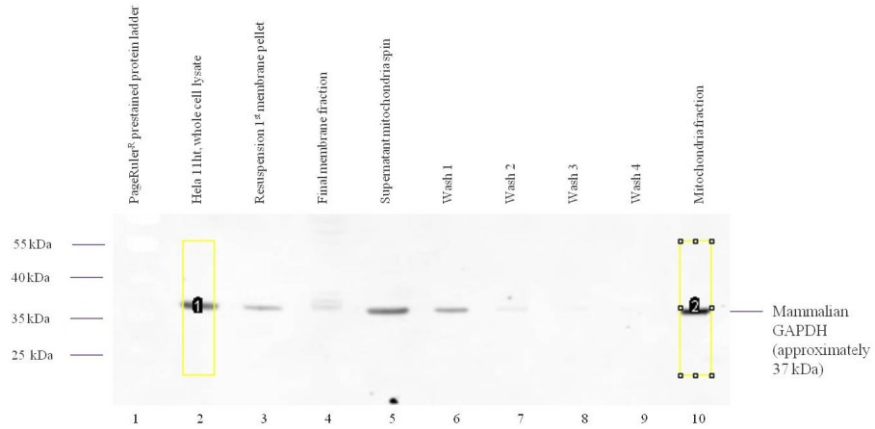

Fig. 2: Blotting windows chosen from figure 19 to compare signals of lane 2 (marked as nr. 1) and lane 2 (marked as nr. 2).

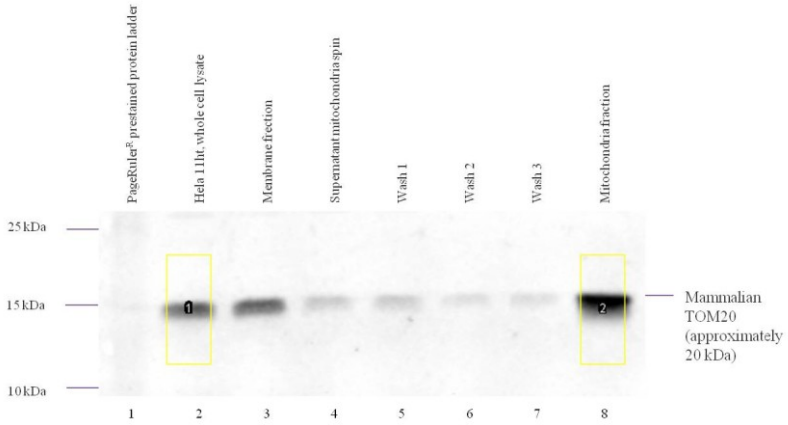

Fig. 3: Blotting windows chosen from figure 20 for quantification of the signal in lane 2 (marked as nr. 1) and lane 10 (marked as nr. 2).

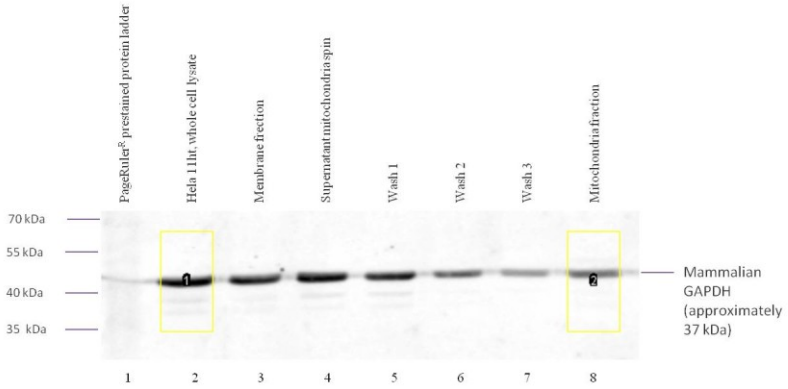

Fig. 4: Windows chosen for signal quantification in lanes 2 (marked as nr.1) and lanes 8 (marked as nr. 2) from figure 21.

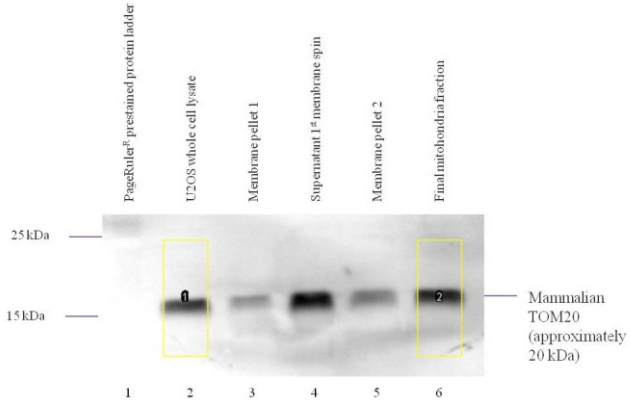

Fig 5: Windows chosen for quantification of TOM20 signal in lanes 2 (marked nr. 1) and 6 (marked nr. 2) from figure 23.

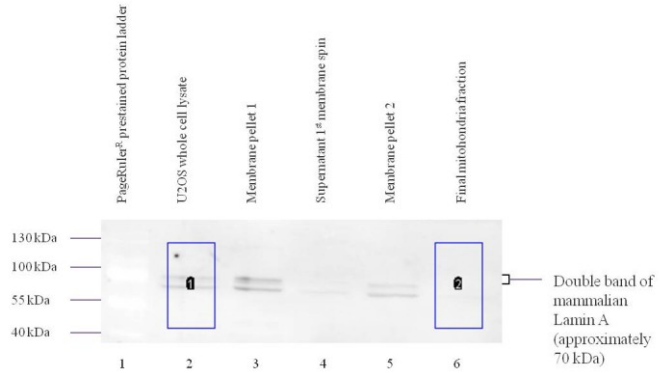

Fig. 6: Windows chosen for quantification of Lamin A signal in lanes 2 (marked nr. 1) and 6 (marked nr. 2) from figure 24.

Fig. 7: Quantification windows chosen from lanes 2 to 7 (marked nr. 1 to 6) from figure 25.

IV. FACS details

FACS details for HeLa EM2-11ht

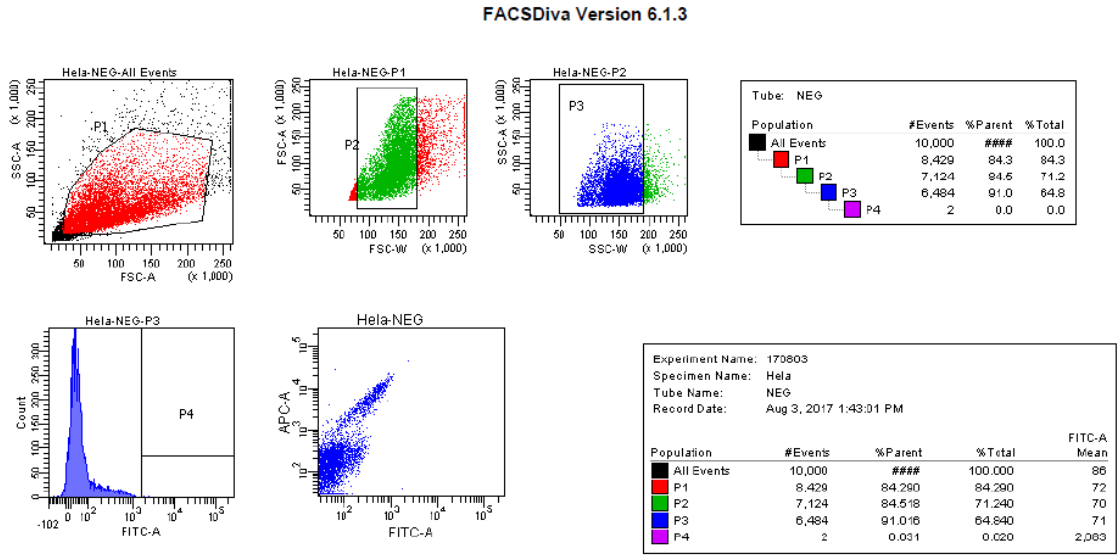

Fig. 8: FACS details for HeLa EM2-11ht negative control (Cornelia Grimmel, FACS Core facility of Tübingen university)

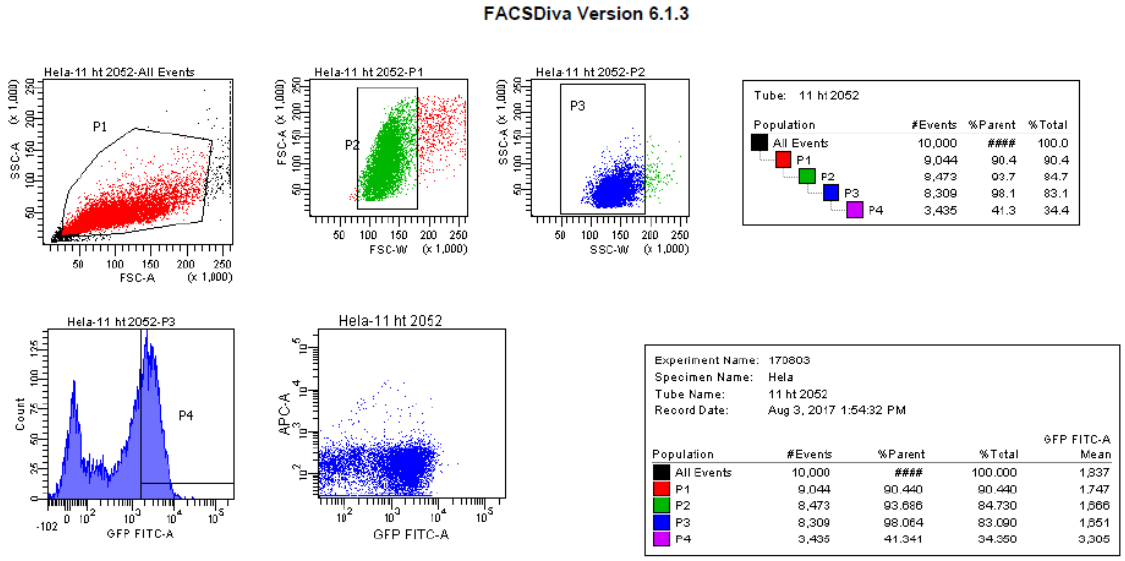

Fig. 9: FACS details for HeLa EM2-11ht$_{1xMCP\text{-}eGFP}$ (Cornelia Grimmel, FACS Core facility of Tübingen university)

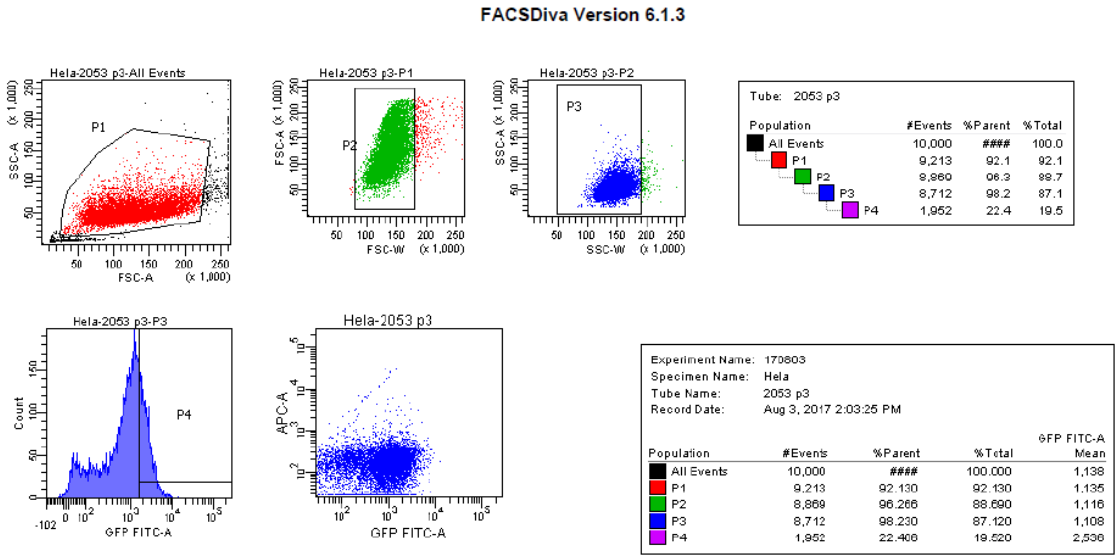

Fig. 10: FACS details for Hela EM2-11ht$_{1xMCP\text{-}eGFP\text{-}BirA*}$ (Cornelia Grimmel, FACS Core facility of Tübingen university)

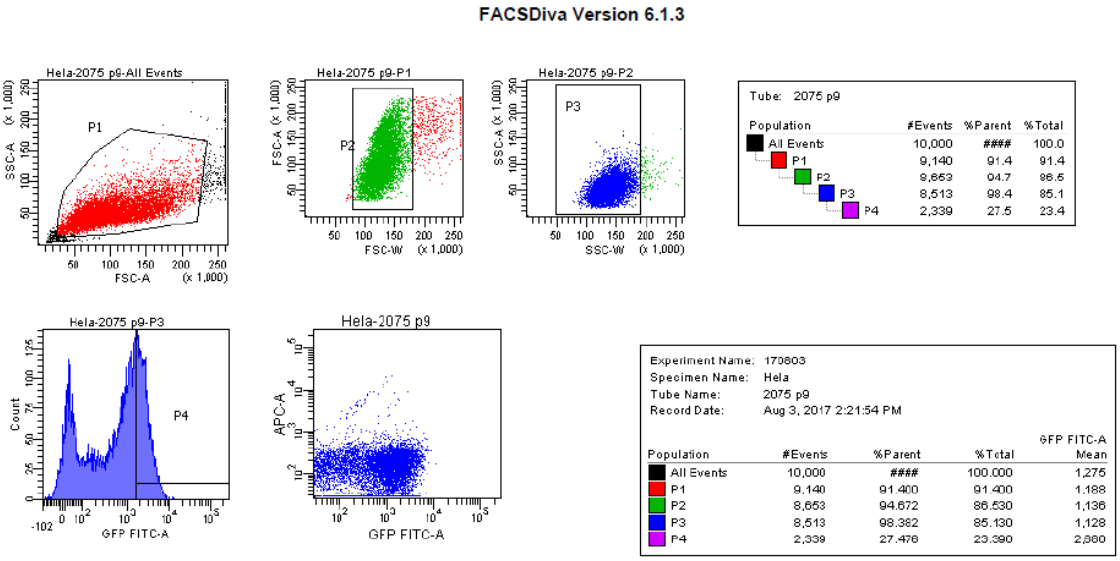

Fig. 11: FACS details for HeLa EM2-11ht$_{2xMCP\text{-}eGFP}$ (Cornelia Grimmel, FACS Core facility of Tübingen university)

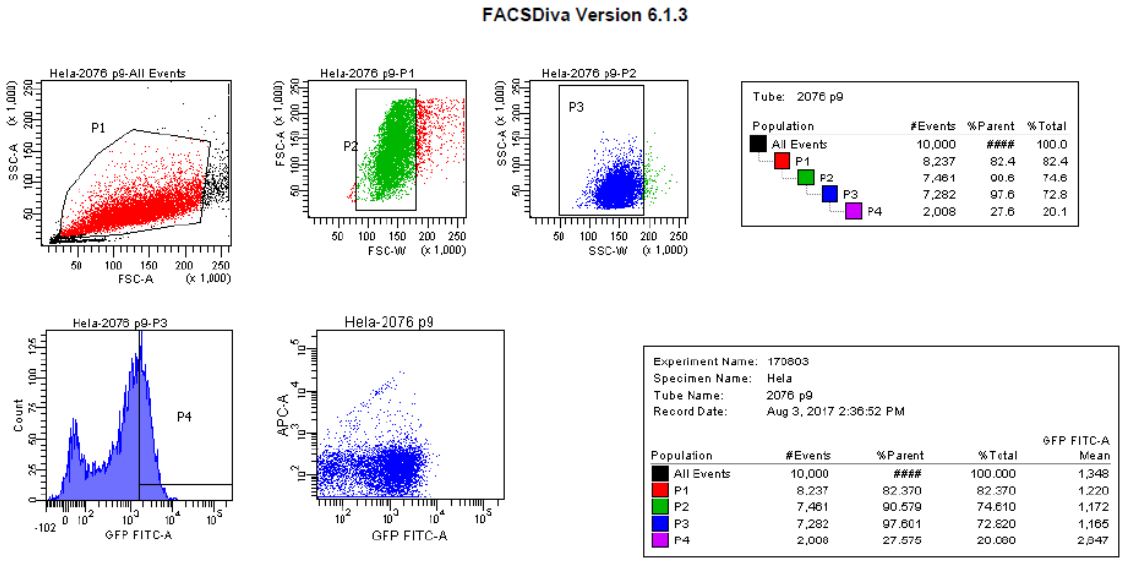

Fig. 12: FACS details for HeLa EM2-11ht$_{2xMCP\text{-}eGFP\text{-}BirA*}$ (Cornelia Grimmel, FACS Core facility of Tübingen university)

FACS details for U2OS T-Rex cells

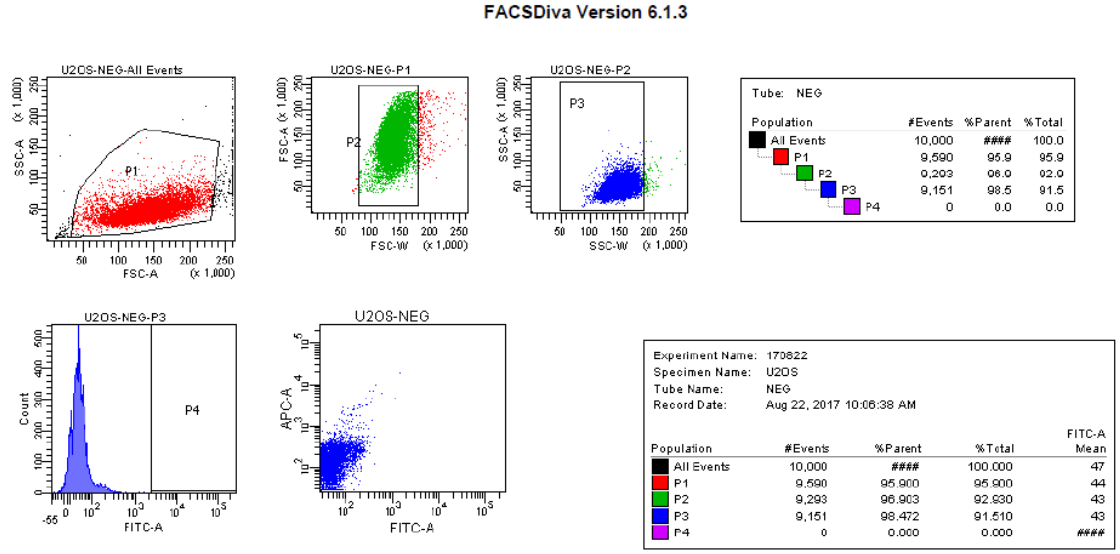

Fig. 13: FACS details for U2OS negative control (Cornelia Grimmel, FACS Core facility of Tübingen university)

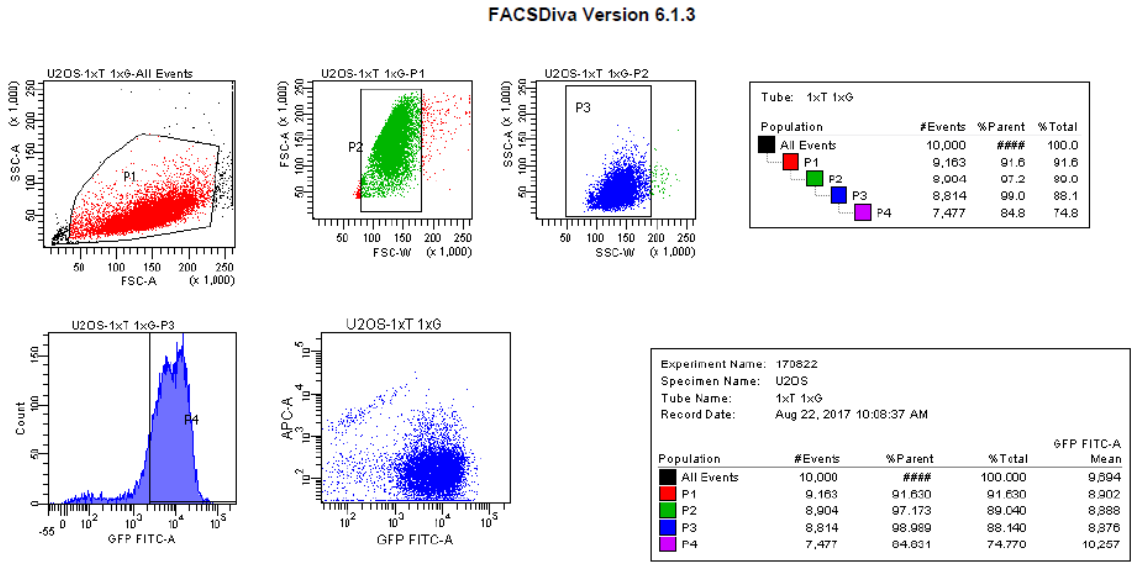

Fig. 14: FACS details for U2OS$_{1xMCP\text{-}eGFP}$ (Cornelia Grimmel, FACS Core facility of Tübingen university)

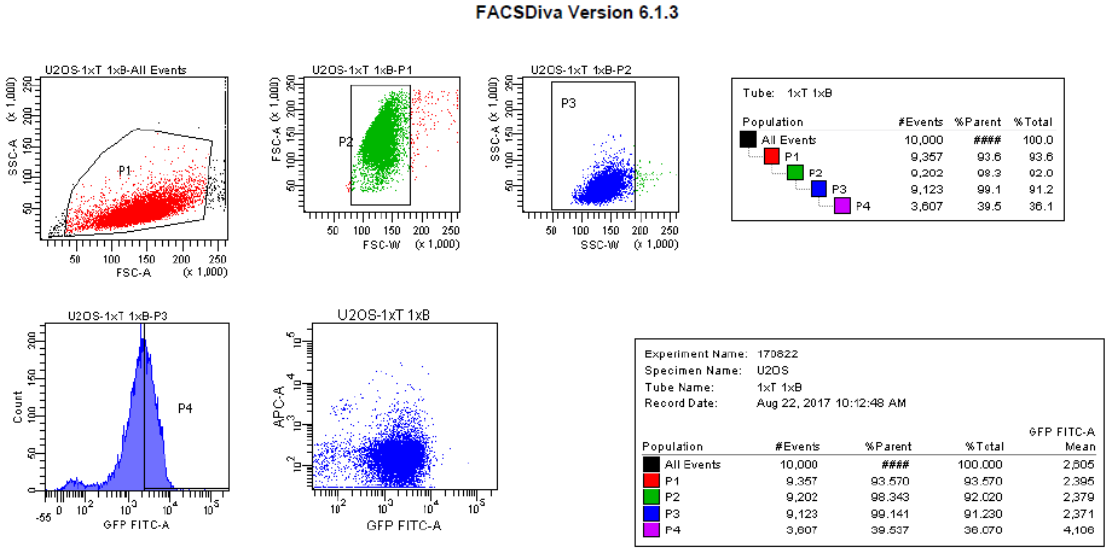

Fig. 15: FACS details for U2OS$_{1xMCP\text{-}eGFP\text{-}BirA*}$ (Cornelia Grimmel, FACS Core facility of Tübingen university)

V. Mass spectrometry details

Table 3: Peptide counts for Potential interactors of the $SOD2_{MS2}$ bait mRNA (mass spectrometry was performed by Dr. Mirita Franz-Wachtel, Proteome center of Tübingen university)

Gene names	**Peptides**									
	Control 1	Control 2a	Control 2b	Sample 1	Sample 2a	Sample 2b	Sample 3a	Sample 3b	Sample 4a	Sample 4b
IGF2BP2	0	0	0	3	3	3	5	4	4	4
LRRC40	0	0	0	2	2	3	2	3	2	2
GPATCH8	0	0	0	2	2	2	2	2	2	2
RAB5C;RAB5A;RAB5B	0	0	0	2	2	2	2	2	2	1
CLUH	3	2	3	4	7	7	9	8	8	8
FXR1	3	4	4	6	8	7	10	11	9	8
LRPPRC	1	0	0	3	0	0	4	3	3	3
LARP1	2	2	2	5	5	5	3	5	2	3
PABPC4	1	2	2	4	8	8	5	6	8	8
PABPC1;PABPC3	3	4	4	5	8	10	9	7	8	8
ATAD3A;ATAD3B	2	0	0	2	0	0	3	4	4	4
FUBP3	0	0	1	1	1	2	2	2	1	1
STAU1	1	2	2	3	5	6	5	5	5	4
ARCN1	0	0	0	0	2	1	2	1	2	1
COPB1	0	1	1	0	1	2	3	3	5	4
VPS13D	4	5	6	7	2	2	25	24	25	25
HSPA4	3	5	4	8	10	10	6	9	7	6
CDC37	1	1	1	3	3	3	3	1	2	2
TOMM34	0	0	0	1	1	0	0	0	3	1

Table 4: Peptide intensities for Potential interactors of the $SOD2_{MS2}$ bait mRNA (mass spectrometry was performed by Dr. Mirita Franz-Wachtel, Proteome center of Tübingen university)

Gene names	**Peptide intensities**									
	Control 1	Control 2a	Control 2b	Sample 1	Sample 2a	Sample 2b	Sample 3a	Sample 3b	Sample 4a	Sample 4b
IGF2BP2	0	0	0	825360	713470	549260	2109400	1356900	639010	630980
LRRC40	0	0	0	168060	401460	604160	327610	479680	211090	222670
GPATCH8	0	0	0	397930	752260	959820	851530	824570	518310	611280
RAB5C;RAB5A;RAB5B	0	0	0	412100	991980	862710	596640	936950	428780	353560
CLUH	415000	512550	938380	740850	2054700	1927400	2967500	2820500	1557800	2009300
FXR1	2835200	3110000	4107600	2908500	2363600	2244700	6456800	7946000	4953700	6157600
LRPPRC	316790	0	0	519610	0	0	794090	971420	542100	566500
LARP1	677110	1398700	1506000	946510	3614800	2612600	1587100	2149900	684220	1301400
PABPC4	0	0	0	1094200	1144900	1003300	294880	533610	741170	817530
PABPC1;PABPC3	890030	3383400	3501100	1873300	8794000	8923100	3912800	4018000	1564900	2514800
ATAD3A;ATAD3B	479470	0	0	432240	0	0	1148700	1359900	1404900	1649600
FUBP3	0	0	372130	173710	167490	461090	425730	477450	190120	273610
STAU1	153930	743500	874130	639740	2882800	3330600	1478000	1787600	1103800	1271700
ARCN1	0	0	0	0	494910	392760	364740	186990	275620	198490
COPB1	0	157360	232240	0	194880	290790	469610	667800	1386300	1861800
VPS13D	1310300	1863100	2359600	1368800	942540	1025900	9023900	8632400	8618800	11352000
HSPA4	381350	2088100	1465200	1504800	4070500	4115100	1434300	2893200	1513200	1294000
CDC37	1175400	985530	1114700	1384200	912780	1021100	1004800	145560	499560	771960
TOMM34	0	0	0	52774	188100	0	0	0	389580	246040

Erklärung zum Eigenanteil

Diese Arbeit wurde im interfakultären Institut für Biochemie unter Betreuung von Prof. Dr. rer. nat. Ralf-Peter Jansen durchgeführt.
Die Konzeption des Arbeitsthemas erfolgte durch Frau Dr. rer. nat. Joyita Mukherjee im Zusammenarbeit mit Prof. Dr. rer. nat. Jansen.
Die Massenspektrometrie wurde durch Frau Dr. rer. nat. Mirita Franz-Wachtel (Proteom Centrum Tübingen) durchgeführt, ein Auszug der Resultate ist in den Tabellen 3 und 4 im Anhang dargestellt. Die Durchflusszytometrie erfolgte in der Flow Cytometry Core facility Tal durch Frau Cornelia Grimmel, sie stellte mir die Details in Form der Abbildungen 8 bis 15 im Anhang zur Verfügung.
Frau Dr. Mukherjee klonierte die Vektoren, die für die transiente Transfektion in Hela S3 Zellen genutzt wurden (Abb. 1, 2 und 3). Darüber hinaus klonierte sie die Plasmide, die für die stabile Integration der Gene für Fusionproteine in Hela EM2-11ht Zellen notwenig waren (Abb. 8).
M. Sc. Alfred Hanswillemenke klonierte den in Abb. 5 dargestellten Vektor und Derivate und stellte freundlicherweise neben den Plasmiden auch die zugehörigen DNA-Sequenzen zur Verfügung.
Die dargestellten Versuche und Auswertungen wurden nach Einarbeitung durch Frau Dr. rer. nat. Joyita Mukherjee und Ruth Schmid von mir eigenständig durchgeführt.
Ich versichere, das Manuskript selbstständig verfasst, nach Anleitung von Prof. Dr. rer. nat. Jansen korrigiert und keine weiteren als die von mir angegebenen Quellen verwendet zu haben.

Jena, den 28.05.2020

Danksagung

„Alle Kraft, die wir fortgeben, kommt erfahren und verwandelt wieder über uns.“

Rainer Maria Rilke

Damit möchte ich mich bei all denen bedanken, die mich bei der Verfassung dieser Arbeit begleitet haben.

Zuerst möchte ich hier Ralf, Joyita, Ruth und der gesamten Arbeitsgruppe *RNA biology* danken, dass sie ihr Wissen mit mir geteilt und mir stets geholfen haben. Ohne sie wäre diese Arbeit nicht möglich gewesen.

Außerdem gilt mein Dank Alfred und Frank, stellvertretend für alle anderen Mitarbeiter des IFIB und der Universität Tübingen, die mich auf unterschiedlichste Weise unterstützt haben.

Danken möchte ich auch meinen Freunden und hier besonders Marion und Henrike, die auch den weiten Weg nach Tübingen nicht gescheut haben.

Ein besonderer Dank gilt meinen Eltern Sylvia und Jürgen sowie meiner Schwester Alexandra für ihre stetige Unterstützung und die Inspiration, die sie mir geben.

Zuletzt möchte ich mich bei Brian bedanken, der mich immer motiviert hat. Für sein Vertrauen in mich.